

**Technical
Document
Series**

Hole Alignment Tolerance Stacking Issues

M&CT-TECH-99-025

October 1999

Mathematics and Computing Technology
Phantom Works

Phantom Works, Mathematics & Computing Technology

A Division of The Boeing Company

THIS DOCUMENT IS:

Controlled by **Mathematics and Engineering Analysis, G-6400**

Prepared under

- Contract
- IR&D
- CD/OH
- Other...

Prepared on **Sun**

Filed under

Document No. **M&CT-TECH-99-025**

Title **Hole Alignment Tolerance Stacking Issues**

Original Release Date **October 1999**

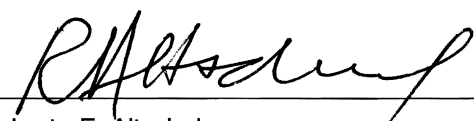
- The information contained herein is NOT BOEING PROPRIETARY or BOEING LIMITED
- Boeing Limited
- Boeing Proprietary

Prepared by:



Fritz Scholz

Approved by:



Roberto E. Altschul

Hole Alignment Tolerance Stacking Issues

Fritz Scholz

M&CT-TECH-99-025

October 1999

Copyright © 1999 The Boeing Company

Phantom Works
Mathematics and Computing Technology
P.O. Box 3707, M/S 7L-21
Seattle, WA 98124-2207

Hole Alignment Tolerance Stacking Issues

Fritz Scholz*

Mathematics and Computing Technology
Boeing Phantom Works

February 24, 1999

Abstract

Each of two parts has K coordination holes with the intent that each hole on one part is paired and to be pinned with a corresponding hole on the other part. While the nominal hole centers for each hole pair are identical, the actual hole centers will deviate from their nominal values in some random fashion reflecting the inherent hole centering accuracy of the drilling process. It is then of some interest to examine the maximal hole center discrepancy among K such hole pairs and to understand how this discrepancy grows with K . We give a plausible and very simple model for assessing this maximal discrepancy statistically and show that the growth of this discrepancy is slow, namely on the order of $\sqrt{\log(K)}$. Although this model formulation assumes the unrealistic true position part alignment on all K nominal centers, it is still useful in that it provides a conservative assessment compared to what might be possible under “best” alignment. Furthermore, its results relate essentially linearly to the common, practical alignment procedure using primary and secondary hole pairs. The statistical treatment of hole center variation is compared to the worst case treatment for both alignment procedures. While the gain of the statistical over worst case treatment is small under true positioning it is substantial under primary/secondary hole alignment. Consequences for minimal clearance and maximal clean-out diameters are derived, assuming no or negligible hole and pin diameter variations. These results can be extended usefully to the situation when triplets of holes, one hole each on one of three parts, need to be pinned. The above results are derived assuming equal hole centering variability from hole to hole. This is extended to hole centering variability that grows linearly with the distances of the nominal hole centers from some reference datum. A further extension deals with matching two parts where each part is built up from k subparts with n holes each. The misalignments of the subparts relative to each other add dependency complications when trying to assess the maximum mismatch between the $K = kn$ holes on each assembly half.

* P.O. Box 3707, MC 7L-22, Seattle WA 98124-2207, e-mail: fritz.scholz@boeing.com

Contents

1	Problem Description and Overview	1
2	Clearance & Clean-Out under True Position Alignment	8
2.1	Single Hole Pair Clearance	8
2.2	Clearance and Clean-Out Distributions for K Holes	10
2.3	Approximations and Quantiles	12
2.4	Clearance Tolerance Stack Criterion and Fallout Rate	16
2.5	Clean-Out Tolerance Stack Criterion and Fallout Rate	17
3	Alignment Using Primary and Secondary Hole Pairs	20
3.1	Maximum Hole Center Distance	22
3.2	Clearance Tolerance Stack and Fallout Rate	31
3.3	Cleanout Tolerance Stack Criterion and Fallout Rate	34
4	Comparison with Worst Case Analysis	36
4.1	Comparison under True Position Alignment	38
4.2	Comparison under Primary/Secondary Hole Alignment	39
5	Three Matched Holes	42
5.1	Clearance for Three Matched Holes, True Position Alignment	42
5.2	Clean-Out for Three Matched Holes, True Position Alignment	47
5.3	Clearance Under Primary/Secondary Hole Triplet Alignment	53
5.4	Clean-Out Under Primary/Secondary Hole Triplet Alignment	60
6	Hole Centering Variation Increasing with Datum Distance	67
7	Mating Coordination Holes on Assembled Parts	75

8	References	89
9	Appendix A Extreme Value Approximation	90
10	Appendix B Geometry of Primary/Secondary Hole Pair Alignment	91
11	Appendix C Clearance and Cleanout for Three Overlapping Holes	98
12	Appendix D Worst Case for Primary/Secondary Hole Pair Alignment	104

1 Problem Description and Overview

We consider various aspects of the coordination hole tolerance stacking problem. They arise when trying to mate two parts, such as stringers to skins, skins to skins, and panels to frames, etc., by placing (temporary) fasteners through matching hole pairs or hole triplets. Usually there will be K such hole pairs or triplets, where $K \geq 2$ and K may be as large as 60 or higher.

When such fasteners are temporary, their function is to act as clamping devices that hold the parts in position while intermediate holes are match-drilled and riveted. Since such riveting fixes the position of the parts relative to each other, these coordination holes also serve the much more important role of defining the geometry or final position of the two parts relative to each other. The temporary fasteners are removed after riveting the intermediate holes. The coordination holes are then cleaned out, i.e., match-drilled with larger, full-sized holes and riveted.

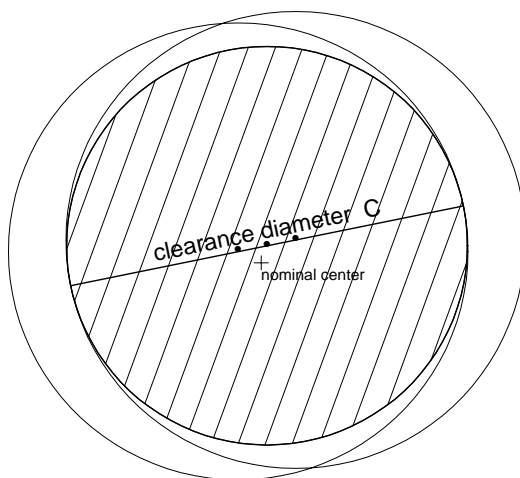
Defining the relative geometry of parts by coordination holes differs from previous practices of using massive tools for joining parts. There the tools carry the geometry information which is transferred to the parts by holding them in place in the tools while match drilling and riveting them. This process results in variation in the geometry as defined on the tool and in variation in fixturing the parts on the tool. The variation in the geometry as defined on the tool acts more like a bias, fixed effect, or mean shift which does not lend itself very well to statistical variation cancellation. Such biases would repeat themselves time and again, unless there is some slow drift in the tool geometry, which represents another systematic variation component.

Although the coordination hole scenario was the original motivation for looking at this problem, the analysis methods proposed here have a wider scope. Namely, they are relevant whenever several particular feature point locations on one part need to be mated to corresponding feature point locations on another part. In the above motivating example these feature point locations would be the hole centers. Typically such feature point locations are subject to variation which leads to mismatches when more than one pair of such feature point locations needs to be aligned. Assessing the maximal size of this mismatch (over all feature point location pairs) from a statistical and worst case perspective is our main goal here.

Although the scope of the methods presented here goes beyond pinning coordination holes we will stay with that application image to avoid complete abstraction. A crucial initial assumption underlying the analysis methods developed here is that during assembly *the parts are aligned by matching the nominal hole center positions for each hole pair*. Since these

nominal hole center positions are also called the *true positions* of these particular features, we refer to this part alignment also as *true position alignment*. This particular alignment is artificial, because it is not at all clear how to accomplish it in practice. However, if it is possible to pin the parts loosely and without interference under true position alignment, it will also be possible to pin the parts under some other nearby alignments as well. It is just a matter of finding such alignments through small motions of the parts relative to each other. Among all these alignments there certainly will be a best one, i.e., with smallest maximum hole center discrepancy. Considering the true position alignment case is therefore in some sense a conservative assessment of the pinning problem. By “conservative” we mean that even if it is established that the parts cannot be pinned under true position alignment, such pinning may still be possible under some other alignment.

Figure 1: Hole Clearance Diameter C



Being able to put fasteners or pins through all the paired holes simultaneously is referred to as the *clearance problem*. Since the paired holes have actual hole centers that deviate from their respective common nominal centers, these paired holes can be viewed as overlapping circles which define a maximal inscribed circle, shown shaded in Figure 1. The common nominal center for both holes is marked by a +. The nominal centers match because true position alignment is assumed here. The diameter of this inscribed circle is called the *clearance diameter*, C , for that particular hole pair. It is a direct function of how far the actual

hole centers deviate from each other.

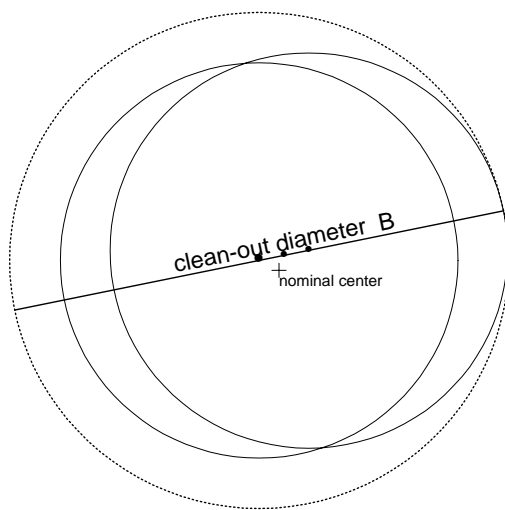
These clearance diameters vary from hole pair to hole pair and it is the smallest one of these K clearance diameters that will give the most problem of placing a fastener through it. Other alignments may certainly produce a smallest clearance diameter (over K hole pairs) that is even larger than the one achieved under true position alignment, but finding this alignment mathematically and analyzing its statistical effects is very complicated at best. The problems of implementing such an alignment in practice may be even more prohibitive, since it would require a high degree of positional part control, which is exactly what coordination holes are supposed to accomplish in a practical fashion. The potential gain of the optimal alignment over the true position alignment may be so small that it will not justify such complications in analysis or practical implementation when aiming for ease of application.

Throughout it is assumed that all coordinate hole fasteners have the same diameter. If the fastener diameters vary as well, with tolerances controlling their variation, then one could use the maximally allowed fastener diameter for a conservative clearance assessment. Similarly, it is assumed that hole diameters are identical. If there is variation among these diameters, then we can take conservatively the smallest toleranced hole diameter for a conservative clearance assessment. There definitely is room here for taking advantage of additional statistical tolerancing, i.e., variation cancellation due to fastener and hole size variation, in addition to the hole centering variation. A first attempt in this direction was made in [4] for the case of two hole pairs with respect to a nearly “best” alignment. There, hole centering and hole and pin size variations as well as deviations from perpendicularity in the hole axes were taken into account in the statistical tolerance stack. However, for K holes and true position alignment this issue of hole and pin size variations has not yet been worked out. If the pin and hole diameter variations are much smaller than the hole centering variation, as assumed here, these effects will have little consequence. However, if these variations are comparable to hole centering variation, then further investigations into statistical stacking of these effects would be beneficial.

Once the parts have been pinned by these temporary fasteners other full-sized holes are match-drilled in-between and riveted. After the parts have been fastened in this way the original coordination hole fasteners used for clamping the parts to each other are removed and bigger full-sized holes are drilled over each hole pair to clean out these overlapping holes. The smallest circle (shown in Figure 2 as the dotted circle), that contains these two circles and is centered on one of them, has diameter B . This is called the *clean-out diameter*, since it is the smallest diameter required to clean out both holes under such centering. These clean-out diameters will vary from hole pair to hole pair. The maximum clean-out diameter over all K hole pairs is a simple function of the maximum distance between hole center pairs.

The control of the maximum clean-out diameter is referred to as the clean-out problem. As long as the maximum clean-out diameter is less than the intended full-sized hole diameter, there is no danger of residual cavities or boundary irregularities in the clean-out holes, i.e., no need for rework or oversized fasteners.

Figure 2: Hole Clean-Out Diameter B



In the context of the minimal clearance diameter a case was made that true position part alignment gives a conservative assessment of the ability to pin the parts. The same is not so clear-cut with respect to the maximum clean-out diameter over all K hole pairs. The reason for the difference is that while trying to pin the parts via coordination holes the parts are still free to move relative to each other, whereas at the clean-out stage the parts are already riveted to each other at intermediate, match-drilled holes. At that stage the parts are certainly not in true position alignment. A plausible (but not completely forcing) argument can be made for treating a maximum clean-out diameter analysis under true position part alignment as reasonable, if not conservative. This argument is as follows. By pinning K hole pairs simultaneously the paired hole centers will be coerced to move closer together in order to permit simultaneous pinning, especially when pinning becomes difficult due to excessive hole centering variations. In such cases the hole centers are likely to be closer together than under true positioning and it is these cases which also pose the biggest clean-out problems. Exceptions to this plausibility argument can be constructed and

more investigations are needed, but at this point we will assume that treating the clean-out problem under true position part alignment will not be too far off the mark from being conservative. Actually it will be seen later that the particular alignment strategy of using primary and secondary coordination holes for a definite and practical alignment provides a counterexample to the above argument. However, in that case this issue of proper treatment of the clean-out problem is resolved in straightforward fashion.

In [1], [2] and [3] we examined an alternate and more realistic alignment model, in which two hole pairs, located farthest apart from each other, were aligned as follows. The parts are moved relative to each other until the centers of the first or primary hole pair are aligned on top of each other (via expanding fasteners or tightly toleranced hole and pin diameters). Then the distant or secondary hole pair is aligned by rotating the parts around the pinned primary hole pair to achieve maximal clearance at that secondary hole pair. This alignment causes the centers of all four holes in the two hole pairs (when projected on a plane perpendicular to the hole axes) to be collinear. This alignment leaves matters mathematically more complex in that the hole center distances of intermediate hole pairs are no longer statistically independent of each other. They all depend on the alignment of the two hole pairs used for alignment, which in turn is affected by the hole centering variation at the primary and secondary hole pairs. These dependencies make a clean analysis of the statistical effects of hole centering variation analytically very complicated. It was found in [1] that using the two hole pairs farthest apart in this alignment is better than choosing any other two hole pairs for such an alignment. This not only minimizes the actual part to part misalignment but also minimizes the maximum hole center discrepancy, i.e., gives best clearance and clean-out results. Although a clean analytical treatment of this alignment procedure was judged to be intractable, we found through extensive simulations a simple link to the results obtained under the impractical method of true position alignment.

In Section 2 we first present the clearance and clean-out problem in the context of one matched hole pair under true position alignment. We show that the clearance and clean-out diameters, C and B , are best studied in terms of the distance D between hole centers. Based on a circular bivariate normal distribution for the hole centering variation we derive the statistical distribution function of D and then extend this to K matched hole pairs, again under true position alignment. From this we derive the distribution functions for the minimal clearance and maximal clean-out diameters for K matched hole pairs. The K hole pairs can all be along one seam or over several seams or arranged in some other spatial form. For example, they could represent hole pairs or paired feature point locations around the perimeter edge of two fuselage sections. As far as pinning is concerned, one can always view the relevant discrepancies locally within a plane. This ignores possible 3-dimensional interference effects which would need to be addressed separately.

Accurate approximations to these distribution functions are then given in terms of the Gumbel distribution from extreme value theory and the effect of K and the hole positioning precision is examined. These approximations show that the ability to simultaneously pin all K hole pairs degrades in direct proportion to the hole centering variability. Furthermore, the degradation is approximately proportional to $\sqrt{\log(K)}$, i.e., the number of hole pairs affects the problem only very mildly. This is certainly surprising in view of other tolerance stacking phenomena where variability contributions of K linearly stacked dimensions would aggregate proportional to \sqrt{K} in root sum square (RSS) stacking or proportional to K in worst case stacking. Of course, we do not have additive accumulation over K variation terms here. Instead we deal with maxima over K terms (hole center discrepancies), each of which is affected by four variation terms (the hole center coordinates).

In Section 3 the effect of the more practical alignment procedure via primary and secondary coordination holes is examined through extensive simulations and related successfully and in simple linear fashion to the analytical model developed in Section 2.

In Section 4 the results of statistical tolerance stacking under true position and primary/secondary hole pair alignment are compared to worst case tolerance stacking under corresponding alignments. In the case of true positioning the gain in maximal hole center mismatch, when using statistical over worst case tolerance stacking, is mild (25% – 10% for $K = 2, \dots, 50$) but under primary/secondary hole pair alignment the gain ranges from 55% – 40% for linear hole patterns and from 33% – 25% for hole patterns arranged equally spaced on the perimeter of a square. Since hole centering accuracy affects the maximum hole center mismatch in a proportional manner, such gains translate directly to the same percentage improvements for hole centering accuracies.

In Section 5 the results of Section 2 for matching K hole pairs under true position alignment are extended to the situation where three parts are to be pinned (e.g. skin, skin and stringer) and thus three holes are matched at each nominal location. This extension is based on considering the worst pair among each triplet and coupling this with Boole’s inequality. This leads to a good approximation for describing extreme hole center discrepancies, which are our primary concern. Here the clearance problem growth relative to K is on the order of $\sqrt{\log(2.4K)}$, i.e., again very slow with K . These results under true position alignment are then again extended to the case which uses primary/secondary hole triplet alignment.

The above results assume equal hole centering accuracy regardless of the locations at which the holes are drilled. This assumption is often not satisfied in practice. Usually the drilling tool is indexed against some datum and the drilling accuracy will degrade somewhat as the drill head moves away from that datum. Systematic location effects (datum to hole variation) have no bearing on the ability to pin parts successfully. Such a common shift

of all hole centers can be compensated by shifting the part correspondingly when aligning it for pinning. Of course such shifts affect the position of the parts relative to each other. In fact, they are possibly the main drivers in part to part misalignment. An increase in centering variation from hole to hole cannot be corrected so easily and its effect may need to be factored in at the tolerance design stage. One way to deal with this is to conservatively assume a constant centering accuracy as it can be attained at the hole center farthest from the datum used as reference during drilling. Since this may be too conservative we reanalyze in Section 6 the results from Section 2 in the context of linearly increasing hole centering variation. Some simple approximations are presented that appear reasonable for extreme clearance and clean-out problems. The results presented here are of exploratory nature since they only cover true position alignment.

Another form of hole centering degradation with distance from datum occurs when differential thermal expansion effects (between drill tool and part to be drilled) play a role. Then there are systematic offsets (typically with linear growth from the datum) and one needs to compensate for these before invoking any of the results presented here. Such compensation should adjust the nominal hole center location based on the ambient temperature and tool/part expansion differential.

Section 7 addresses a further extension. Here the two parts or subassemblies to be joined by coordination holes are themselves built up from subparts, each subpart already predrilled with its respective coordination holes. The assembly from subparts to part or subassembly is another source of variation (affecting all holes on the same subpart jointly, i.e., in a dependent manner) which needs to be accounted for when examining whether the two built up parts or subassemblies can be pinned successfully at all coordination holes. This problem is examined only in a rather limited setting and the intent is to gain a preliminary understanding of how such correlated variation affects the analysis. Although this question arose originally in support of JSF it came up again within the context of fitting cargo liners to built up frames. Ultimately it is planned to build a simulation software tool which has sufficient flexibility to help address various further such inquiries.

Sections 2, 3, and 5 are accompanied by boxed rules or guidelines for planning tolerance stack analyses. Their purpose is to serve as direct entry points without having to read through the underlying analyses. Sections 6 and 7 are exploratory investigations. Further progress in these areas is definitely possible and could lead to similar boxed rules or guidelines, but a definite case for their need has to be made before embarking on this.

2 Clearance & Clean-Out under True Position Alignment

Suppose two locally flat parts 1 and 2 are to be pinned by placing a pin of diameter δ through a hole with diameter d in part 1 and (by proper alignment of part 2 with respect to part 1) at the same time also through a corresponding hole of diameter d on part 2. For $\delta < d$ such pinning should always be possible, if we align the hole centers on top of each other. This assumes that there are no other part interferences.

Although the alignment just mentioned may work fine with just one hole pair to be pinned, it is usually no longer possible if several hole pairs need to be aligned simultaneously and if the actual hole centers deviate from the respective nominal hole centers. It is assumed that the nominal hole centers are matched perfectly by design and thus could be aligned perfectly by true position alignment. Note the distinction made between “actual hole centers” and “nominal hole centers.” It is extremely unlikely that the actual hole centers on part 1 could simultaneously match the corresponding actual hole centers on part 2 through some alignment. Bearing this in mind we assume for now that the parts are aligned on their true position, as intended by the design.

2.1 Single Hole Pair Clearance

Focussing on hole centering issues we disregard part thickness and thus perpendicularity issues (see [4] for some treatment of that) and view the two parts as planar and aligned in true position within a common two-dimensional coordinate system. Within this coordinate system we denote the common nominal hole centers by (μ, ν) and the actual hole centers by (X_1, Y_1) and (X_2, Y_2) , respectively. See Figure 1, where (μ, ν) is marked by a + and (X_1, Y_1) and (X_2, Y_2) are marked as the two outside • marks on the clearance diameter. The middle • represents the center of the maximal clearance circle.

Assume that X_1, Y_1, X_2, Y_2 are independent and normally distributed random variables with means μ for X_1 and X_2 and ν for Y_1 and Y_2 and with variances σ_1^2 for X_1 and Y_1 and σ_2^2 for X_2 and Y_2 . These assumptions mean that the hole centering variation on either part is described by a circular bivariate normal distribution centered on (μ, ν) with the radial accuracy governed by σ_1 in the case of (X_1, Y_1) and by σ_2 in the case of (X_2, Y_2) . This variation model is backed by theoretical considerations as the only one that has independent variations in the X and Y directions and which has an isotropic bivariate probability density, i.e., a density that is constant at points equidistant from the nominal center (μ, ν) . This means that hole center deviations from the nominal center are equally likely in all directions. The fact that we allow for different σ 's reflects the possibly different processes that may be applied in drilling the holes on the two parts. For example, it may be possible to center

holes more accurately on stringers than on skin panels.

A consequence of the above variation model is that the probability of “the distance of (X_i, Y_i) from nominal center (μ, ν) being bounded by x ” is given by

$$P\left(\sqrt{(X_i - \mu)^2 + (Y_i - \nu)^2} \leq x\right) = 1 - \exp\left(-\frac{x^2}{2\sigma_i^2}\right) \quad \text{for } i = 1, 2 .$$

Here $\exp(y) = e^y$ is the exponential function and we denote by $\log(z) = \log_e(z)$ its inverse, often also denoted by $\ln(z)$.

In particular, from the defining relation of the quantile x_p relative to p ($0 < p < 1$), namely

$$P\left(\sqrt{(X_i - \mu)^2 + (Y_i - \nu)^2} \leq x_p\right) = 1 - \exp\left(-\frac{x_p^2}{2\sigma_i^2}\right) = p = .9973$$

we obtain

$$x_{.9973} = x_p = \sigma_i \sqrt{-2 \log(1 - p)} = \sigma_i \sqrt{-2 \log(1 - .9973)} = 3.439\sigma_i ,$$

i.e., a $3.439\sigma_i$ radial zone around (μ, ν) will contain 99.73% of all actual hole centers. This can be viewed as a bivariate analogy to the 99.73% of all X_i (or Y_i) values falling within the customary $3\sigma_i$ of μ (or ν) in the univariate framework. The factor 3.439 (as opposed to 3) adjusts for the fact that we deal with a two-dimensional variation criterion.

If the radial tolerance for hole centering is specified by T_i for holes on part i , we may, in keeping with the above $3\sigma_i$ vis-à-vis .9973 paradigm for one-dimensional tolerances, want to link this radial tolerance to σ_i as follows:

$$T_i = 3.439 \sigma_i \quad \text{or} \quad \sigma_i = T_i/3.439 . \quad (1)$$

The distance between the pair of actual hole centers is denoted by D and can be expressed as

$$D = \sqrt{(X_1 - X_2)^2 + (Y_1 - Y_2)^2} .$$

This distance D also is the amount by which the two holes (circles) of radius r or diameter $d = 2r$ are shifted relative to each other, leaving us with a diameter $C = 2r - D = d - D$ for the largest clearance circle that can fit within the two offset holes. A negative value for C indicates that there is no clearance within the two holes at all, at least not in the assumed true position alignment. If $d - D < \delta$ there is insufficient clearance for a pin with diameter δ .

The corresponding diameter for a clean-out hole, centered on one of the two hole centers, is $B = 2(r + D) = d + 2D$. If we center the clean-out hole halfway between the two hole centers, then the clean-out diameter is $B' = d + D$. This latter diameter may be relevant¹ when drilling full-sized holes. Then one is concerned with a rivet passing through the clearance diameter and the subsequently “upset” rivet filling at most a circle of a certain size, namely the smallest one containing both circles. This circle coincides with the one associated with the diameter B' .

Under the above assumptions the differences $X_1 - X_2$ and $Y_1 - Y_2$ are independent and normally distributed random variables with mean zero and common variance $\tau^2 = \sigma_1^2 + \sigma_2^2$. Thus the distribution function of D , or the probability that the distance D between two hole centers is bounded by x , is given by

$$P(D \leq x) = 1 - \exp\left(-\frac{x^2}{2\tau^2}\right) \quad \text{for } x \geq 0.$$

The fact that the hole drilling accuracies could differ from part to part is of no great impact, since in the end only $\tau^2 = \sigma_1^2 + \sigma_2^2$ matters.

2.2 Clearance and Clean-Out Distributions for K Holes

If K hole pairs are aligned on nominal positions we can ask: What is the maximum diameter for a pin that would fit all hole pairs simultaneously? This diameter is the minimum of K statistically independent hole clearances, i.e.,

$$C_{K,\min} = \min(C_1, \dots, C_K) = \min(d - D_1, \dots, d - D_K) = d - \max(D_1, \dots, D_K),$$

where C_i is the clearance for the i^{th} true position aligned hole pair. Similarly, the worst clean-out diameter among the K holes is given by the maximum of K statistically independent clean-out hole diameters, i.e.,

$$B_{K,\max} = \max(B_1, \dots, B_K) = d + 2 \max(D_1, \dots, D_K)$$

or

$$B'_{K,\max} = \max(B'_1, \dots, B'_K) = d + \max(D_1, \dots, D_K),$$

where B_i and B'_i are the respective clean-out diameters for the i^{th} true position aligned hole pair.

¹pointed out to me by Mark Boberg

The reason for being able to invoke statistical independence here is that the random deviations of each hole center from nominal are assumed to be independent and don't influence each other through the alignment process, since the alignment is assumed to be keyed on the fixed nominal centers. Although datum to hole variation would affect all holes on the same part by a common shift (which causes dependence from hole to hole), one can ignore this variation source as far as pinning and clean-out is concerned. One would simply assume an alignment that negates that common shift, i.e., use a modified true position alignment. Since true position alignment is artificial (not realizable), there is no loss in using the further artificial construct of a modified true position alignment.

The exact statistical distributions of $C_{K,\min}$, $B_{K,\max}$, and $B'_{K,\max}$ are easily derived in terms of the distribution of

$$M_K = \max(D_1, \dots, D_K) .$$

Namely,

$$P(C_{K,\min} \leq x) = P(d - \max(D_1, \dots, D_K) \leq x) = 1 - P(M_K \leq d - x) , \quad x \leq d$$

$$P(B_{K,\max} \leq x) = P(2M_K + d \leq x) = P(M_K \leq [x - d]/2) , \quad x \geq d$$

and

$$P(B'_{K,\max} \leq x) = P(M_K + d \leq x) = P(M_K \leq x - d) \quad x \geq d .$$

From the independence of centering errors for each hole pair and the true position alignment assumption we get for $x \geq 0$

$$\begin{aligned} P(M_K \leq x) &= P(D_1 \leq x, \dots, D_K \leq x) = P(D_1 \leq x) \times \dots \times P(D_K \leq x) \\ &= [P(D \leq x)]^K = \left[1 - \exp\left(-\frac{x^2}{2\tau^2}\right) \right]^K \end{aligned}$$

From this it follows that

$$P(C_{K,\min} \leq x) = 1 - \left[1 - \exp\left(-\frac{[d - x]^2}{2\tau^2}\right) \right]^K \quad \text{for } x \leq d$$

$$P(B_{K,\max} \leq x) = \left[1 - \exp\left(-\frac{[(x - d)/2]^2}{2\tau^2}\right) \right]^K \quad \text{for } x \geq d,$$

and

$$P(B'_{K,\max} \leq x) = \left[1 - \exp\left(-\frac{[x-d]^2}{2\tau^2}\right) \right]^K \quad \text{for } x \geq d.$$

2.3 Approximations and Quantiles

For large K the above distributions can be approximated, providing a clearer insight into the effects of τ and K on the growth of the clearance and clean-out problem. It turns out that these approximations are also useful for small to moderate K , provided they are applied to the appropriate distribution tail. Fortunately, this tail happens to be just the one that is of most concern in each respective case.

First we develop the approximation for $P(M_K \leq x)$ as follows:

$$\begin{aligned} H_K(x) = P(M_K \leq x) &= \left[1 - \exp\left(-\frac{x^2}{2\tau^2}\right) \right]^K \approx \left[\exp\left(-\exp\left\{-\frac{x^2}{2\tau^2}\right\}\right) \right]^K \\ &= \mathcal{G}\left(\frac{x^2}{2\tau^2} - \log(K)\right) = \mathcal{H}_K(x), \end{aligned} \quad (2)$$

where $\tau^2 = \sigma_1^2 + \sigma_2^2$ and $\mathcal{G}(x) = \exp(-\exp[-x])$ is the Gumbel distribution function known from extreme value theory. The above approximation invokes

$$1 - \alpha \approx \exp(-\alpha)$$

which is good for small values of α . Here we used $\alpha = \exp(-x^2/(2\tau^2))$, which is small for large x . Thus the approximation for $H_K(x)$ should work well for all $K \geq 2$, provided x is large. The latter is the case of main interest. For large K the approximation will tend to get better for other x values as well. This is demonstrated later in the context of quantiles.

It should be pointed out that the approximation $\mathcal{H}_K(x)$ for $H_K(x)$ is not based on the traditional approach taken in extreme value theory. There one usually determines normalizing constants a_K and b_K such that the following limiting relationship holds uniformly for all x

$$P(b_K[M_K - a_K] \leq x) \longrightarrow G(x) \quad \text{as } K \rightarrow \infty,$$

where $G(x)$ is a distribution function which can be only one of three different types. In Appendix A we show that with $a_K = \tau\sqrt{2\log(K)}$ and $b_K = \sqrt{2\log(K)}/\tau$ we have that $G(x) = \mathcal{G}(x)$, which is one of these three distribution types. Thus for all $x \geq 0$ and for large K we can also approximate

$$H_K(x) = P(M_K \leq x) = P(b_K[M_K - a_K] \leq b_K[x - a_K]) \approx \mathcal{G}(b_K[x - a_K]). \quad (3)$$

For $K = 2, 3, 5, 10, 30, 60$ the respective plots in Figure 3 show the true densities of the M_K distributions as a solid line, compared with the density from our first approximation (2) as a dotted line, and that of the second approximation (3) as a dashed line. The first approximation is excellent for high M_K values even for small K and overall quite good for $K \geq 10$. The second approximation is not good for small K and even for $K = 30$ and $K = 60$ it still shows substantially higher density in the important, right tail. One sees clearly how slowly the distributions shift to the right as K increases from 2 to 60, and they also appear to get more concentrated at the same time. This latter observation is confirmed below when looking at quantile differences.

It should be pointed out that $\mathcal{H}_K(x)$ is not a statistical distribution function, since it does not increase from zero to one. Instead it increases from $\exp(-K)$ to one for $x \geq 0$ and is not meant to serve as approximation for $x < 0$. Thus it should not surprise that the derivative of $\mathcal{H}_K(x)$, shown as dotted line in Figure 3, does not integrate to one over the range $[0, \infty)$. Instead it integrates only to $1 - \exp(-K)$. This is particularly pronounced in Figure 3 for $K = 2$, where the total areas under the solid and dotted curves don't appear to match. The solid and dashed curves represent genuine densities, but the dashed curve does extend to the left of $x = 0$, which is again pronounced for $K = 2$.

The exact p -quantile $m_{K,p}$ of M_K is defined by

$$p = P(M_K \leq m_{K,p}) = \left[1 - \exp\left(-\frac{m_{K,p}^2}{2\tau^2}\right) \right]^K$$

which we solve for $m_{K,p}$ as

$$m_{K,p} = \tau \sqrt{-2 \log(1 - p^{1/K})}.$$

For $p \approx 1$ and thus $p^{1/K}$ even closer to 1 we have from $-\log(1 - x) \approx x$ for small x as excellent approximation

$$1 - p^{1/K} \approx -\log\left(1 - [1 - p^{1/K}]\right) = -\log\left(p^{1/K}\right) = -\frac{\log p}{K}$$

and thus

$$m_{K,p} \approx \tau \sqrt{-2 \log[-\log(p)] + 2 \log(K)}. \quad (4)$$

This approximation is good for any $K \geq 2$, provided $p \approx 1$. For large K it is valid for all $p \in (0, 1)$, as long as $p^{1/K}$ is reasonably close to 1. Note that for any $p > 0$ we have $p^{1/K} \approx 1$ provided K is large enough.

Figure 3: Distribution of M_K for $\sigma_1 = \sigma_2 = .01$

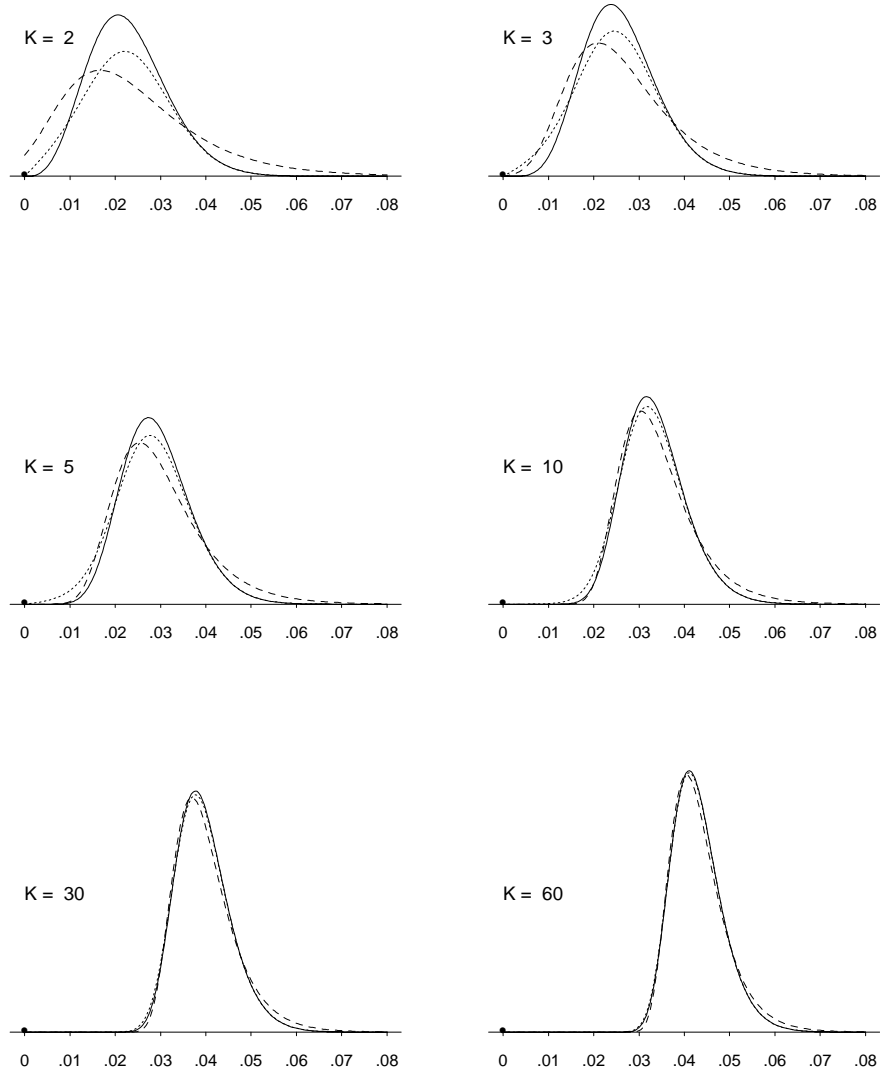
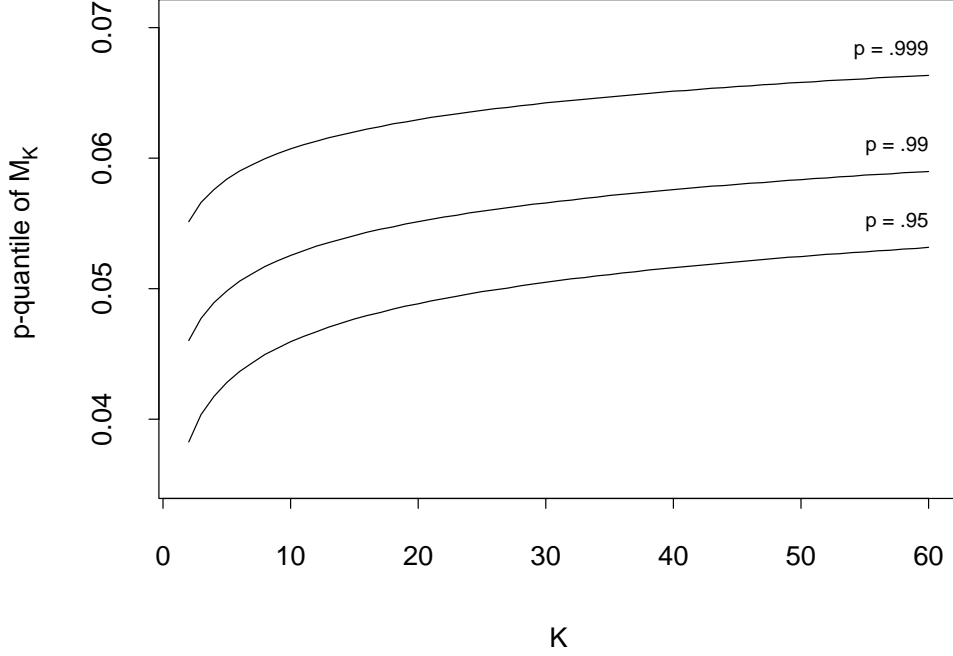


Figure 4: Growth of $m_{K,p}$ with Respect to K when $\sigma_1 = \sigma_2 = .01$



The exact and approximate quantile representations clearly show the dependence on the hole centering precision parameter τ . It simply scales the distribution of M_K , i.e., if τ increases by a factor κ , then the distribution of M_K will spread out to the right from zero by that factor κ . Also note the slow increase of $m_{K,p}$ with respect to K , namely through $\log(K)$ under the square root. See Figure 4 for a graphical illustration of this slow growth effect.

Concerning the spread of the distribution of M_K we can look at the difference of two of its quantiles. Let $0 < p < q < 1$ and denoting $A = -2\log[-\log(q)] > -2\log[-\log(p)] = B$ we have

$$\begin{aligned}
 m_{K,q} - m_{K,p} &\approx \tau\sqrt{A + 2\log(K)} - \tau\sqrt{B + 2\log(K)} \\
 &= \tau \frac{A + 2\log(K) - [B + 2\log(K)]}{\sqrt{A + 2\log(K)} + \sqrt{B + 2\log(K)}} = \frac{\tau(A - B)}{\sqrt{A + 2\log(K)} + \sqrt{B + 2\log(K)}}
 \end{aligned}$$

which slowly decreases to zero at the rate of $1/\sqrt{\log(K)}$ as $K \rightarrow \infty$.

2.4 Clearance Tolerance Stack Criterion and Fallout Rate

The corresponding exact formula and approximation for the p -quantile of the minimum clearance diameter $C_{K,\min}$ derives from the above relations as follows.

$$p = P(C_{K,\min} \leq c_{K,\min,p}) = 1 - P(M_K \leq d - c_{K,\min,p})$$

$$\implies 1 - p = P(M_K \leq d - c_{K,\min,p}) = P(M_K \leq m_{K,1-p})$$

i.e.,

$$\implies c_{K,\min,p} = d - m_{K,1-p} = d - \tau \sqrt{-2 \log [1 - (1 - p)^{1/K}]} \quad (5)$$

$$\approx d - \tau \sqrt{-2 \log [-\log(1 - p)] + 2 \log(K)}$$

with the last approximation being excellent for small p for any $K \geq 2$.

When the pin diameter δ is less than the quantile $c_{K,\min,p}$ we have

$$P(C_{K,\min} > \delta) \geq P(C_{K,\min} > c_{K,\min,p}) = 1 - p$$

and we can conclude that the minimum clearance $C_{K,\min}$ over all K hole pairs is greater than the pin diameter δ for at least $100(1 - p)\%$ of the part assemblies to be pinned. The condition $\delta < c_{K,\min,p}$ translates to

$$d - \tau \sqrt{-2 \log [1 - (1 - p)^{1/K}]} > \delta$$

or

$$\tau \sqrt{-2 \log [1 - (1 - p)^{1/K}]} < d - \delta .$$

Using the approximation for small p this becomes

$$\tau \sqrt{-2 \log [-\log(1 - p)] + 2 \log(K)} < d - \delta , \quad (6)$$

where $d - \delta$ is the nominal margin between hole and pin diameter. If this is to be satisfied for 99.73% of all assemblies, which is in keeping with the traditional interpretation of end

tolerances ($T_e \sim 3\sigma_e$), we would choose $p = .0027$ in (6). Furthermore, according to (1) we should take

$$\tau = \sqrt{\sigma_1^2 + \sigma_2^2} = \frac{1}{3.439} \sqrt{T_1^2 + T_2^2},$$

where T_i is the radial hole centering tolerance for part i . Here the conversion $\sigma_i = T_i/3.439$ reflects our previous interpretation that 99.73% of all actual hole centers are within the circular zone with radius T_i around the respective i^{th} nominal hole center.

With this the clearance criterion (6) becomes

$$\frac{1}{3.439} \sqrt{T_1^2 + T_2^2} \sqrt{11.826 + 2 \log(K)} = \sqrt{T_1^2 + T_2^2} \sqrt{1 + 2 \log(K)/11.826} < d - \delta.$$

Conversely, one can ask for the rate p of assembly fallout (not all holes can be pinned) for a given nominal gap $d - \delta$. Since this rate is not necessarily near zero we should not use the approximation. Clearly we have $p = 1$ for $d < \delta$ and for $d \geq \delta$ we get

$$\begin{aligned} p &= P(C_{K,\min} < \delta) = P(d - M_K < \delta) = P(M_K > d - \delta) \\ &= 1 - \left[1 - \exp\left(-\frac{1}{2} \left[\frac{d - \delta}{\tau}\right]^2\right) \right]^K \\ &= 1 - \left[1 - \exp\left(-\frac{11.826(d - \delta)^2}{2(T_1^2 + T_2^2)}\right) \right]^K. \end{aligned}$$

The Rule 1 box summarizes the clearance tolerance stack criterion and the clearance fallout rate in terms of the radial tolerances for hole centering.

2.5 Clean-Out Tolerance Stack Criterion and Fallout Rate

Similarly one obtains the corresponding exact formula and approximation for the p -quantiles of the maximum clean-out diameter $B_{K,\max}$, namely

$$\begin{aligned} p &= P(B_{K,\max} \leq b_{K,\max,p}) \\ &= P(M_K \leq [b_{K,\max,p} - d]/2) = P(M_K \leq m_{K,p}). \end{aligned}$$

Thus one obtains $b_{K,\max,p} = d + 2m_{K,p}$ or, using the approximation for $p \approx 1$,

$$b_{K,\max,p} \approx d + 2\tau \sqrt{-2 \log[-\log(p)] + 2 \log(K)},$$

with the interpretation that 100 p % of such assemblies will have the clean-out diameter bounded from above by this quantile $b_{K,\max,p}$.

Rule 1

Clearance under True Position Alignment

Given 2 parts, each with a set of K nominally matched coordination holes (in any pattern), and given that these holes are centered with radial tolerance T_i on part i , $i = 1, 2$, then these two parts can be pinned successfully at all K coordination hole pairs with 99.73% assurance for such assembly if

$$d - \delta > \sqrt{T_1^2 + T_2^2} \sqrt{1 + \frac{2 \log(K)}{11.826}} .$$

Here d and δ are the common hole and pin diameters. If these themselves are toleranced one can conservatively work with the worst case dimensions of these with respect to the clearance issue, namely with tightest hole diameters and widest pin diameters (maximum material condition).

Conversely, for given $d - \delta \geq 0$ the assembly fallout rate p of insufficient clearance at some hole pair among the K pairs to be pinned is given by

$$p = 1 - \left[1 - \exp \left(-\frac{11.826(d - \delta)^2}{2(T_1^2 + T_2^2)} \right) \right]^K .$$

For $d - \delta < 0$ the assembly fallout rate obviously is $p = 1$ or 100%.

Assumptions: The hole centering variation is reasonably described by a circular bivariate normal distribution, centered on nominal hole centers (matching for both parts), and is independent from hole to hole (hole to hole variation). It is assumed that the radius T_i for the circular hole centering tolerance zones captures 99.73% of all drilled hole centers.

Furthermore, the parts are assumed to be aligned in true position. Although this latter alignment is not practical it is still not the best possible one for minimizing clearance problems.

When the diameter d_f of the full-sized holes, which are drilled for clean-out purposes, is at least as large as the quantile $b_{K,\max,p}$ we have

$$p = P(B_{K,\max} \leq b_{K,\max,p}) \leq P(B_{K,\max} \leq d_f) .$$

Under that condition we can conclude that the full-sized hole diameter d_f will clean out all K coordination hole pairs for at least $100p\%$ of the part assemblies.

If this is again to happen for 99.73% of all assemblies, we would take $p = .9973$ in the formula above and for τ we take the same value as before. Hence

$$b_{K,\max,.9973} \approx d + \frac{2}{3.439} \sqrt{T_1^2 + T_2^2} \sqrt{-2 \log[-\log(.9973)] + 2 \log(K)} < d_f$$

or

$$\sqrt{T_1^2 + T_2^2} \sqrt{1 + [2 \log(K)]/11.826} < (d_f - d)/2 .$$

For the other formulation of clean-out diameter this would yield

$$p = P(B'_{K,\max} \leq b'_{K,\max,p}) = P(M_K \leq b'_{K,\max,p} - d) = P(M_K \leq m_{K,p})$$

so that $b'_{K,\max,p} = d + m_{K,p}$ or, using the approximation for $p \approx 1$,

$$b'_{K,\max,p} \approx d + \tau \sqrt{-2 \log[-\log(p)] + 2 \log(K)} ,$$

with the interpretation that $100p\%$ of such assemblies will have the maximal clean-out diameter $B'_{K,\max}$ bounded from above by this quantile $b'_{K,\max,p}$. The considerations for full-sized hole drilling parallel those from before, leading now to the more relaxed requirement

$$\sqrt{T_1^2 + T_2^2} \sqrt{1 + [2 \log(K)]/11.826} < d_f - d .$$

Conversely, for given $d_f - d \geq 0$, one may ask for the rate p of fallout, i.e., for the proportion of assemblies with clean-out problems. In the context of the first clean-out centering, leading to $B_{K,\max}$, one obtains

$$\begin{aligned} p &= P(B_{K,\max} > d_f) = 1 - P(B_{K,\max} \leq d_f) = 1 - P(M_K \leq [d_f - d]/2) \\ &= 1 - \left[1 - \exp \left(-\frac{1}{2} \left[\frac{(d_f - d)/2}{\tau} \right]^2 \right) \right]^K \\ &= 1 - \left[1 - \exp \left(-\frac{11.826 [(d_f - d)/2]^2}{2(T_1^2 + T_2^2)} \right) \right]^K \end{aligned}$$

When dealing with the other clean-out formulation, leading to $B'_{K,\max}$, the fallout rate is calculated in the same manner, but replacing $(d_f - d)/2$ by $d_f - d$ in the above formula.

With respect to clean-out issues the Rule 2 box summarizes the tolerance stack criterion and the assembly fallout rate in terms of the radial tolerances for hole centering.

3 Alignment Using Primary and Secondary Hole Pairs

Here we consider an alignment process that comes close to common practice. The two parts are aligned by pinning two pairs of coordination holes. The pairs to be pinned are chosen so that they are maximally apart. Simulations reported in [1] appear to show that this choice of hole pairs is best among all other choices of hole pairs, both in terms of minimizing part misalignment and in terms of reducing hole clearance and clean-out problems.

In the alignment considered here the first of the two hole pairs, called the primary hole pair, is pinned perfectly, i.e., the centers of the holes in this pair match, either by employing an expanding temporary fastener or by using a tightly toleranced hole/fastener combination. The other and secondary hole pair is aligned by the necessary rotation around the pinned primary hole pair and by pushing a temporary, expanding fastener through the secondary hole pair and expanding that fastener so that the hole centers of all four involved holes are collinear when projected onto the plane perpendicular to the hole center axes. For this to be possible it is assumed that the parts have the required freedom to move or rotate relative to each other. Of course it is possible that the hole center variations are so extreme that there is insufficient clearance at the secondary hole pair to get the fastener through. Whether pinning of the secondary hole pair is possible or not, for purposes of analysis it is assumed that after alignment the primary hole centers match and that they are collinear with the pair of secondary hole centers, i.e., the secondary hole centers are as close as possible to each other given the constraint of matching the primary hole centers.

After this alignment the clearance at the primary hole pair is obviously maximal and at the secondary hole pair it is somewhat reduced. For the intermediate hole pairs the clearances are presumably negatively impacted, because the nominal centers for all these hole pairs are now misaligned. Since the actual hole centers are aimed at the nominal centers, it is likely that the maximal hole center discrepancy over these $K - 2$ intermediate paired hole centers is somewhat increased over what it would be under true position alignment. To a small extent this may be offset by the “better” than true position alignment at the primary hole pair. The net effect on the maximal hole center distance over all K hole pairs is not obvious. We denote the maximum of the distances between the K hole center pairs after the primary/secondary hole pair alignment by \tilde{M}_K .

Rule 2

Clean-Out under True Position Alignment

Given 2 parts, each with a set of K nominally matched coordination holes (in any pattern), and given that these holes are centered with radial tolerance T_i on part i , $i = 1, 2$, then the respective pairs of coordination holes on these two parts can be cleaned out successfully at all K locations with 99.73% assurance if

$$(d_f - d)/2 > \sqrt{T_1^2 + T_2^2} \sqrt{1 + \frac{2 \log(K)}{11.826}}.$$

Here d_f and d are the common diameters of the full-sized (clean-out) holes and coordination holes, respectively. If these themselves are toleranced one can conservatively work with the worst case dimensions of these as far as clean-out is concerned, namely with the minimum value for d_f and the maximum value for d .

Conversely, for given $d_f - d \geq 0$ one determines the fallout rate p of an excessive clean-out diameter requirement at some hole pair among the K pairs to be cleaned out as

$$p = 1 - \left[1 - \exp \left(- \frac{11.826 [(d_f - d)/2]^2}{2(T_1^2 + T_2^2)} \right) \right]^K.$$

If $d_f - d < 0$ the fallout rate is $p = 1$ or 100%.

Assumptions: The hole centering variation is reasonably described by a circular bivariate normal distribution, centered on nominal hole centers (matching for both parts), and is independent from hole to hole (hole to hole variation). It is assumed that the radius T_i for the circular hole centering tolerance zones captures 99.73% of all drilled hole centers.

The parts are assumed to be aligned in true position. Although this latter alignment is not practical it is still not the best possible one for minimizing clean-out problems.

The clean-out holes are assumed to be centered on one of the respective coordination hole centers. If the clean-out holes are centered midway between the two respective coordination hole centers, i.e., centered on the clearance gaps, we can replace $(d_f - d)/2$ by the more relaxed $d_f - d$ in the two formulas above.

Caveat: See the discussion on page 4 concerning the possibly not quite conservative nature of this rule, which is based on true position alignment.

3.1 Maximum Hole Center Distance

An analytical investigation of these alignment effects on \tilde{M}_K proved intractable and it was decided to attack this problem via extensive simulations. Two sets of simulations were investigated, one with nominal hole centers equally spaced along a straight line and the other with nominal hole centers equally spaced along the perimeter of a square including the corners. These simulations show that the high quantiles of the \tilde{M}_K distribution are significantly higher under this two hole pair alignment when compared to the corresponding quantiles of M_K under true position alignment.

Previously it was argued that even true position alignment was not the best possible one, and now it seems that this two hole pair alignment, which comes closer to assembly reality, may give away even more. This means that tighter hole centering tolerances are needed in order to allow for the variation effects in this alignment process.

In the simulations we assume a common σ for hole centering accuracy on either part. However, the results can also be used when the hole centering accuracy is different for the two parts to be pinned, i.e., are characterized by standard deviations σ_1 and σ_2 for parts 1 and 2, respectively. In that case one simply interprets $\sigma = \sqrt{(\sigma_1^2 + \sigma_2^2)/2} = \tau/\sqrt{2}$ as the “common” σ . The justification for this is given at the end of Appendix B. There it is also demonstrated that the distribution of \tilde{M}_K/σ , aside from the linear or square pattern of equally spaced nominal hole centers, depends only on K and not on σ . This distributional independence from σ holds, provided σ is small compared to the hole to hole spacings, which certainly is not a restrictive limitation. By simulating the distribution of the normalized ratio \tilde{M}_K/σ we get direct access (by simple scaling) to the distribution of \tilde{M}_K for any reasonable σ .

The first set of simulations assumes that the nominal hole centers are equally spaced along a line. For each $K \in \{2, 3, \dots, 10, 12, 14, 16, 20, 25, 30, 40, 50, 60\}$ a set of 50,000 simulations was run. This means that for each run the hole center variations at all K hole center pairs were independently simulated, i.e., the X and Y deviations from nominal at each hole center were independently generated from a normal distribution with mean zero and standard deviation σ . The resulting value of \tilde{M}_K/σ was calculated and this process was then repeated independently 50,000 times for each K .

The second set of simulations assumes that the nominal hole centers are equally spaced along the perimeter of a square with points at the corners. This means that K must be a multiple of 4. Two diagonally opposing corner points were used as primary and secondary points for alignment. Again \tilde{M}_K denotes the maximum of the K distances between respective hole center pairs after the above primary/secondary hole pair alignment. The distribution of the normalized \tilde{M}_K/σ , depending only on K for $K \in \{4, 8, 12, 16, 20, 24\}$, was obtained

by running 50,000 simulations for each K .

For each K the 50,000 simulated values of \tilde{M}_K/σ (for the linear as well as the square hole center patterns) were sorted in increasing order. The resulting ordered values can be viewed as the 50,000 sample p_i -quantiles $\hat{m}_{K,p_i}/\sigma$, for $p_i = i/50,001$, $i = 1, \dots, 50,000$. These normalized sample quantiles, for p_i not too close to zero or one, can be viewed as good estimates of the actual p -quantiles $\tilde{m}_{K,p}/\sigma$ of \tilde{M}_K/σ . Here $\tilde{m}_{K,p}$ is defined by the property

$$P(\tilde{M}_K \leq \tilde{m}_{K,p}) = p.$$

These normalized sample quantiles, $\hat{m}_{K,p_i}/\sigma \approx \tilde{m}_{K,p_i}/\sigma$, were compared against the corresponding quantiles

$$m_{K,p_i}/\sigma = 2\sqrt{-\log(1 - p_i^{1/K})}$$

of the M_K/σ distribution. Recall that M_K is the maximal hole center distance under true position alignment and its distribution does not depend on the pattern of nominal hole centers. For the respective values of K the plots of $\hat{m}_{K,p_i}/\sigma \approx \tilde{m}_{K,p_i}/\sigma$ against $m_{K,p_i}/\sigma$ for $i = 1, \dots, 50,000$ are shown in Figures 5-7 for the linear and square hole center patterns.

For linear hole patterns and $K \geq 3$ the plots look consistently quite linear for $p_i \geq .001$ and for $K = 2$ linearity sets in for $p_i \geq .3$. In the linear pattern case the respective quantiles are indicated by the dashed horizontal lines.

For square hole patterns the linearity is strong for $p_i \geq .50$, i.e., between the .50- and .99-quantiles. In the square pattern case these segments are marked by the +’s. The more pronounced scatter of the very extreme upper points is quite natural and should not be construed as evidence against the continuation of that linear behavior.

In the linear pattern case least squares lines (dashed) were fitted to the upper 70% (for $K = 2$) and 99.9% (for $K \geq 3$) of the points. In the square pattern case least squares lines (dashed) were fitted to the upper 50% of the points. The solid lines represent the main diagonals where $\tilde{m}_{K,p}/\sigma = m_{K,p}/\sigma$. These diagonals are shown to give a perspective to the actual difference between $\tilde{m}_{K,p}/\sigma$ and $m_{K,p}/\sigma$. The intercept and slope coefficients (α_K, β_K) of the fitted least squares lines were plotted against K in Figure 8 and smoothed (for $K > 2$) using a smoothing spline. The smoothed values are presented in Table 1 for the K values for which simulations were run, while interpolated values were saved for use in a spreadsheet tool. Note that although the table values were generated assuming a common σ for hole centering accuracy on both parts, they can also be used when we deal with differing accuracies represented by σ_1 and σ_2 , simply by taking $\sigma = \sqrt{(\sigma_1^2 + \sigma_2^2)}/2 = \tau/\sqrt{2}$.

Figure 5: Quantile Comparison of Primary/Secondary Hole versus True Position Alignment
 $\tilde{m}_{K,p}/\sigma$ versus $m_{K,p}/\sigma$ for Linear Patterns

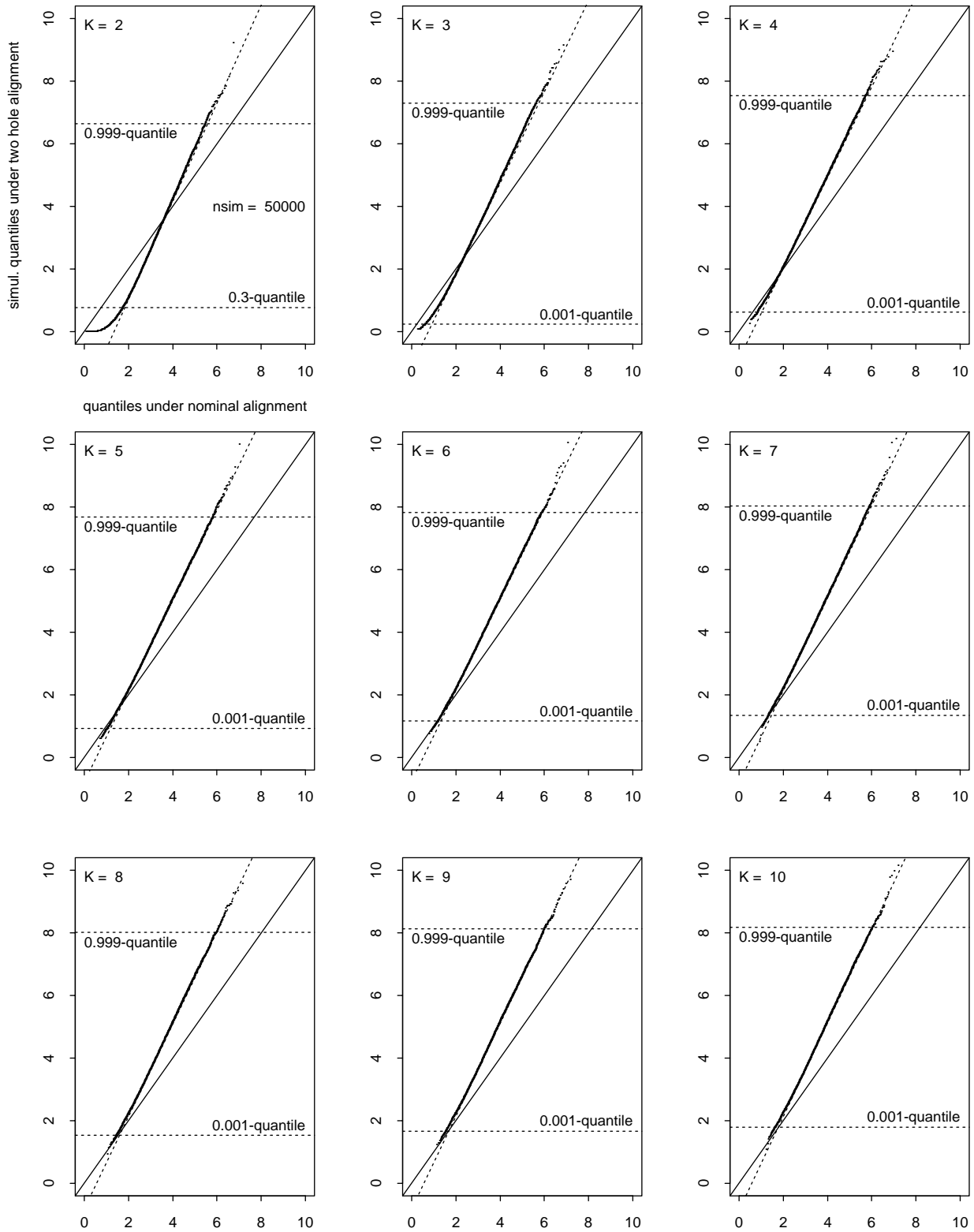


Figure 6: Quantile Comparison of Primary/Secondary Hole versus True Position Alignment
 $\tilde{m}_{K,p}/\sigma$ versus $m_{K,p}/\sigma$ for Linear Patterns

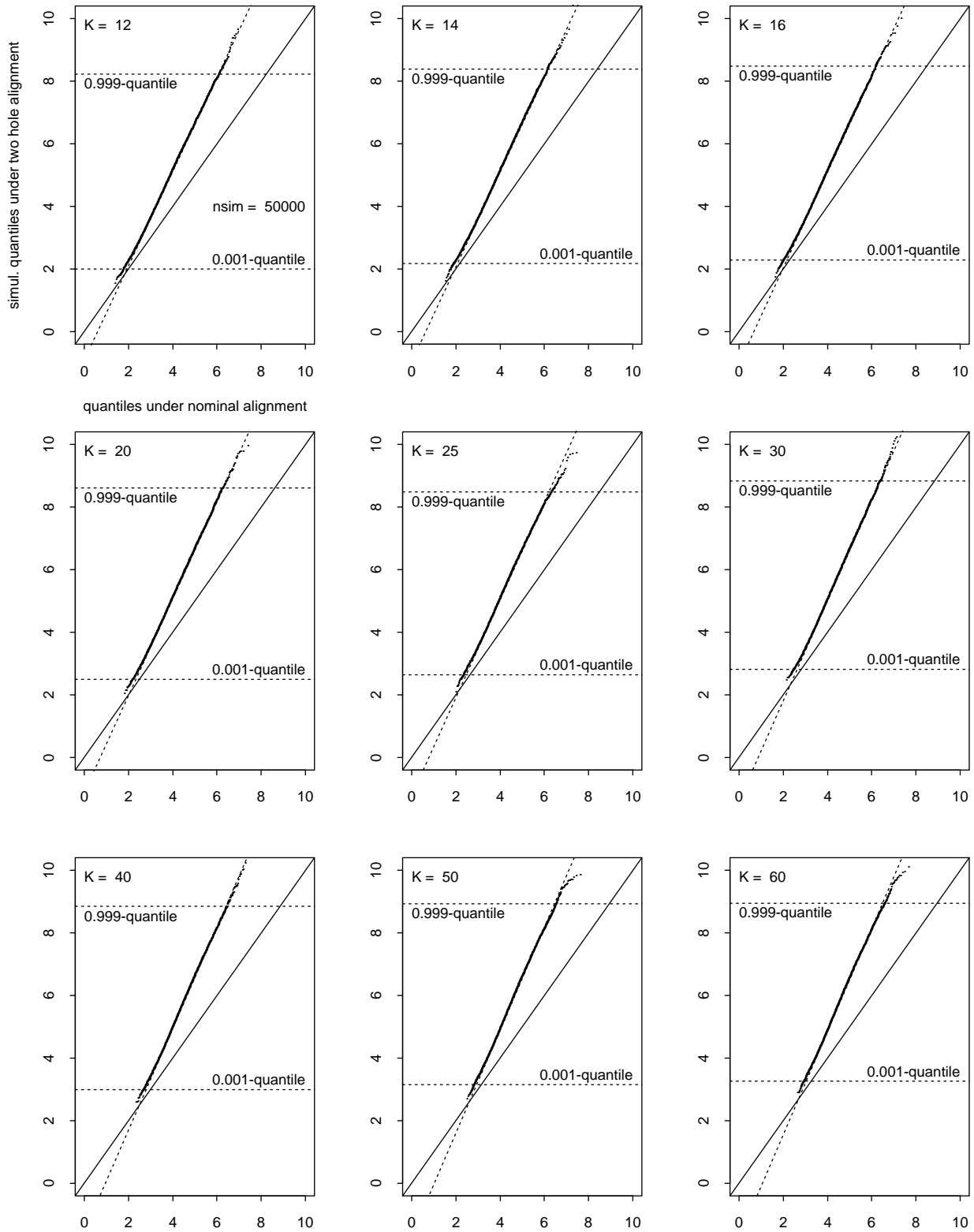


Figure 7: Quantile Comparison of Primary/Secondary Hole versus True Position Alignment
 $\tilde{m}_{K,p}/\sigma$ versus $m_{K,p}/\sigma$ for Square Patterns

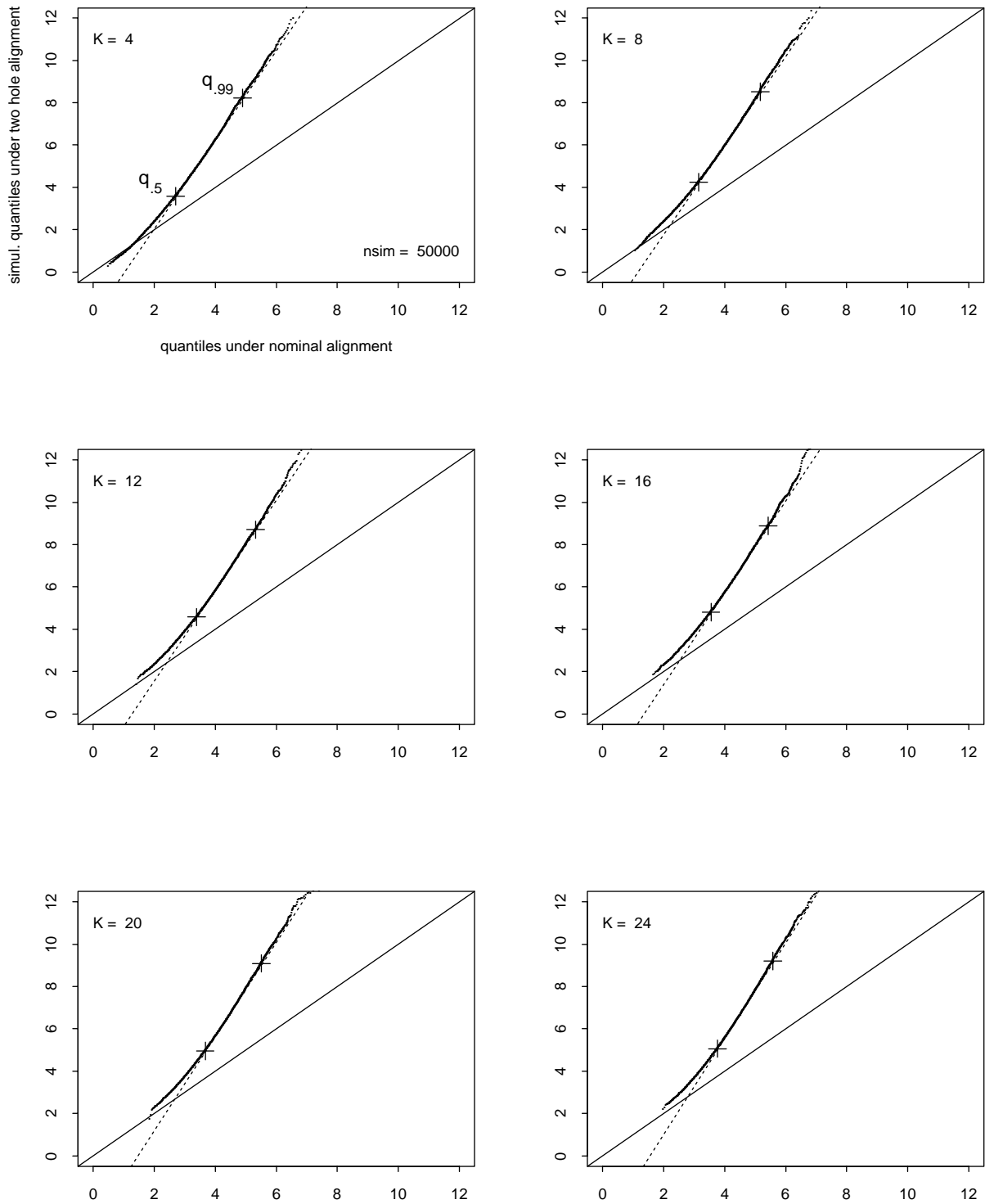


Figure 8: Smoothing Splines for Intercepts and Slopes

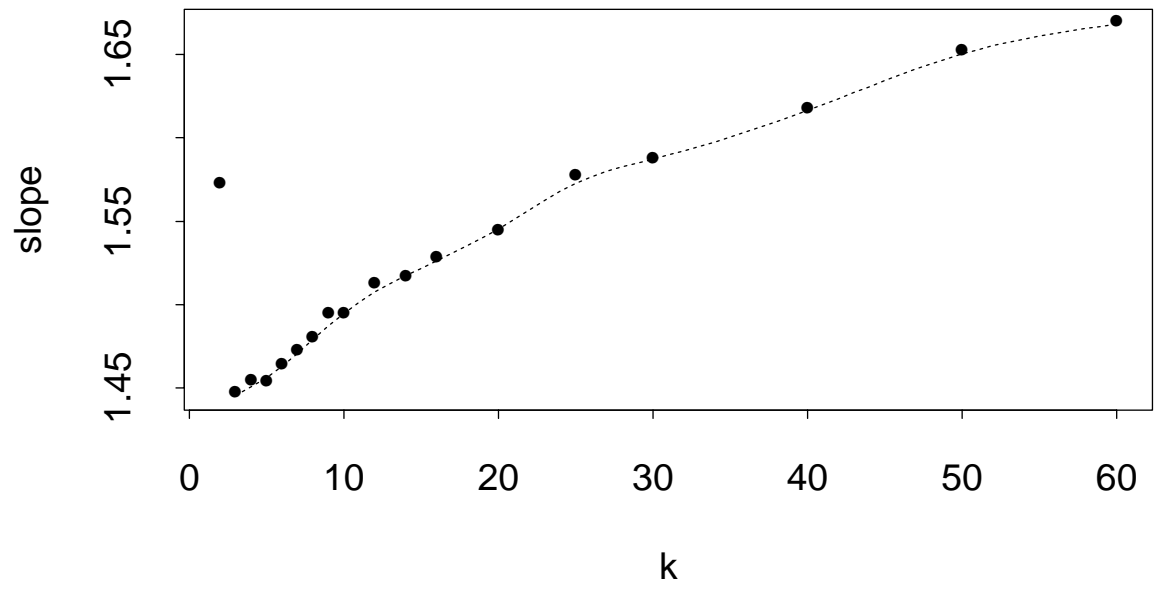
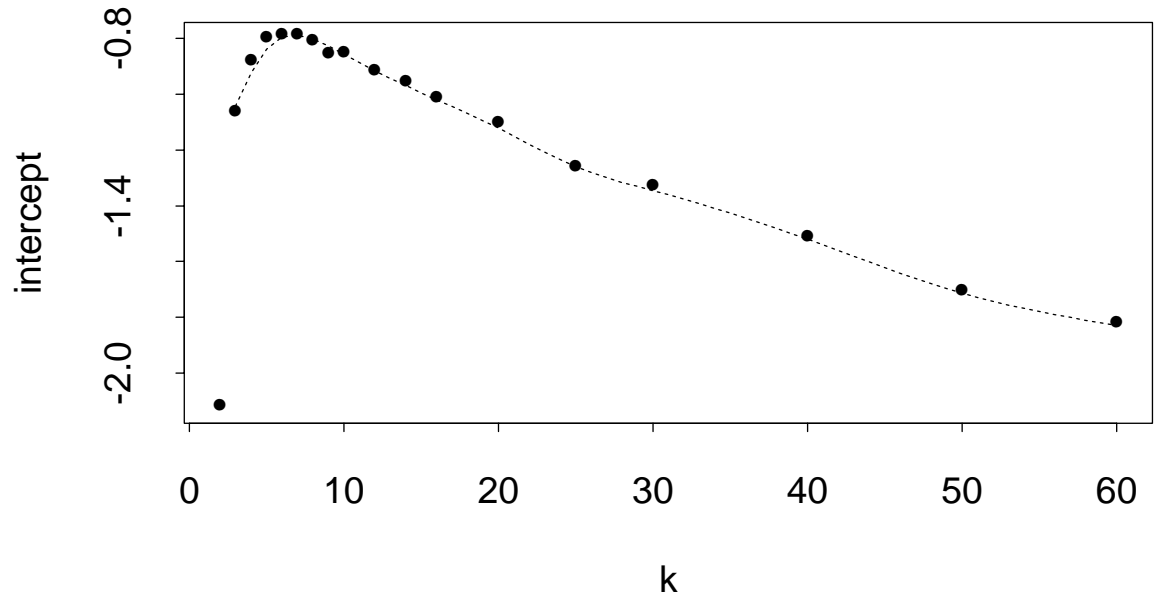


Table 1: Coefficients for Linear Quantile Relationships

$$\tilde{m}_{K,p}/\sigma = \alpha_K + \beta_K m_{K,p}/\sigma \quad \text{or} \quad \tilde{m}_{K,p} = \alpha_K \sigma + \beta_K m_{K,p}$$

linear patterns for nominal hole centers								
valid for $p \geq .3$ at $K = 2$ & $p \geq .001$ for $K \geq 3$								
K	α_K	β_K	K	α_K	β_K	K	α_K	β_K
2	-2.127	1.571	8	-0.802	1.479	20	-1.122	1.545
3	-1.043	1.446	9	-0.828	1.487	25	-1.260	1.573
4	-0.923	1.451	10	-0.857	1.495	30	-1.346	1.587
5	-0.838	1.456	12	-0.916	1.508	40	-1.520	1.616
6	-0.796	1.463	14	-0.969	1.517	50	-1.713	1.650
7	-0.788	1.471	16	-1.020	1.526	60	-1.830	1.668

square patterns for nominal hole centers								
valid for $p \geq .5$								
K	α_K	β_K	K	α_K	β_K	K	α_K	β_K
4	-2.198	2.107	12	-2.744	2.139	20	-3.300	2.229
8	-2.469	2.108	16	-2.975	2.171	24	-3.545	2.267

A plot with all the fitted least squares lines superimposed is given in Figure 9, with $K = 2$ represented by the lowest dotted line for the linear patterns and with $K = 4$ represented by the highest dashed line for the square patterns. For each hole center geometry (linear or square) there is remarkably little difference in these lines for $K > 2$. That the relation between $\hat{m}_{K,p} \approx \tilde{m}_{K,p}$ and $m_{K,p}$ is so strongly linear is fortuitous. It begs for a true analytical explanation, especially since the type of geometric hole centering pattern (linear or square) still seems to have a strong impact on the coefficients of the linear relationships. On intuitive grounds one might suspect that this linear relationship results in some average way from the tiltings underlying the primary/secondary hole alignment scheme.

Seeing no reasonably easy path to such an explanation we chose instead to borrow the exact analytical expression for $m_{K,p}$ and, building on the empirically observed linearity, obtained a simple formula for $\tilde{m}_{K,p}$ as well, namely for $K = 2$ & $p \geq .30$ and $K \geq 3$ & $p \geq .001$ ($p \geq .50$ in the square hole pattern case)

$$\begin{aligned} \tilde{m}_{K,p} &\approx \alpha_K \sigma + \beta_K m_{K,p} = \frac{\tau}{\sqrt{2}} \left[\alpha_K + 2\beta_K \sqrt{-\log(1 - p^{1/K})} \right] \\ &\approx \frac{\tau}{\sqrt{2}} \left[\alpha_K + 2\beta_K \sqrt{-\log[-\log(p)] + \log(K)} \right], \end{aligned} \quad (7)$$

where the last approximation is reasonable only for $p \approx 1$.

It is clear that the upper quantiles of \tilde{m}_{K,p_i} are consistently and significantly higher than those of m_{K,p_i} . From Figure 10, which displays the percent increase in the .9973-quantile of \tilde{M}_K over the .9973-quantile of M_K , we see that this increase in the linear pattern case ranges mostly from 25% to 35%. Only for $K = 2$ is this increase as low as 15%. For the square pattern case the increase is more pronounced at 65%.

Since σ , which governs the hole centering accuracy, affects the maximal discrepancies between hole centers in a proportional fashion, one sees that relying on primary/secondary hole pair alignment in setting tolerance requirements on hole centering could easily result in 25-35% or 65% tighter tolerances than needed under true position alignment. This tightening of tolerances could be viewed as the tolerance contribution due to the assembly process, i.e., it is the cost of the practicality of primary/secondary hole pair alignment.

Figure 9: Linear Quantile Relationships for Upper Quantiles of $\tilde{m}_{K,p_i}/\sigma$ versus $m_{K,p_i}/\sigma$.

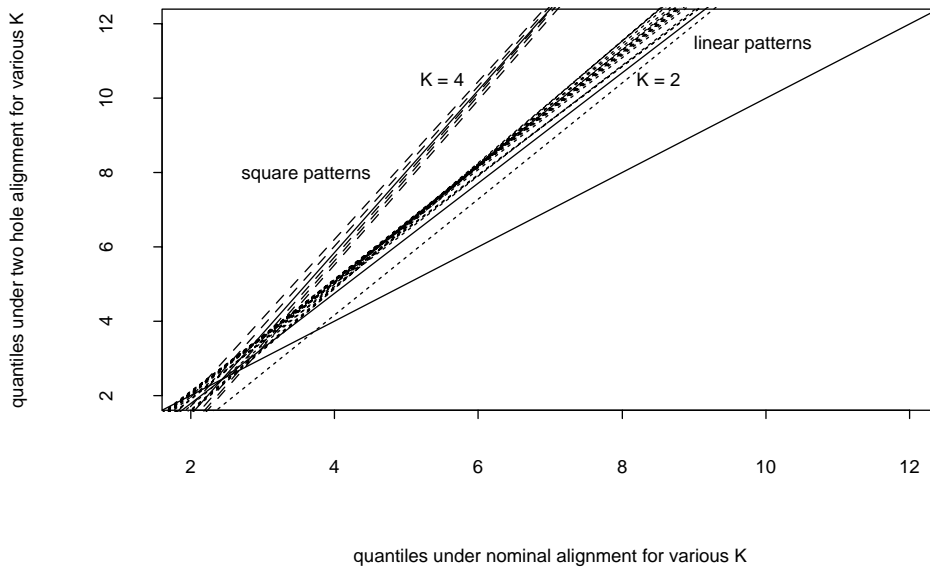
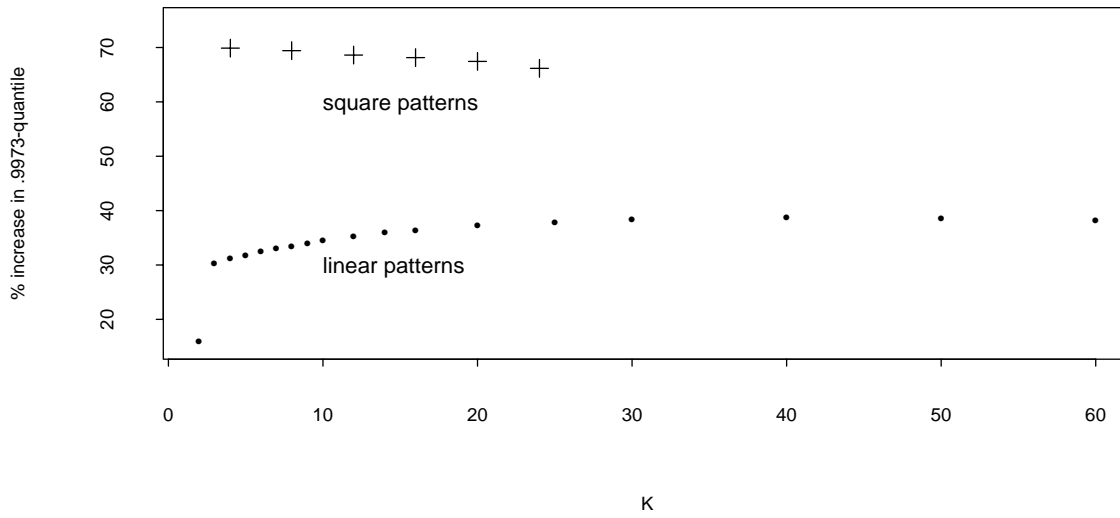


Figure 10: Percent Increase in $\tilde{m}_{K,.9973}$ over $m_{K,.9973}$.



3.2 Clearance Tolerance Stack and Fallout Rate

If $\tilde{C}_{K,\min}$ denotes the minimum clearance diameter over K hole pairs under the primary/secondary hole pair alignment one obtains from (7) as in (5) the following relationship for the p -quantile $\tilde{c}_{K,\min,p}$ of $\tilde{C}_{K,\min}$

$$\begin{aligned}\tilde{c}_{K,\min,p} = d - \tilde{m}_{K,1-p} &\approx d - \tau \left[\frac{\alpha_K}{\sqrt{2}} + \beta_K \sqrt{-2 \log(1 - [1 - p]^{1/K})} \right] \\ &\approx d - \tau \left[\frac{\alpha_K}{\sqrt{2}} + \beta_K \sqrt{-2 \log[-\log(1 - p)] + 2 \log(K)} \right],\end{aligned}$$

where the first approximation is good for $K = 2$ & $p \leq .70$ and $K \geq 3$ & $p \leq .999$ for linear hole patterns and for $p \leq .50$ for square hole patterns while the second approximation should only be used for $p \approx 0$ for either pattern.

When the pin diameter δ is less than the quantile $\tilde{c}_{K,\min,p}$ we have

$$P(\tilde{C}_{K,\min} > \delta) \geq P(\tilde{C}_{K,\min} > \tilde{c}_{K,\min,p}) = 1 - p.$$

In that case the minimum clearance $\tilde{C}_{K,\min}$ over all K hole pairs under the primary/secondary hole pair alignment is greater than the pin diameter δ for at least $100(1 - p)\%$ of the part assemblies to be pinned. The condition $\delta < \tilde{c}_{K,\min,p}$ translates to

$$\tau \left[\frac{\alpha_K}{\sqrt{2}} + \beta_K \sqrt{-2 \log(1 - [1 - p]^{1/K})} \right] < d - \delta. \quad (8)$$

Using the approximation for small p this becomes

$$\tau \left[\frac{\alpha_K}{\sqrt{2}} + \beta_K \sqrt{-2 \log[-\log(1 - p)] + 2 \log(K)} \right] < d - \delta. \quad (9)$$

To ensure successful pinning of 99.73% of all assemblies, we would choose $p = .0027$ in (8) or (9). With the same motivation as before we take

$$\tau = \sqrt{\sigma_1^2 + \sigma_2^2} = \frac{1}{3.439} \sqrt{T_1^2 + T_2^2},$$

which results in the following requirement on the nominal hole to pin clearance $d - \delta$

$$d - \delta > \sqrt{T_1^2 + T_2^2} \left(\frac{\alpha_K}{3.439\sqrt{2}} + \beta_K \sqrt{1 + \frac{2 \log(K)}{11.826}} \right).$$

Conversely, one can again ask for the assembly fallout rate p (not all holes can be pinned) for a given nominal gap $d - \delta$, i.e., we want

$$p = P(\tilde{C}_{K,\min} < \delta) = P(\tilde{M}_K > d - \delta) \quad \text{or} \quad P(\tilde{M}_K \leq d - \delta) = 1 - p. \quad (10)$$

By the definition of the quantile $\tilde{m}_{K,p}$ we have that equation (10) is satisfied whenever $\tilde{m}_{K,1-p} = d - \delta$. Since we have an accurate representation of $\tilde{m}_{K,1-p}$ for $K = 2$ & $p \leq .70$ and $K \geq 3$ & $p \leq .999$ (for $p \leq .50$ for square hole patterns), we can find p by solving this latter (approximate) equation, i.e.,

$$\begin{aligned} d - \delta &= \frac{\tau}{\sqrt{2}} \left[\alpha_K + 2\beta_K \sqrt{-\log(1 - [1 - p]^{1/K})} \right] \\ &= \frac{1}{3.439} \sqrt{T_1^2 + T_2^2} \left[\frac{\alpha_K}{\sqrt{2}} + \beta_K \sqrt{-2 \log(1 - [1 - p]^{1/K})} \right] \end{aligned}$$

for p . Solving this equation for p results in the following assembly fallout rate p for given nominal gap $d - \delta$

$$P(\tilde{C}_{K,\min} < \delta) = p = 1 - \left[1 - \exp \left(-\frac{1}{2} \left[\frac{3.439(d - \delta)}{\beta_K \sqrt{T_1^2 + T_2^2}} - \frac{\alpha_K}{\beta_K \sqrt{2}} \right]^2 \right) \right]^K.$$

For $K = 2$ & $p > .70$ and $K \geq 3$ & $p > .999$ ($p > .50$ for square hole patterns) the accuracy of this expression deteriorates somewhat. Obviously we should have $p = 1$ if $d - \delta \leq 0$ and for $d - \delta = 0$ the above formula reduces to

$$p = 1 - \left[1 - \exp \left(-\frac{1}{4} \left[\frac{\alpha_K}{\beta_K} \right]^2 \right) \right]^K,$$

which gives the values .865, .998 for $K = 2, 3$ in the linear hole pattern case and the values .997, .99995 for $K = 4, 8$ in the square hole pattern case.

The above derivations are summarized in the modified Rule 1a which gives the tolerance clearance requirement on the nominal clearance gap $d - \delta$ and the clearance fallout rate for given $d - \delta$ under primary/secondary hole pair alignment, both in terms of the radial tolerances for hole centering.

Rule 1a

Clearance under Primary/Secondary Hole Pair Alignment

Given 2 parts, each with a set of K nominally matched coordination holes (equally spaced in a linear or square pattern), and given that these holes are centered with radial tolerance T_i on part i , $i = 1, 2$, then these two parts can be pinned successfully at all coordination hole pairs with 99.73% assurance for such assembly if

$$d - \delta > \sqrt{T_1^2 + T_2^2} \left(\frac{\alpha_K}{3.439\sqrt{2}} + \beta_K \sqrt{1 + \frac{2 \log(K)}{11.826}} \right).$$

Here d and δ are the common hole and pin diameters. If these themselves are toleranced one can conservatively work with the worst case dimensions of these, i.e., with maximum material condition (tightest hole diameter and widest pin diameter). The values of α_K and β_K can be read from Table 1.

Conversely, for given $d - \delta > 0$ the assembly fallout rate p of insufficient clearance at some hole pair, among the K pairs to be pinned, is

$$p = 1 - \left[1 - \exp \left(-\frac{1}{2} \left\{ \frac{3.439(d - \delta)}{\beta_K \sqrt{T_1^2 + T_2^2}} - \frac{\alpha_K}{\beta_K \sqrt{2}} \right\}^2 \right) \right]^K.$$

This is reasonably accurate when $K = 2$ & $p \leq .70$ $K \geq 3$ & $p \leq .999$ ($p \leq .50$) for linear (quadratic) hole patterns but still useful otherwise. Of course for $d - \delta \leq 0$ the fallout rate is $p = 1$ or 100%.

Assumptions: The hole centering variation is reasonably described by a circular bivariate normal distribution, centered on nominal hole centers (matching for both parts), and is independent from hole to hole (hole to hole variation). It is assumed that the radius T_i for the circular hole centering tolerance zone captures 99.73% of all drilled hole centers.

The nominal coordination hole centers are equally spaced along a line or along the periphery of a square, including the corners.

Here it is assumed that the parts are aligned by the primary/secondary hole pair alignment process, i.e., perfect on the primary hole pair and by rotation best possible at the secondary hole pair. Among the K hole pairs the primary and secondary pairs are chosen to be as far apart as possible.

3.3 Cleanout Tolerance Stack Criterion and Fallout Rate

Similarly, Rule 2a is converted from Rule 2, i.e., gives clean-out requirements on $d_f - d$ and the clean-out fallout rate for given $d_f - d$ under primary/secondary hole pair alignment in terms of the radial tolerances for hole centering.

We note that the caveat at the bottom of Rule 2 is missing in Rule 2a. The reason for this is that under primary/secondary hole alignment it is assumed that the parts are fixed relative to each other while intermediate holes are match-drilled and riveted. It is assumed that this process does not disturb the alignment². This was not the case under true position alignment where this alignment was not achievable in practice and where pinning the coordination holes would definitely not leave the parts in true position alignment while match-drilling and riveting intermediate holes.

²This ignores possible expansion effects due to riveting.

Rule 2a

Clean-Out under Primary/Secondary Hole Pair Alignment

Given 2 parts, each with a set of K nominally matched coordination holes, and given that these holes are centered with radial tolerance T_i on part i , $i = 1, 2$, then the coordination holes on these two parts can be cleaned out successfully at all K locations with 99.73% assurance if

$$(d_f - d)/2 > \sqrt{T_1^2 + T_2^2} \left(\frac{\alpha_K}{3.439\sqrt{2}} + \beta_K \sqrt{1 + \frac{2 \log(K)}{11.826}} \right).$$

Here d_f and d are the common full-sized (clean-out) hole and coordination hole diameters, respectively. If these themselves are toleranced one can conservatively work with the worst case dimensions of these, i.e., with minimum value for d_f and maximum value for d . The values of α_K and β_K can be read from Table 1.

Conversely, for given $d_f - d$ one determines the fallout rate p of an excessive clean-out diameter at some hole pair among the K pairs to be cleaned out as

$$p = 1 - \left[1 - \exp \left(-\frac{1}{2} \left\{ \frac{3.439(d_f - d)/2}{\beta_K \sqrt{T_1^2 + T_2^2}} - \frac{\alpha_K}{\beta_K \sqrt{2}} \right\}^2 \right) \right]^K.$$

This is reasonably accurate when $K = 2$ & $p \leq .70$ and $K \geq 3$ & $p \leq .999$ ($p \leq .50$) for linear (quadratic) hole patterns but still useful otherwise. Of course for $d_f - d \leq 0$ the fallout rate is $p = 1$ or 100%.

Assumptions: The hole centering variation is reasonably described by a circular bivariate normal distribution, centered on nominal hole centers (matching for both parts), and is independent from hole to hole (hole to hole variation). It is assumed that the radius T_i for the circular hole centering tolerance zone captures 99.73% of all drilled hole centers.

The nominal coordination hole centers are equally spaced along a line or along the periphery of a square, including the corners.

Here it is assumed that the parts are aligned by the primary/secondary hole pair alignment process, i.e., perfect on the primary hole pair and by rotation best possible at the secondary hole pair. Among the K hole pairs the primary and secondary pairs are chosen to be as far apart as possible. The clean-out holes are assumed to be centered on one of the respective coordination hole centers. If the clean-out holes are centered midway between the two respective coordination hole centers, i.e., centered on the clearance gaps, we can replace $(d_f - d)/2$ by the more relaxed $d_f - d$ in the above two formulas.

4 Comparison with Worst Case Analysis

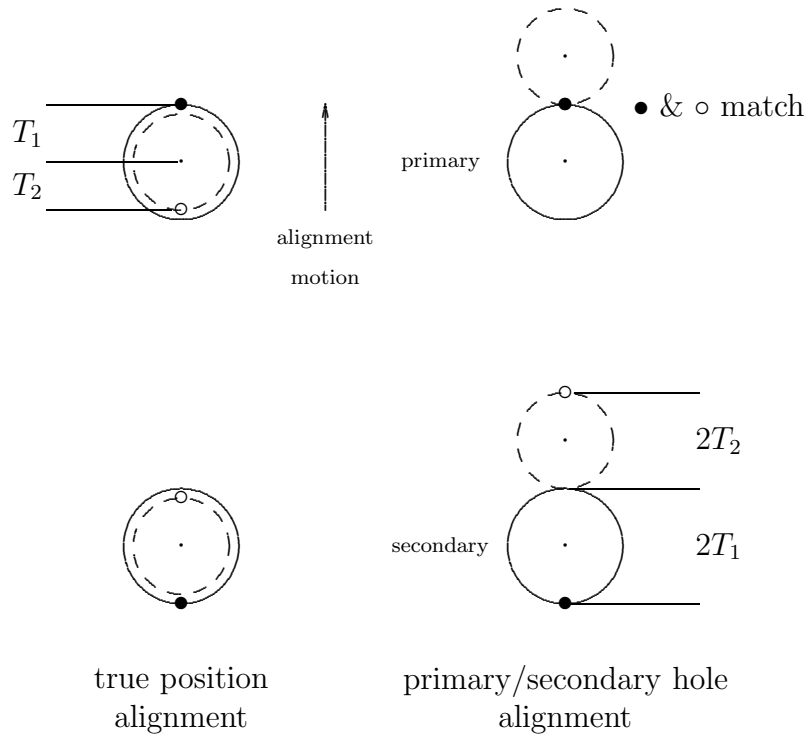
So far the clearance and clean-out problem was examined from a statistical point of view. This is contrasted here with the worst case tolerance stack analysis. For reasons of fair comparisons we will distinguish two types of worst case analyses. In the first we assume that the parts are aligned in nominal or true position and in the second we employ the same type of primary/secondary hole pair alignment considered previously.

We assume that the hole centers on part i are toleranced by circular zones with respective radii T_i , $i = 1, 2$. Such circular zones are shown in nominal alignment on the left side of Figure 11 for two hole pairs. The circles there do not represent the actual holes but the circular tolerance zones for the hole centers. These zones are centered on the nominal hole centers, indicated by \cdot 's, while the actual hole centers, chosen for illustration in worst case fashion, are indicated by \circ 's and \bullet 's. Both the circular zones and the respective distances between them are shown in exaggeratedly large and small dimensions for the purpose of compact illustration. Also for illustration the radii for the two circular zones are chosen to be different to be able to distinguish the two circles when aligned in true position. In nominal or true position alignment the farthest any two hole centers can be apart from each other is $T_1 + T_2$. The left side of Figure 11 shows that this is possible.

On the right side of Figure 11 we show a different alignment of the parts, namely by centering the actual hole centers of the primary hole pair on top of each other and leaving the actual hole centers of the secondary hole pair as close to each other as possible. This results in all four hole centers being collinear and the primary pair matching. This alignment of secondary and primary hole pairs results in a mismatch of $2T_1 + 2T_2$ between the pair of secondary hole centers. When pinning these two hole pairs one may become aware of this large mismatch and may want to trade some of that mismatch at the cost of undoing the perfect match at the top hole pair on the right side, i.e., if possible one would move back in the direction of the alignment shown on the left.

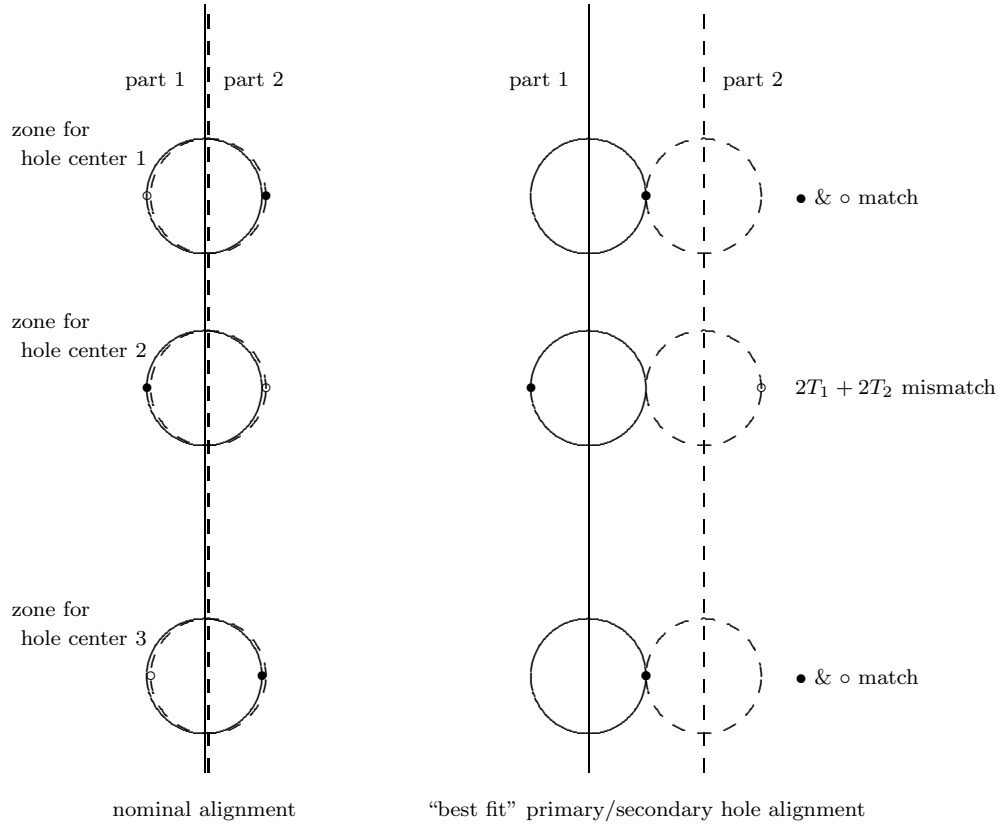
That this is not always so recognizable is shown in Figure 12, where on the left side three pairs of hole centering zones are shown with actual hole centers indicated by \bullet 's on part 1 and by \circ 's on part 2. The parts on the left are shown in nominal alignment with dashed and solid circular zones shown only slightly offset for clarity. Note that the \bullet and \circ are never more than $T_1 + T_2$ apart in this alignment. On the right side the same set of zones and actual hole centers is shown in the best possible alignment for primary and secondary hole centers, namely matching in both cases. However, the intermediate hole center pair now shows a $2T_1 + 2T_2$ mismatch. Without looking at these intermediate hole pairs this mismatch would not be discovered during the alignment of primary and secondary hole pairs.

Figure 11: Comparing True Position & Primary/Secondary Hole Alignment



In comparing statistical with worst case tolerance stacking methodology one should compare them under true position alignment and then again under primary/secondary two hole alignment. It turns out that while there is little gain in statistical tolerancing over worst case tolerancing under true position alignment, there is significant gain ($\approx 50\%$ reduction in end tolerance for maximum hole mismatch) of statistical over worst case tolerancing under the commonly used primary/secondary hole pair alignment.

Figure 12: Worst Case in “Best Fit” Primary/Secondary Hole Alignment



4.1 Comparison under True Position Alignment

Here the worst case mismatch between hole centers was shown to be $m_{wc,1} = T_1 + T_2$, regardless of the number of holes involved and the geometric pattern of the holes. Statistically we can bound the maximum mismatch between K pairs of hole centers, aligned in true position and without regard to geometric pattern, by $m_{K,.9973}$, which covers almost all (99.73%) assemblies. Note that

$$m_{K,.9973} \approx \tau \sqrt{-2 \log[-\log(.9973)] + 2 \log(K)} = \sqrt{T_1^2 + T_2^2} \sqrt{1 + \frac{2 \log(K)}{11.826}}$$

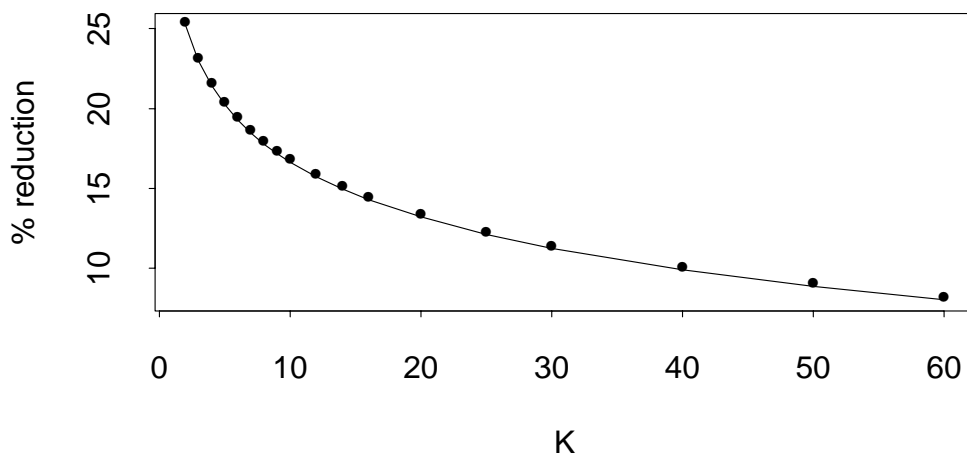
For easier comparison assume $T_1 = T_2 = T$. The percentage reduction of $m_{K,.9973}$ relative

to $m_{wc,1}$ is then

$$R_K = 100 \times \frac{m_{wc,1} - m_{K,.9973}}{m_{wc,1}} \%$$

This percent reduction, R_K , is plotted against K in Figure 13. The gain of statistical over worst case tolerancing, initially at 25% for $K = 2$ and dropping to 15% at $K = 14$, may not be sufficient justification for entering the complications of statistical tolerance stacking, at least under true position alignment and as far as clearance and clean-out issues are concerned. However, recall that true position alignment is not really a viable assembly option. It was used only as an intermediate step in a better understanding of the primary/secondary hole alignment scheme.

Figure 13: Percent Reduction in Maximum Hole Center Mismatch Statistical versus Worst Case Tolerance Stack under True Position Alignment



4.2 Comparison under Primary/Secondary Hole Alignment

Under the commonly used primary/secondary hole alignment it appeared from Figure 12 that the worst case hole center mismatch is $m_{wc,2} = 2(T_1 + T_2)$. Under the same alignment the maximum mismatch between K pairs of hole centers can be bounded statistically for

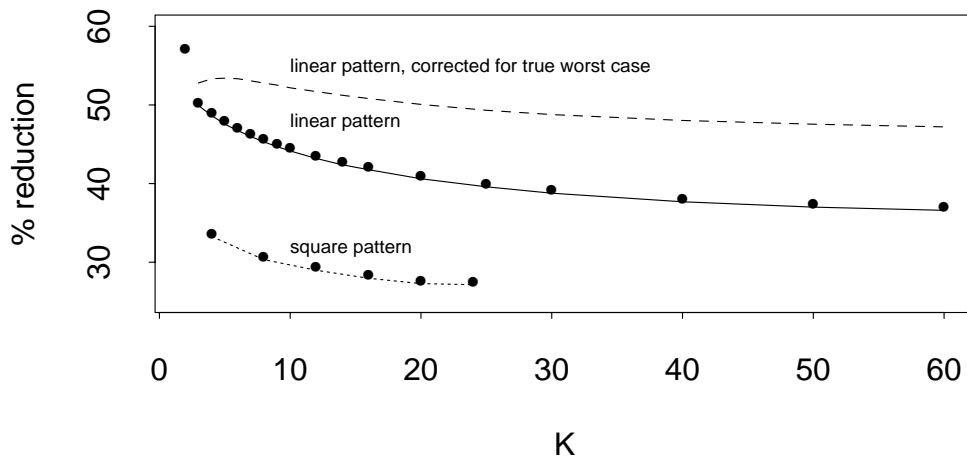
almost all (99.73%) assemblies by

$$\tilde{m}_{K,.9973} = \sqrt{T_1^2 + T_2^2} \left(\frac{\alpha_K}{3.439\sqrt{2}} + \beta_K \sqrt{1 + \frac{2 \log(K)}{11.826}} \right),$$

where the appropriate coefficients α_K and β_K are taken from Table 1. For easier comparison assume $T_1 = T_2 = T$. The percentage reduction of $\tilde{m}_{K,.9973}$ relative to $m_{wc,2}$ is

$$\tilde{R}_K = 100 \times \frac{m_{wc,2} - \tilde{m}_{K,.9973}}{m_{wc,2}} \%$$

Figure 14: Percent Reduction in Maximum Hole Center Mismatch Statistical versus Worst Case Tolerance Stack Primary/Secondary Hole Alignment, Linear and Square Patterns



This percent reduction, \tilde{R}_K , is plotted against K as the two bottom curves in Figure 14 for linear and square patterns, respectively. The top curve will be explained later. The percentage gain here is substantially higher than under true position alignment. The separate point for $K = 2$ under the linear pattern reflects the fact that the smoothing was done only

for the cases $K > 2$. This separate treatment for $K = 2$ seems justified on visual grounds but may also be explained by the fact that the alignment procedure affects clearance at both holes favorably when $K = 2$. However, as soon as $K > 2$ one has at least one hole that is most likely affected negatively by the alignment as far as clearance is concerned.

At the start of this subsection we stated that “it appeared . . . that the worst case hole center mismatch is $m_{wc,2} = 2(T_1 + T_2)$.” Although this appeared quite plausible at first glance, it turns out that this understates the worst case mismatch by about 6 – 20% for $K > 2$, at least for coordination holes in a linear and equally spaced pattern. This is explained in Appendix D. For the special case of a linear and equally spaced nominal hole center pattern with equal centering tolerances, i.e., $T_1 = T_2 = T$, it is argued there that the worst case separation of hole centers is

$$4T \times \frac{1}{2} \left(1 + \sqrt{1 + \left(\frac{K-2}{K-1} \right)^2} \right) = 4T \times \psi_K .$$

Note that the factor ψ_K , which modifies $4T$, is greater than 1 for $K > 2$. A plot of ψ_K against K is given in Figure 46 of Appendix D. The values of ψ_K rise quickly from $\psi_3 = 1.059$, $\psi_4 = 1.10$, to $\psi_{10} = 1.17$, and asymptote at $\psi_\infty = (1 + \sqrt{2})/2 \approx 1.21$.

When comparing statistical tolerancing with worst case analysis we should thus look at the following corrected percentage reduction

$$\begin{aligned} \hat{R}_K &= 100 \left[\frac{\psi_K m_{wc,2} - \tilde{m}_{K,.9973}}{\psi_K m_{wc,2}} \right] \% \\ &= 100 \left[\frac{m_{wc,2} - \tilde{m}_{K,.9973}}{m_{wc,2}} + \frac{\tilde{m}_{K,.9973}}{m_{wc,2}} \times \left(1 - \frac{1}{\psi_K} \right) \right] \% \\ &= \left[\tilde{R}_K + (100 - \tilde{R}_K) \times \left(1 - \frac{1}{\psi_K} \right) \right] \% . \end{aligned}$$

When before we had a percentage reduction of $\tilde{R}_{10} \approx 43\%$ for $K = 10$, we should, based on the true worst case and using $\psi_{10} = 1.17$, have computed a correct percentage reduction of

$$\hat{R}_{10} = [43 + (100 - 43) \times (1 - 1/1.17)] \% = 51.3\% .$$

This percentage reduction, adjusted to the true worst case, is shown as the curve at the top of Figure 14.

Since the primary/secondary alignment scheme comes close to general practice it appears that a significant gain over worst case stacking can be realized from statistical stacking.

5 Three Matched Holes

The development for two matched holes at each nominal location can be generalized to three holes at each such location. This situation arises for example when trying to pin three parts, such as two skin panels and a stringer along one common seam of coordination holes. Following the same strategy as for pinning two holes at each location we first focus on the case when the parts are aligned in true position and cover again the case of clearance and clean-out. After that we examine how this relates to primary/secondary hole triplet alignment, but limit this investigation to a linear and equally spaced pattern of nominal hole centers.

5.1 Clearance for Three Matched Holes, True Position Alignment

The necessary ingredients for finding clearance and clean-out diameters for a triplet of coordination holes, all aligned on the same nominal center or in true position alignment, can be found in [2]. For easy reference purposes the relevant parts are reproduced in Appendix C. The step of going from one such triplet to K of them is the same as before, invoking again statistical independence. Unfortunately, the statistical distribution of the clearance diameter for three overlapping holes in true position is not very tractable. However, reasonably clean approximations are feasible. For extreme clearance (small) and clean-out (large) diameters it is possible to offer a rationale for using the previous results for hole pairs also for triplets. This rationale is based on the following consideration. It seems that the extremes in question will, for the most part, occur when two of the three circles are too far apart, so that the presence of the third circle is irrelevant. What we are suggesting is that the probability of all three circles being active contributors to an extremely low clearance or extremely large clean-out is negligible.

In [2] (see also Appendix C) we saw that the clearance diameter at one hole triplet site is of the form $2r - U$, where $2r$ is the common hole diameter and U is a complicated function of the hole center distances $|\overline{P_1P_2}|$, $|\overline{P_1P_3}|$, $|\overline{P_2P_3}|$, assuming all three parts in true position alignment, i.e., aligned at the nominal $P = (\mu, \nu)$, while the actual hole centers are at P_i , $i = 1, 2, 3$. Of course this is viewed with all three holes as projected onto a common plane so that the three holes are represented as three circles, which usually overlap and define a largest circle with clearance diameter $2r - U$ that fits within the intersection of all three circles.

The above rationale suggests that for large U -values we essentially have

$$U \approx \max\{|\overline{P_1P_2}|, |\overline{P_1P_3}|, |\overline{P_2P_3}|\}.$$

For large x this leads to the following approximation for $P(U \leq x)$:

$$\begin{aligned}
P(U \leq x) &\approx P\left(|\overline{P_1 P_2}| \leq x, |\overline{P_1 P_3}| \leq x, |\overline{P_2 P_3}| \leq x\right) \\
&\approx P\left(|\overline{P_1 P_2}| \leq x\right) P\left(|\overline{P_1 P_3}| \leq x\right) P\left(|\overline{P_2 P_3}| \leq x\right) \\
&= \left[1 - \exp\left(-\frac{x^2}{2\tau_{12}^2}\right)\right] \left[1 - \exp\left(-\frac{x^2}{2\tau_{13}^2}\right)\right] \left[1 - \exp\left(-\frac{x^2}{2\tau_{23}^2}\right)\right] \\
&= \left[1 - \exp\left(-\frac{x^2}{2\tau^2}\right)\right]^3
\end{aligned}$$

with $\tau_{ij}^2 = \sigma_i^2 + \sigma_j^2$, and where in the last equality we assume that $\sigma_1 = \sigma_2 = \sigma_3 = \sigma$ for the three hole drilling processes, and thus $\tau = \tau_{12} = \tau_{13} = \tau_{23} = \sigma\sqrt{2}$. This latter simplification is not necessary, but makes the effect of dealing with hole triplets more transparent.

The above approximation for $P(U \leq x)$ (with the further simplification) yields the following approximation for the p -quantile U_p of U , namely:

$$U_p \approx \hat{U}_{1,p} = 2\sigma\sqrt{-\log[1 - p^{1/3}]}$$

As a second approximation, derived by trial and error from the first, we propose

$$U_p \approx \hat{U}_{2,p} = 2\sigma\sqrt{-\log[1 - p^{1/2.4}]},$$

which would be consistent with the following form for the approximate distribution function of U

$$P(U \leq x) \approx \left[1 - \exp\left(-\frac{x^2}{4\sigma^2}\right)\right]^{2.4}$$

To check the suggested approximations we simulated 50,000 such hole triplets (with $\sigma = .01$ and linear hole pattern with a gap of 20 between adjacent nominal hole centers) and observed the true U value each time. Figure 15 compares the sorted observed U -values, i.e., $U_{(1)} \leq \dots \leq U_{(n)}$, $n = 50,000$, against \hat{U}_{1,p_i} with $p_i = i/(n+1)$, $i = 1, \dots, n$. The straight line represents the main diagonal. The few stragglers at the high end should not be viewed as significant deviation from the main diagonal. They are to be expected as part of normal statistical variation. It is quite evident that the suggested approximation is very good for high p -quantiles of U , say for $p \geq .95$, but then tends to deteriorate mildly for the lower values of p . The second approximation $\hat{U}_{2,p}$, shown in Figure 16, is reasonably good over the

Figure 15: Approximation Quality for High U -Quantiles

Based on $\hat{U}_{1,p} = 2\sigma\sqrt{-\log[1 - p^{1/3}]}$, $\sigma = .01$

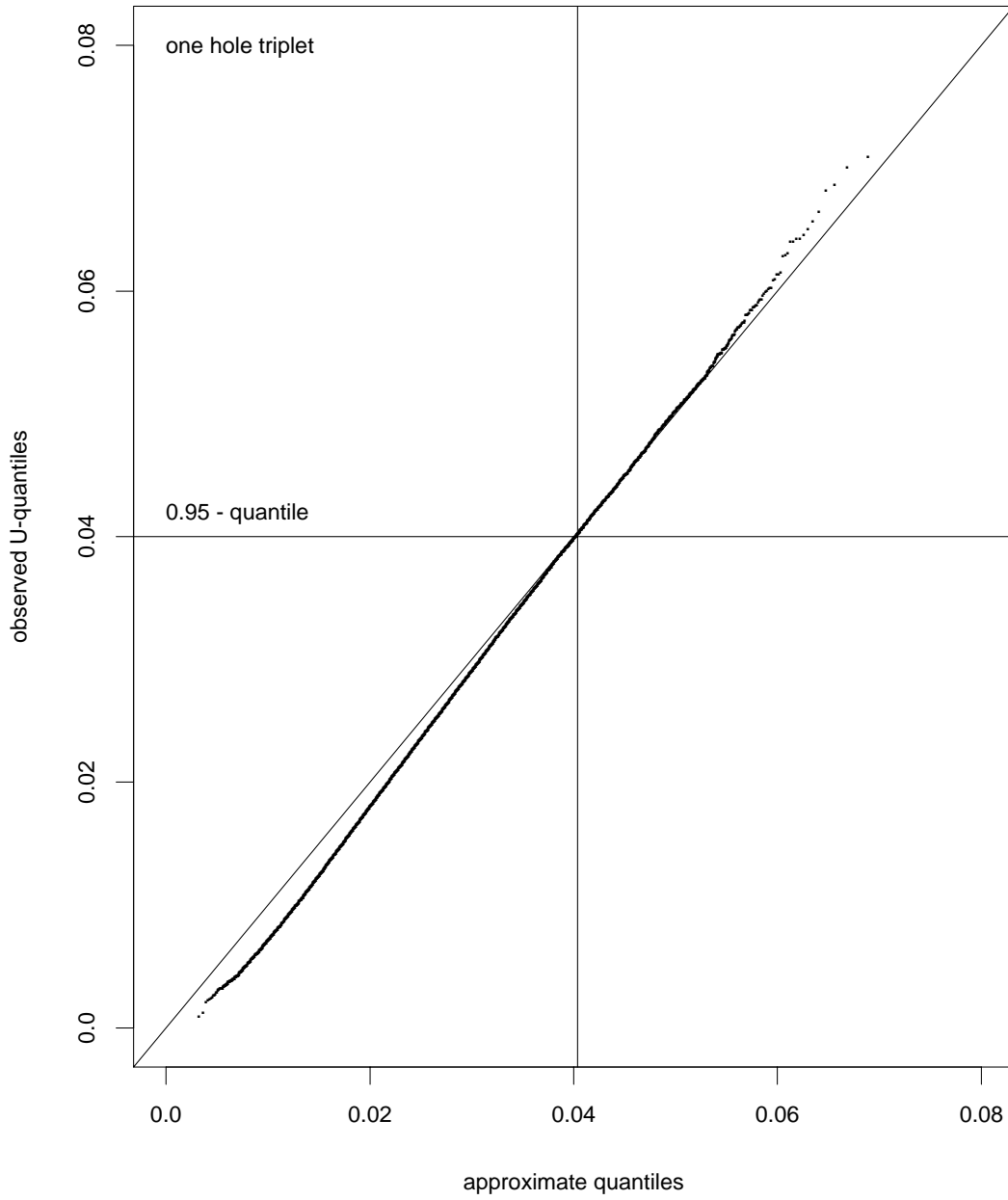
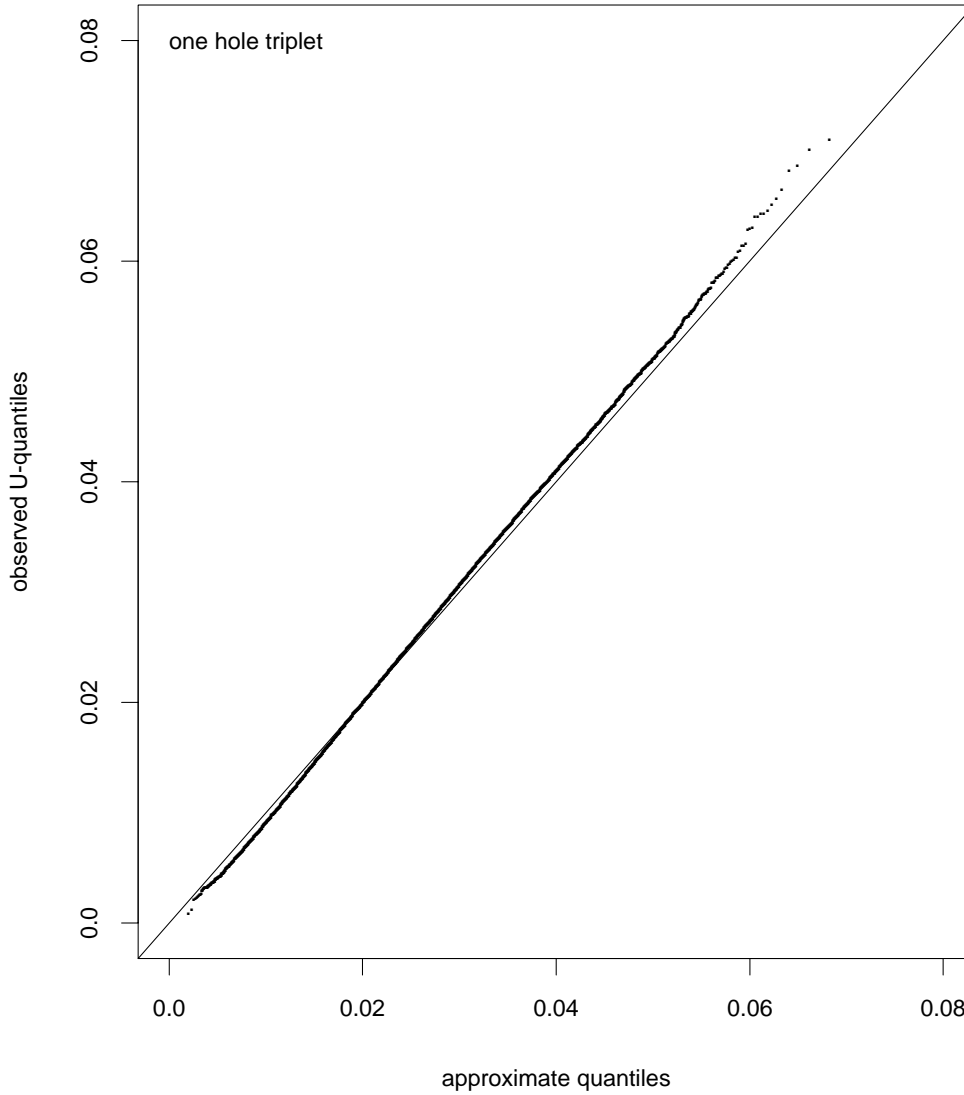


Figure 16: Approximation Quality for High U -Quantiles

Based on $\hat{U}_{2,p} = 2\sigma\sqrt{-\log[1 - p^{1/2.4}]}$, $\sigma = .01$



full range of p -values, although not quite as close as $\widehat{U}_{1,p}$ for $p \geq .95$. However, this second approximation tends to be superior when two or more hole triplets are involved.

When considering K such hole triplets and denoting by U_i the clearance loss at the i^{th} hole triplet we find as before that

$$M_{K3} = \max(U_1, \dots, U_K)$$

is the relevant quantity in describing the minimum clearance diameter

$$C_{K3,\min} = \min(C_1, \dots, C_K) = \min(2r - U_1, \dots, 2r - U_K) = d - M_{K3} .$$

We then have, assuming again $\sigma_1 = \sigma_2 = \sigma_3 = \sigma$,

$$P(M_{K3} \leq x) = [P(U_1 \leq x)]^K \approx \left[1 - \exp\left(-\frac{x^2}{4\sigma^2}\right) \right]^{2.4K} .$$

The corresponding approximation for the p -quantile $m_{K3,p}$ of M_{K3} is then

$$m_{K3,p} \approx \widehat{m}_{K3,p} = 2\sigma \sqrt{-\log(1 - p^{1/2.4K})} .$$

Employing the same approximation as before, we also have for $p \approx 1$

$$m_{K3,p} \approx \bar{m}_{K3,p} = 2\sigma \sqrt{-\log[-\log(p)] + \log(2.4K)} .$$

Note that going from two to three holes at each pinning location amounts to increasing K to $2.4K$. However, that effect is softened by the way $2.4K$ enters the formulas for $\widehat{m}_{K3,p}$ or $\bar{m}_{K3,p}$.

To check the suggested approximate behavior of $\widehat{m}_{K3,p}$ we simulated 50,000 sets of K such hole triplets (with $\sigma = .01$ and with linear pattern of nominal hole centers, equally spaced with gaps of 20 between adjacent hole centers) and observed the true M_{K3} value each time. Figure 17 compares the sorted observed M_{K3} -values, i.e., $M_{K3(1)} \leq \dots \leq M_{K3(n)}$, $n = 50,000$, against \widehat{m}_{K3,p_i} with $p_i = i/(n+1)$, $i = 1, \dots, n$. The straight line represents the main diagonal. It is quite evident that the suggested approximation is quite good even for quantiles as low as the .001-quantile or lower.

The approximate p -quantile $c_{K3,\min,p}$ for the minimal clearance diameter is

$$\begin{aligned} c_{K3,\min,p} &= d - m_{K3,1-p} \approx d - \widehat{m}_{K3,1-p} \\ &= d - 2\sigma \sqrt{-\log(1 - [1 - p]^{1/2.4K})} = \widehat{c}_{K3,\min,p} \\ &\approx d - 2\sigma \sqrt{-\log[-\log(1 - p)] + \log(2.4K)} = \bar{c}_{K3,\min,p} , \end{aligned}$$

where the last approximation holds for small p . From the previous findings about the approximation of $\widehat{m}_{K3,p}$ it follows that the approximation $\widehat{c}_{K3,\min,p}$ is quite good for all p .

Again we use the conversion of $T_1 = T_2 = T_3 = T$ to σ , i.e., $\sigma = T/3.439$. In order to be able to pin 99.73% of all assemblies we need $\bar{c}_{K3,\min,.0027} > \delta$ or

$$d - \delta > \frac{1}{3.439} T \sqrt{2} \sqrt{-2 \log[-\log(.9973)] + 2 \log(2.4K)} = T \sqrt{2} \sqrt{1 + 2 \log(2.4K)/11.826} .$$

Conversely, one can ask for the rate p of assembly fallout (not all hole triples can be pinned, i.e., $C_{K3,\min} < \delta$) for a given nominal gap $d - \delta$. Clearly we have $p = 1$ for $d < \delta$ and for $d \geq \delta$ we have

$$\begin{aligned} p &= P(C_{K3,\min} < \delta) = P(M_{K3} > d - \delta) = 1 - P(M_{K3} \leq d - \delta) \\ &= 1 - \left[1 - \exp \left\{ -\frac{(d - \delta)^2}{4\sigma^2} \right\} \right]^{2.4K} . \end{aligned}$$

The Rule 3 box summarizes the clearance tolerance stack criterion and fallout rate in terms of the radial tolerances for hole centering.

5.2 Clean-Out for Three Matched Holes, True Position Alignment

In [2] (see also Appendix C) it was seen that the smallest clean-out diameter of a hole centered on one of the three holes, say on hole 1, is

$$B = d + 2 \max \left(|\overline{P_1 P_2}|, |\overline{P_1 P_3}| \right) .$$

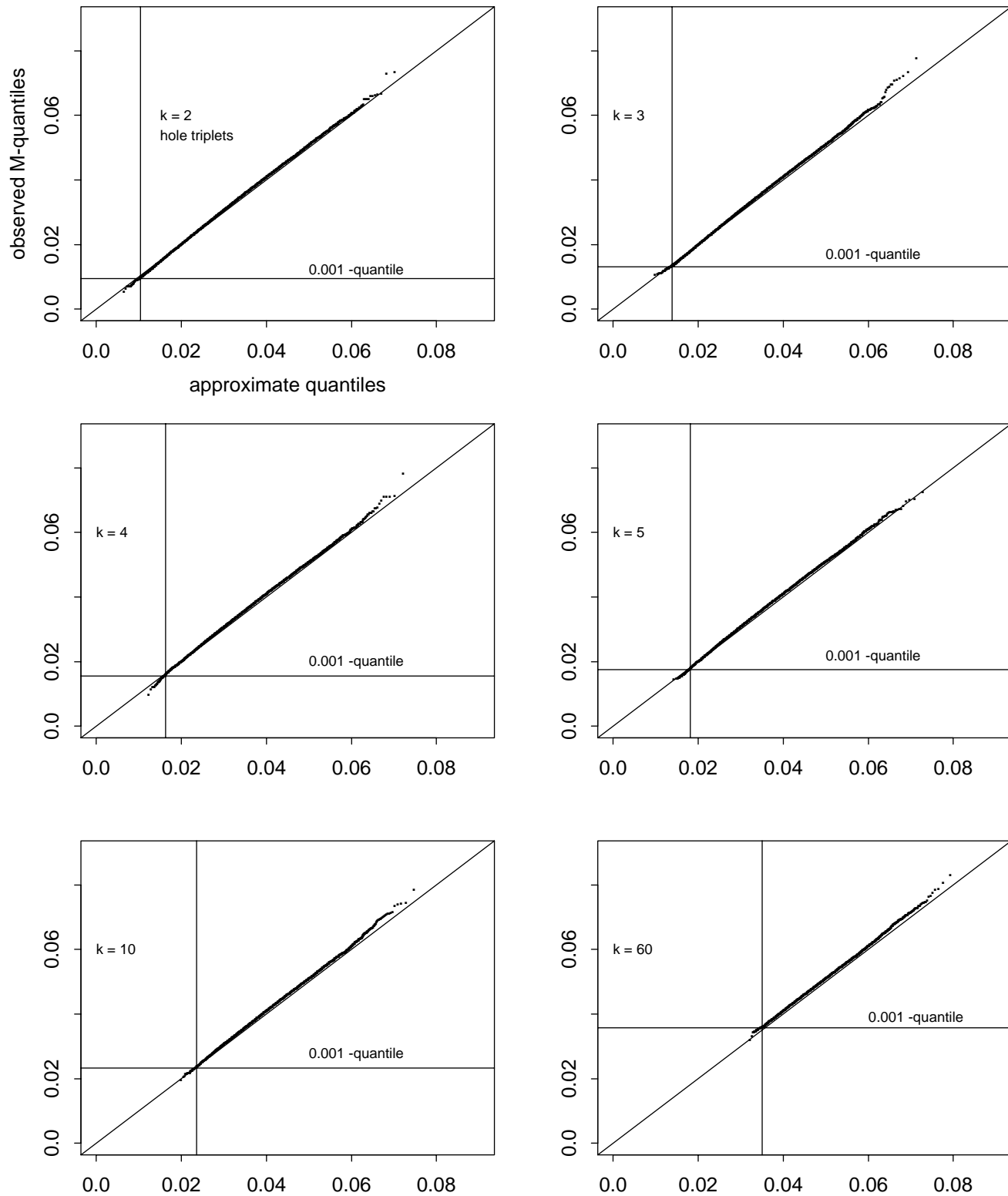
The quantity $V = \max \left(|\overline{P_1 P_2}|, |\overline{P_1 P_3}| \right)$, although simpler in nature than U , still has a complicated distribution. For large values x the probability $P(V \leq x)$ can be effectively approximated as follows

$$\begin{aligned} P(V \leq x) &= P \left(|\overline{P_1 P_2}| \leq x, |\overline{P_1 P_3}| \leq x \right) \approx P \left(|\overline{P_1 P_2}| \leq x \right) P \left(|\overline{P_1 P_3}| \leq x \right) \\ &= \left[1 - \exp \left(-\frac{x^2}{2\tau_{12}^2} \right) \right] \times \left[1 - \exp \left(-\frac{x^2}{2\tau_{13}^2} \right) \right] = \left[1 - \exp \left(-\frac{x^2}{2\tau^2} \right) \right]^2 , \end{aligned}$$

where in the last equality we assume again $\sigma_1 = \sigma_2 = \sigma_3 = \sigma$ and thus $\tau = \tau_{12} = \tau_{13} = \sigma\sqrt{2}$. This yields the following approximation for the p -quantile V_p of V for $p \approx 1$, namely

$$V_p \approx \widehat{V}_p = 2\sigma \sqrt{-\log(1 - p^{1/2})} .$$

Figure 17: Approximation Quality for M_{K3} -Quantiles



Rule 3

Clearance For Three Parts, True Position Alignment

Given 3 parts, each with a set of K nominally matched coordination holes, and given that these holes are centered with the same radial tolerance T on all three parts (otherwise assume conservatively the largest tolerance that applies), then these three parts can be pinned successfully at all K coordination hole triplets with 99.73% assurance for such assembly if

$$d - \delta > T \sqrt{2} \sqrt{1 + 2 \log(2.4K)/11.826} .$$

Here d and δ are the common hole and pin diameters. If these themselves are toleranced one can conservatively work with the worst case dimensions of these, i.e., with maximum material condition (tightest hole diameter and widest pin diameter).

Conversely, for given $d - \delta \geq 0$ the assembly fallout rate p of insufficient clearance at some hole triplet among the K triplets to be pinned is given by

$$p \approx 1 - \left[1 - \exp \left\{ -\frac{(d - \delta)^2 11.826}{4T^2} \right\} \right]^{2.4K} .$$

For $d - \delta < 0$ the assembly fallout rate obviously is $p = 1$ or 100%.

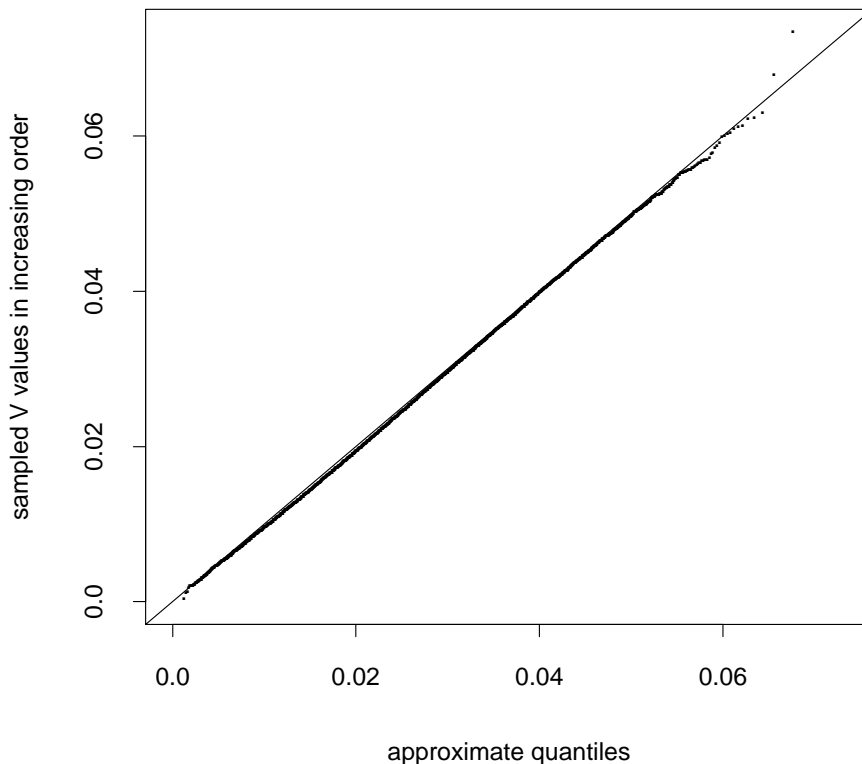
Assumptions: The hole centering variation is reasonably described by a circular bivariate normal distribution, centered on nominal hole centers (matching for all three parts), and is independent from hole to hole (hole to hole variation).

It is assumed that the radius T for the circular hole centering tolerance zones captures 99.73% of all drilled hole centers.

Furthermore, the parts are assumed to be aligned in true position. Although this latter alignment is not practical it is still not the best possible one for minimizing clearance problems.

To check the suggested approximation we simulated 50,000 such hole triplets (with $\sigma = .01$ and linear nominal hole center pattern, with gaps of 20 between adjacent hole centers) and observed the true V value each time. Figure 18 compares the sorted observed V -values, i.e., $V_{(1)} \leq \dots \leq V_{(n)}$, $n = 50,000$, against \hat{V}_{p_i} with $p_i = i/(n+1)$, $i = 1, \dots, n$. The straight line represents the main diagonal. It is quite evident that the suggested approximation is very good over the full range of p -values.

Figure 18: Approximation Quality for High V -Quantiles



When considering K such hole triplets we find, as before, that

$$M'_{K3} = \max(V_1, \dots, V_K)$$

is the relevant quantity in describing the maximum clean-out diameter

$$B_{K3,\max} = \max(B_1, \dots, B_K) = \max(2r + 2V_1, \dots, 2r + 2V_K) = d + 2M'_{K3}.$$

We have, assuming again $\sigma_1 = \sigma_2 = \sigma_3 = \sigma$ and thus $\tau = \tau_{12} = \tau_{13} = \sigma\sqrt{2}$, that

$$P(M'_{K3} \leq x) = [P(V_1 \leq x)]^K \approx \left[1 - \exp\left(-\frac{x^2}{2\tau^2}\right)\right]^{2K}$$

The corresponding p -quantile $m'_{K3,p}$ of M'_{K3} is approximated by

$$m'_{K3,p} \approx 2\sigma \sqrt{-\log[1 - p^{1/2K}]} = \widehat{m}'_{K3,p}.$$

Given the excellent approximation quality of \hat{V}_p for all p there was no need to verify the approximation quality for $\widehat{m}'_{K3,p}$.

The p -quantile approximation for the maximum clean-out diameter is thus

$$b_{K3,\max,p} = d + 2m'_{K3,p} \approx d + 4\sigma \sqrt{-\log[1 - p^{1/2K}]} = \hat{b}_{K3,\max,p}$$

and for $p \approx 1$ this becomes

$$b_{K3,\max,p} \approx d + 4\sigma \sqrt{-\log[-\log(p)] + \log(2K)} = \bar{b}_{K3,\max,p}.$$

Using again the identification $\sigma = T/3.439$ and aiming for 99.73% of all assemblies without clean-out problems, we must have

$$\bar{b}_{K3,\max,.9973} = d + 2\sqrt{2}T \frac{1}{3.439} \sqrt{-2\log[-\log(.9973)] + 2\log(2K)} < d_f$$

or

$$\sqrt{2}T \sqrt{1 + 2\log(2K)/11.826} < (d_f - d)/2.$$

Conversely, for given $d_f - d \geq 0$ one may ask for the rate p of fallout, i.e., for the proportion of assemblies with clean-out problems. This rate p is obtained as

$$\begin{aligned} p &= P(B_{K3,\max} > d_f) = 1 - P(B_{K3,\max} \leq d_f) \\ &= 1 - P(M'_{K3} \leq [d_f - d]/2) \\ &= 1 - \left\{1 - \exp\left(-\frac{[d_f - d]^2}{16\sigma^2}\right)\right\}^{2K}. \end{aligned}$$

The Rule 4 box summarizes the clean-out tolerance stack criterion in terms of the radial tolerances for hole centering.

Rule 4

Clean-Out For Three Parts, True Position Alignment

Given 3 parts, each with a set of K nominally matched coordination holes, and given that these holes are centered with common radial tolerance T on all three parts (otherwise take conservatively the largest of the centering tolerances as common value), then the coordination holes on these three parts can be cleaned out successfully at all K locations with 99.73% assurance if

$$(d_f - d)/2 > \sqrt{2} T \sqrt{1 + 2 \log(2K)/11.826} .$$

Here d_f and d are the common full-sized (clean-out) hole and coordination hole diameters, respectively. If these themselves are toleranced one can conservatively work with the worst case dimensions of these, i.e., with minimum value for d_f and maximum value for d .

Conversely, for given $d_f - d$ one determines the fallout rate p of an excessive clean-out diameter at some hole triplet among the k to be cleaned out as

$$p = 1 - \left\{ 1 - \exp \left(- \frac{[d_f - d]^2 11.862}{16T^2} \right) \right\}^{2K} .$$

Assumptions: The hole centering variation is reasonably described by a circular bivariate normal distribution, centered on nominal hole centers (matching for all three parts), and is independent from hole to hole (hole to hole variation). The clean-out holes are assumed to be centered on one of the respective coordination hole centers.

It is assumed that the radius T for the circular hole centering tolerance zones captures 99.73% of all drilled hole centers.

The parts are assumed to be aligned in true position. Although this latter alignment is not practical it is still not the best possible one for minimizing clean-out problems.

Caveat: See the discussion on page 4 concerning the possibly not quite conservative nature of this rule, which is based on true position alignment.

5.3 Clearance Under Primary/Secondary Hole Triplet Alignment

Here we consider the clearance issue for K triplets of holes, nominally equally spaced in a linear pattern, when the first and last hole triplet are used for primary and secondary hole triplet alignment. This means that a hole triplet at one end of the linear pattern is pinned first such that the hole centers of all three holes coincide. Although this may not be exactly achievable one can aim for it by using an expanding fastener or tightly toleranced hole and pin diameters. Then the three parts are rotated around the pinned primary hole triplet to get maximal clearance at the secondary hole triplet at the other end of the linear pattern. This secondary hole triplet is then pinned with an expanding fastener. The working assumption is that, after pinning these two hole triplets, the coinciding three primary hole centers (when projected on the plane perpendicular to the hole barrel axis) are collinear with the three secondary hole centers (when projected similarly). This may not be achievable exactly but one can come close. Once this alignment is effected the locations of all K holes on each of the three parts are assumed to be fixed. Because of this alignment the diameter of clearance at the i^{th} hole triplet is reduced from the common hole diameter d by the amount U_i . As was shown in Appendix C this amount U_i depends on the pairwise distances between the three hole centers at that location.

The minimum clearance diameter $\tilde{C}_{K3,\min}$ over all K hole triplets can again be expressed as

$$\tilde{C}_{K3,\min} = d - \max(U_1, \dots, U_K) = d - \tilde{M}_{K3} .$$

Because the alignment is driven by the hole centering variations at the primary and secondary alignment hole triplets it is evident that the U_i are no longer statistically independent. Furthermore, their distributions vary with i . For this reason we write \tilde{M}_{K3} and $\tilde{C}_{K3,\min}$ instead of M_{K3} and $C_{K3,\min}$ which were used under true position alignment.

As in the case of pinning K hole pairs by primary/secondary hole pair alignment, it is analytically not feasible to get the exact distribution of \tilde{M}_{K3} . Thus we simulated the distribution of \tilde{M}_{K3} for $K = 2, 3, \dots, 10, 12, 14, 16, 20, 25, 30, 40, 50$, and 60 by simulating $N = 50,000$ instances of \tilde{M}_{K3} for each such K . The hole centering variation was again simulated by a circular bivariate normal distribution, using $\sigma = .01$ and a nominal hole center gap of 20. The hope is that the quantiles of the simulated \tilde{M}_{K3} values relate linearly to the quantiles

$$\widehat{m}_{K3,p} = 2\sigma \sqrt{-\log(1 - p^{1/2.4K})} ,$$

i.e., we hope that the p -quantile $\tilde{m}_{K3,p}$ of \tilde{M}_{K3} satisfies the following approximate relationship

$$\tilde{m}_{K3,p}/\sigma \approx \alpha_K + \beta_K \widehat{m}_{K3,p}/\sigma \quad \text{or} \quad \tilde{m}_{K3,p} \approx \alpha_K \sigma + \beta_K \widehat{m}_{K3,p} .$$

Table 2: Coefficients for Linear Quantile Relationships

$$\tilde{m}_{K3,p}/\sigma = \alpha_K + \beta_K \widehat{m}_{K3,p}/\sigma \quad \text{or} \quad \tilde{m}_{K3,p} = \alpha_K \sigma + \beta_K \widehat{m}_{K3,p}$$

valid for $p \geq .1$ for $K = 2$ and for all p for $K > 2$.

K	α_K	β_K	K	α_K	β_K	K	α_K	β_K
2	-2.491	1.674	8	-0.970	1.540	20	-1.265	1.597
3	-1.386	1.562	9	-0.983	1.544	25	-1.367	1.614
4	-1.209	1.549	10	-1.004	1.549	30	-1.424	1.621
5	-1.077	1.539	12	-1.058	1.560	40	-1.589	1.646
6	-1.002	1.536	14	-1.111	1.570	50	-1.745	1.671
7	-0.972	1.537	16	-1.168	1.580	60	-1.820	1.680

Plotting the ordered values $\tilde{M}_{(1)} \leq \dots \leq \tilde{M}_{(N)}$ of the $N = 50,000$ simulated values of \tilde{M}_{K3}/σ against the corresponding quantiles $\widehat{m}_{K3,p_i}/\sigma$, $p_i = 1/(N+1), i = 1, \dots, N$, shows that the pattern is indeed quite linear as Figures 19 and 20 illustrate. In each plot the abscissa represents the $\widehat{m}_{K3,p_i}/\sigma$ value and the ordinate the corresponding value $\tilde{M}_{(i)}$. Aside from the point patterns each of the plots shows two slanted lines. One is the main diagonal which is shown for comparison purpose and the other is a least squares line fitted to the point pattern. Only in the case $K = 2$ we used the upper 90% of the plotted points for least squares fitting. In all other cases all points were used in the fitting process. The special treatment of $K = 2$ accounts for the fact that the linear pattern does not seem to extend to the lower 10% of the points. This special phenomenon presumably results from the fact that for $K = 2$ we have no intermediate hole triplets between primary and secondary alignment triplets and it is probably the intermediate triplets that dominate the behavior of \tilde{M}_{K3} for $K > 2$. The horizontal dashed lines are the indicated quantiles of the simulated \tilde{M}_{K3}/σ values.

The straight line fits are so good that the actual point patterns are mostly obscured, except for strays at either end and the already explained deviant behavior for $K = 2$ at the low end. The intercepts and slopes of these lines, when plotted against K , still show some simulation roughness as shown in Figure 21. To smooth out this roughness we fitted a smoothing spline for $K > 2$ and tabulated instead the smoothed values in Table 2 for those values of K for which simulations were run. For other values of K we used the smoother for interpolation purposes and saved those intercept and slope values for a spreadsheet tool.

Figure 19: Quantile Comparison of \tilde{M}_{K3}/σ and $\widehat{m}_{K3,p}/\sigma$

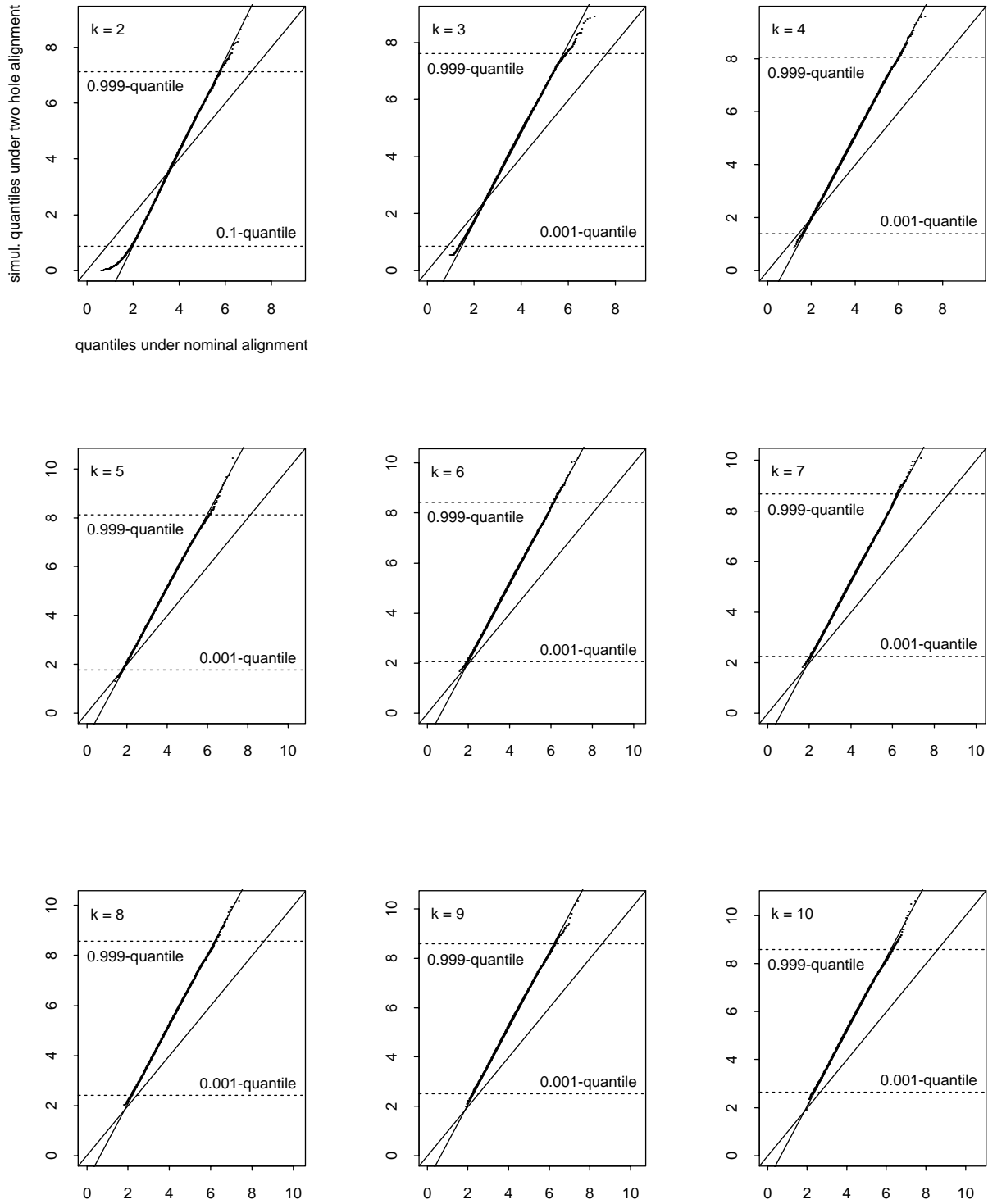


Figure 20: Quantile Comparison of \tilde{M}_{K3}/σ and $\widehat{m}_{K3,p}/\sigma$

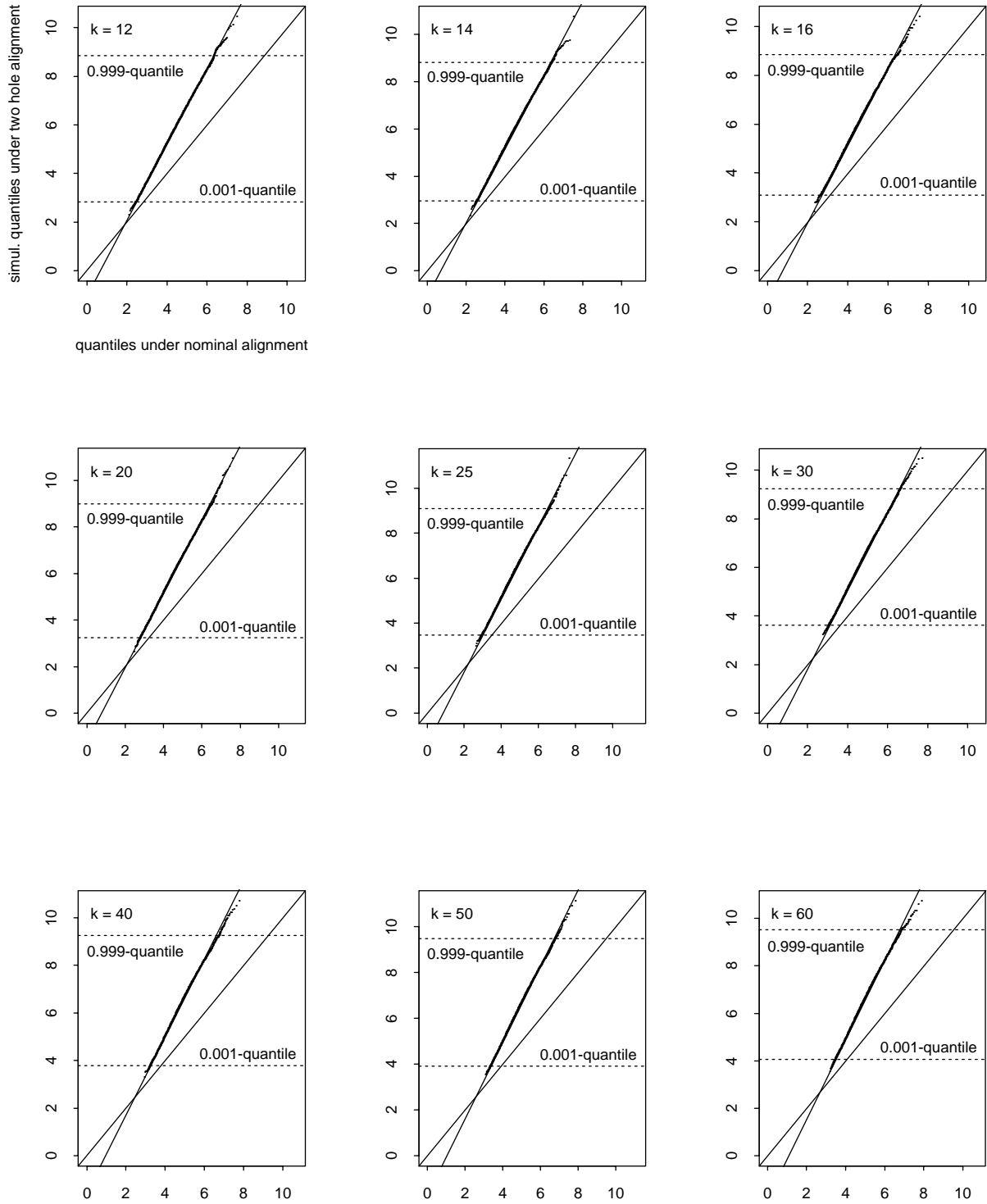
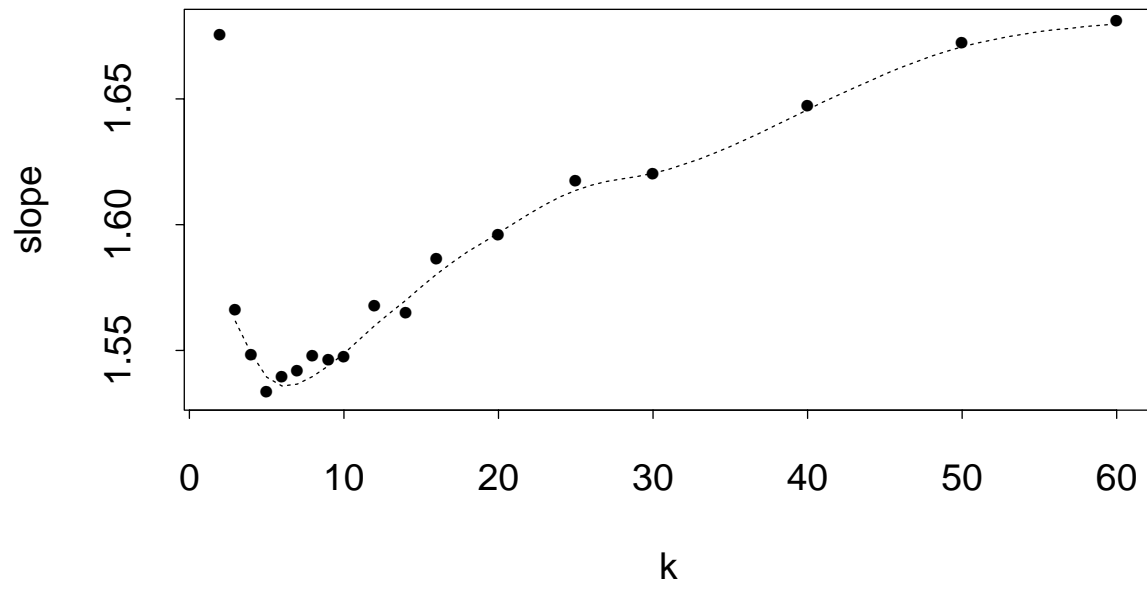
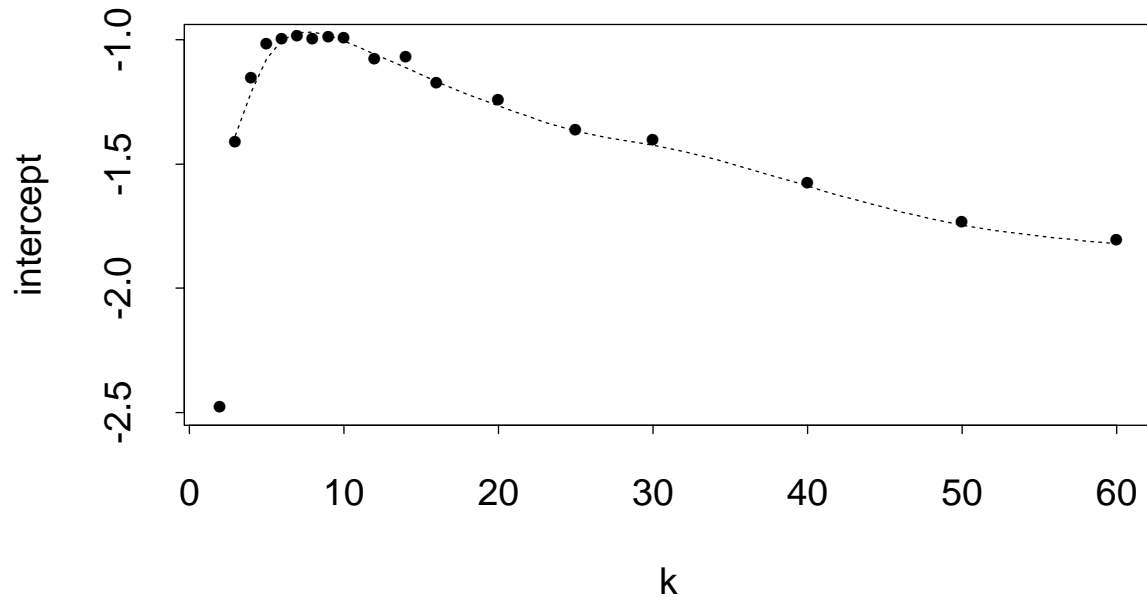


Figure 21: Smoothing Splines for Intercepts and Slopes



Although these tabled values arose out of a simulation using very specific values for σ and inter-hole gaps, their validity extends to other such choices of σ and inter-hole gaps as long as one is small compared to the other, as is usually the case.

As before, the obtained representation

$$\tilde{m}_{K3,p} = \alpha_K \sigma + \beta_K \widehat{m}_{K3,p} = \sigma \left[\alpha_K + 2\beta_K \sqrt{-\log(1 - p^{1/2.4K})} \right]$$

translates to the following corresponding quantile representation for $\tilde{C}_{K3,\min}$, namely

$$\tilde{c}_{K3,\min,p} = d - \tilde{m}_{K3,1-p} = d - \sigma \left\{ \alpha_K + 2\beta_K \sqrt{-\log(1 - [1 - p]^{1/2.4K})} \right\}, \quad (11)$$

which is reasonably valid for $p \leq .9$ for $K = 2$ and for all p for $K > 2$.

For $p \approx 0$ one can further approximate this by

$$\tilde{c}_{K3,\min,p} \approx d - \sigma \left\{ \alpha_K + 2\beta_K \sqrt{-\log(-\log[1 - p]) + \log(2.4K)} \right\}, \quad (12)$$

showing clearly the benign effect of K . The case $p \approx 0$ is most relevant for clearance concerns.

In order for 99.73% of all such three part assemblies to pin successfully we need that $\tilde{c}_{K3,\min,.0027} > \delta$, where δ is the common pin diameter. Relating again σ to the hole centering tolerance T via $\sigma = T/3.439$ (assuming 99.73% of all hole centers are within radius T of nominal center) this translates to the following condition for successful pinning of the three parts

$$d - \delta > \frac{T}{3.439} \left\{ \alpha_K + 2\beta_K \sqrt{-\log(1 - [1 - .0027]^{1/2.4K})} \right\}$$

or using (12)

$$d - \delta > T\sqrt{2} \left[\frac{\alpha_K}{3.439\sqrt{2}} + \beta_K \sqrt{1 + \frac{2\log(2.4K)}{11.826}} \right].$$

Conversely, one can ask for given $d - \delta$: What is the proportion p of assemblies for which the three parts cannot be pinned successfully? From the quantile relationship (11) one obtains

$$p = 1 - \left[1 - \exp \left(-\frac{1}{2} \left\{ \frac{3.439(d - \delta)}{\beta_K T \sqrt{2}} - \frac{\alpha_K}{\beta_K \sqrt{2}} \right\}^2 \right) \right]^{2.4K}.$$

The above is summarized in the Rule 3a box. When comparing this to Rule 1a one should keep in mind that in Rule 3a we assumed a common hole centering tolerance T for all three parts.

Rule 3a

Clearance under Primary/Secondary Hole Triplet Alignment

Given 3 parts, each with a set of K nominally matched coordination holes (equally spaced and in a linear pattern), and given that these holes are centered with common radial tolerance T on all three parts, then these three parts can be pinned successfully at all coordination hole triplets with 99.73% assurance for such assembly if

$$d - \delta > T\sqrt{2} \left[\frac{\alpha_K}{3.439\sqrt{2}} + \beta_K \sqrt{1 + \frac{2 \log(2.4K)}{11.826}} \right].$$

Here d and δ are the common hole and pin diameters. If these themselves are toleranced one can conservatively work with the worst case dimensions of these, i.e., with maximum material condition (tightest hole diameter and widest pin diameter). The values of α_K and β_K can be read from Table 2.

Conversely, for given $d - \delta > 0$ the assembly fallout rate p of insufficient clearance at some hole triplet among the K triplets to be pinned is

$$p = 1 - \left[1 - \exp \left(-\frac{1}{2} \left\{ \frac{3.439(d - \delta)}{\beta_K T \sqrt{2}} - \frac{\alpha_K}{\beta_K \sqrt{2}} \right\}^2 \right) \right]^{2.4K}.$$

This is reasonably accurate when $p \leq .90$ for $K = 2$ and for all p when $K > 2$. Of course for $d - \delta \leq 0$ the fallout rate is $p = 1$ or 100%.

Assumptions: The hole centering variation is reasonably described by a circular bivariate normal distribution, centered on nominal hole centers (matching for all three parts), and is independent from hole to hole (hole to hole variation). It is assumed that the common radius T for the circular hole centering tolerance zones captures 99.73% of all drilled hole centers.

The nominal coordination hole centers are equally spaced along a line.

Here it is assumed that the parts are aligned by the primary/secondary hole triplet alignment process, i.e., perfect on the primary hole triplet and by rotation best possible at the secondary hole triplet. Among the K hole triplets the primary and secondary triplets are chosen to be as far apart as possible.

5.4 Clean-Out Under Primary/Secondary Hole Triplet Alignment

Here we consider the clean-out issue for K triplets of holes, nominally equally spaced in a linear pattern, when the first and last hole triplets are used for primary and secondary hole triplet alignment as explained in the previous section. It is assumed that the clean-out holes are all centered on the holes in one of the three parts pinned. The choice of that part is based on practicality considerations. Because of the primary/secondary hole triplet alignment the diameter of the clean-out hole at the i^{th} hole triplet is increased over the common hole diameter d by the amount $2V_i$. As was shown in Appendix C the quantity V_i depends on the pairwise distances between the three hole centers at that location under the given alignment.

The maximum clean-out diameter $\tilde{B}_{K3,\max}$ over all K hole triplets can again be expressed as

$$\tilde{B}_{K3,\max} = d + 2 \max(V_1, \dots, V_K) = d + 2\tilde{M}'_{K3}.$$

Because the alignment is driven by the hole centering variations at the primary and secondary alignment hole triplets it is evident that the V_i are no longer statistically independent. Furthermore, their distributions vary with i . For this reason we write \tilde{M}'_{K3} and $\tilde{B}_{K3,\max}$ instead of M'_{K3} and $B_{K3,\max}$ which were used under true position alignment.

As in the case of pinning K hole pairs by primary/secondary hole pair alignment, it is analytically not feasible to get the exact distribution of \tilde{M}'_{K3} . Thus we simulated the distribution of \tilde{M}'_{K3} for $K = 2, 3, \dots, 10, 12, 14, 16, 20, 25, 30, 40, 50$, and 60 by simulating $N = 50,000$ instances of \tilde{M}'_{K3} for each such K . The hole centering variation was again simulated by a circular bivariate normal distribution, using $\sigma = .01$ and a nominal hole center gap of 20. The hope is that the quantiles of the simulated \tilde{M}'_{K3} values relate linearly to the quantiles

$$\widehat{m}'_{K3,p} = 2\sigma \sqrt{-\log(1 - p^{1/2K})},$$

i.e., we hope that the p -quantile $\tilde{m}'_{K3,p}$ of \tilde{M}'_{K3} satisfies the following approximate relationship

$$\tilde{m}'_{K3,p}/\sigma \approx \alpha_K + \beta_K \widehat{m}'_{K3,p}/\sigma \quad \text{or} \quad \tilde{m}'_{K3,p} \approx \alpha_K \sigma + \beta_K \widehat{m}'_{K3,p}.$$

Plotting the ordered values $\tilde{M}'_{(1)} \leq \dots \leq \tilde{M}'_{(N)}$ of the $N = 50,000$ simulated values of \tilde{M}'_{K3}/σ against the corresponding quantiles $\widehat{m}'_{K3,p_i}/\sigma$, $p_i = 1/(N+1)$, $i = 1, \dots, N$, shows that the pattern is indeed quite linear as Figures 22 and 23 illustrate.

In each plot the abscissa represents the $\widehat{m}'_{K3,p_i}/\sigma$ value and the ordinate the corresponding value $\tilde{M}'_{(i)}$. In addition to the point patterns each of the plots shows two slanted lines. One is the main diagonal which is shown for comparison purpose and the other is a least squares line fitted to the point pattern.

Figure 22: Quantile Comparison of \tilde{M}'_{K3}/σ and $\widehat{m}'_{K3,p}/\sigma$

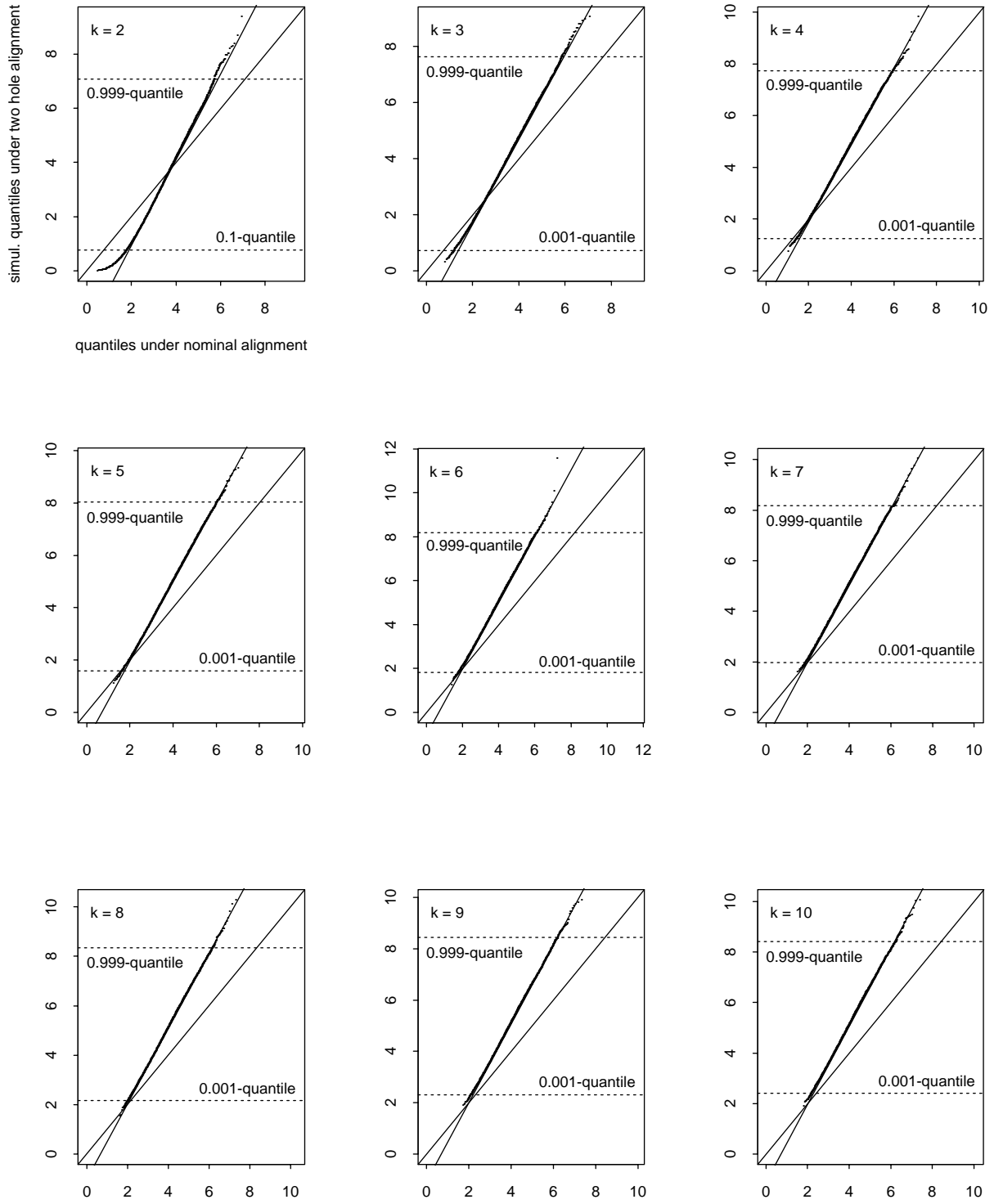
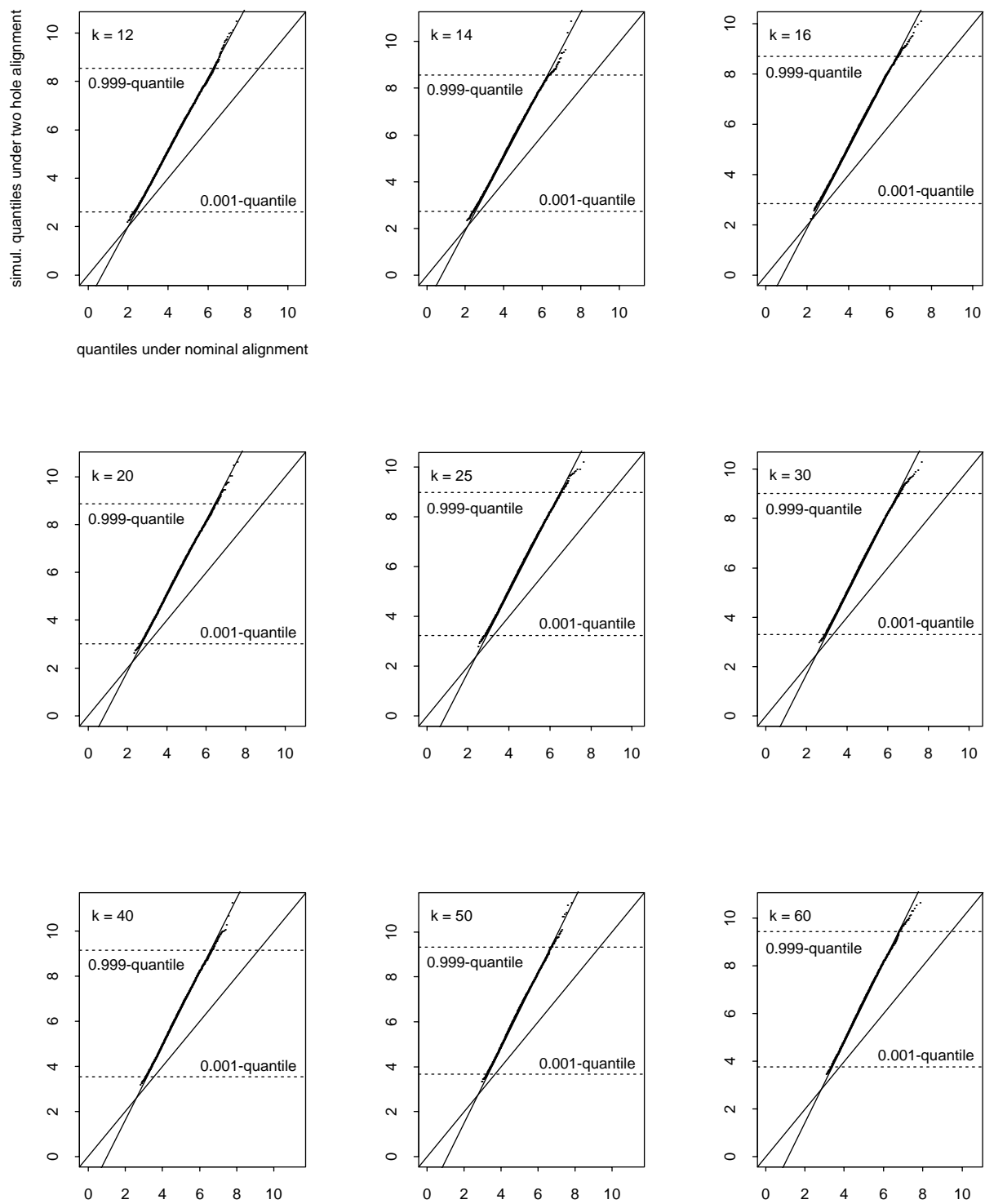


Figure 23: Quantile Comparison of \tilde{M}'_{K3}/σ and $\widehat{m}'_{K3,p}/\sigma$



Only in the case $K = 2$ we used the upper 90% of the plotted points for least squares fitting. In all other cases all points were used in the fitting process. The special treatment of $K = 2$ was already commented on in the previous section. The horizontal dashed lines are the indicated quantiles of the simulated M'_{K3}/σ values.

The straight line fits are again so good that the actual point patterns are mostly obscured, except for strays at either end and the already explained deviant behavior for $K = 2$ at the low end. The intercepts and slopes of these lines, when plotted against K , still show some simulation roughness as shown in Figure 24. To smooth out this roughness and to facilitate interpolation of α_K and β_K for other intermediate values of K we fitted a smoothing spline for $K > 2$ and tabulated instead the smoothed values in Table 3 which shows these coefficients only for those values of K for which simulations were run. However, other values were interpolated and are used in a spreadsheet software tool. Although these tabled values arose out of a simulation using very specific values for σ and inter-hole gaps, their validity extends to other such choices of σ and inter-hole gaps as long as one is small compared to the other, as is usually the case.

As before, the obtained representation

$$\tilde{m}'_{K3,p} = \alpha_K \sigma + \beta_K \widehat{m}'_{K3,p} = \sigma \left[\alpha_K + 2\beta_K \sqrt{-\log(1 - p^{1/2K})} \right]$$

translates to the following corresponding quantile representation for $\tilde{B}_{K3,\max}$, namely

$$\tilde{b}_{K3,\max,p} = d + 2\tilde{m}'_{K3,p} = d + 2\sigma \left[\alpha_K + 2\beta_K \sqrt{-\log(1 - p^{1/2K})} \right], \quad (13)$$

which is reasonably valid for $p \geq .1$ for $K = 2$ and for all p for $K > 2$.

For $p \approx 1$ one can further approximate this by

$$\tilde{b}_{K3,\max,p} \approx d + 2\sigma \left\{ \alpha_K + 2\beta_K \sqrt{-\log[-\log(p)] + \log(2K)} \right\}, \quad (14)$$

showing clearly the benign effect of K . The case $p \approx 1$ is most relevant for clean-out concerns.

In order for 99.73% of all such three part assemblies to clean out successfully we need that $\tilde{b}_{K3,\max,.9973} < d_f$, where d_f is the common clean-out diameter. Relating again σ to the hole centering tolerance T via $\sigma = T/3.439$ (assuming 99.73% of all hole centers are within radius T of nominal center) this translates to the following condition for successful clean-out of the holes on the three parts

Figure 24: Smoothing Splines for Intercepts and Slopes

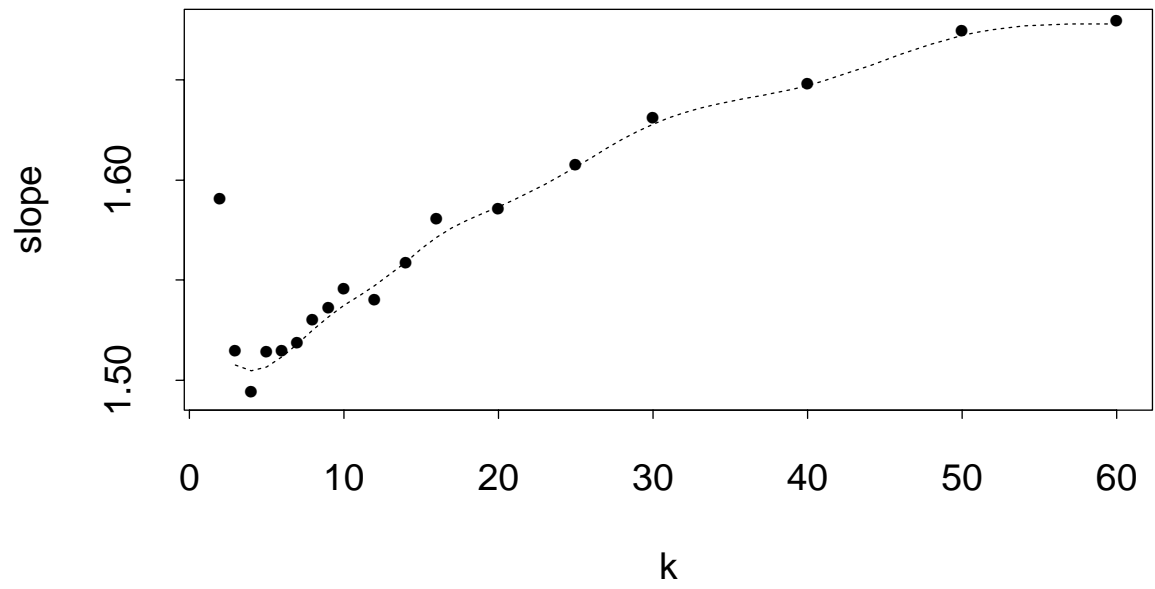
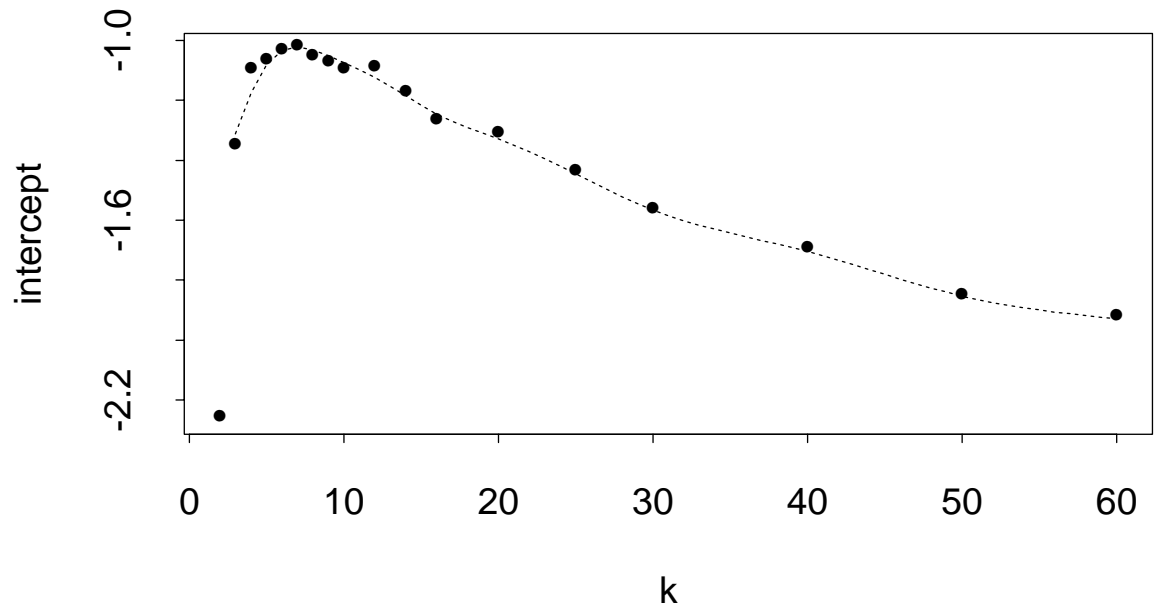


Table 3: Coefficients for Linear Quantile Relationships

$$\tilde{m}'_{K3,p}/\sigma = \alpha_K + \beta_K \widehat{m}'_{K3,p}/\sigma \quad \text{or} \quad \tilde{m}'_{K3,p} = \alpha_K \sigma + \beta_K \widehat{m}'_{K3,p}$$

valid for $p \geq .1$ for $K = 2$ and for all p for $K > 2$.

K	α_K	β_K	K	α_K	β_K	K	α_K	β_K
2	-2.265	1.589	8	-1.031	1.525	20	-1.328	1.587
3	-1.312	1.508	9	-1.050	1.532	25	-1.445	1.607
4	-1.173	1.505	10	-1.073	1.537	30	-1.565	1.628
5	-1.080	1.507	12	-1.123	1.547	40	-1.704	1.647
6	-1.034	1.512	14	-1.184	1.559	50	-1.853	1.672
7	-1.021	1.518	16	-1.245	1.571	60	-1.929	1.678

$$(d_f - d)/2 > \frac{T}{3.439} \left[\alpha_K + 2\beta_K \sqrt{-\log(1 - .9973^{1/2K})} \right]$$

or using (14)

$$(d_f - d)/2 > T\sqrt{2} \left[\frac{\alpha_K}{3.439\sqrt{2}} + \beta_K \sqrt{1 + \frac{2\log(2K)}{11.826}} \right].$$

Conversely, one can ask for given $d_f - d$: What is the proportion p of assemblies for which the holes on the three parts cannot be cleaned out successfully? From the quantile relationship (13) one obtains

$$p = 1 - \left[1 - \exp \left(-\frac{1}{2} \left\{ \frac{3.439(d_f - d)/2}{\beta_K T \sqrt{2}} - \frac{\alpha_K}{\beta_K \sqrt{2}} \right\}^2 \right) \right]^{2K}.$$

The above is summarized in the Rule 4a box. When comparing this to Rule 2a one should keep in mind that in Rule 4a we assumed a common hole centering tolerance T for all three parts.

Rule 4a

Clean-Out under Primary/Secondary Hole Triplet Alignment

Given 3 parts, each with a set of K nominally matched coordination holes, and given that these holes are centered with common radial tolerance T on all three parts (otherwise take conservatively the largest of the centering tolerances as common value), then the coordination holes on these three parts can be cleaned out successfully at all K locations with 99.73% assurance if

$$(d_f - d)/2 > T \sqrt{2} \left(\frac{\alpha_K}{3.439\sqrt{2}} + \beta_K \sqrt{1 + \frac{2 \log(2K)}{11.826}} \right) .$$

Here d_f and d are the common full-sized (clean-out) hole and coordination hole diameters, respectively. If these themselves are toleranced one can conservatively work with the worst case dimensions of these, i.e., with minimum value for d_f and maximum value for d . The values of α_K and β_K can be read from Table 3.

Conversely, for given $d_f - d$ one determines the fallout rate p of an excessive clean-out diameter at some hole pair among the K pairs to be cleaned out as

$$p = 1 - \left[1 - \exp \left(-\frac{1}{2} \left\{ \frac{3.439(d_f - d)/2}{\beta_K T \sqrt{2}} - \frac{\alpha_K}{\beta_K \sqrt{2}} \right\}^2 \right) \right]^{2K} .$$

This is reasonably accurate when $K = 2$ & $p \leq .90$ and for all p for $K \geq 3$. Of course for $d_f - d \leq 0$ the fallout rate is $p = 1$ or 100%.

Assumptions: The hole centering variation is reasonably described by a circular bivariate normal distribution, centered on nominal hole centers (matching for all three parts), and is independent from hole to hole (hole to hole variation). It is assumed that the radius T for the circular hole centering tolerance zone captures 99.73% of all drilled hole centers.

The nominal coordination hole centers are equally spaced along a line.

Here it is assumed that the parts are aligned by the primary/secondary hole triplet alignment process, i.e., perfect on the primary hole triplet and by rotation best possible at the secondary hole triplet. Among the K hole triplet the primary and secondary triplets are chosen to be as far apart as possible. The clean-out holes are assumed to be centered on the respective coordination hole centers of one of the parts, chosen on practicality grounds.

6 Hole Centering Variation Increasing with Datum Distance

So far hole centering variation has been assumed to be the same from hole to hole. Here we reexamine the maximal hole center mismatch issue when the hole centering variation increases linearly with the distance from some datum.

There is no boxed rule given here, since this section represents more of an exploratory study of what happens when the drilling accuracy deteriorates. Another reason for not giving a boxed rule is that it was not clear how to express tolerances on such a deterioration of drilling accuracy. The reader who wants to use the methods given here is advised to read the section as a whole and make the necessary modification concerning the specifics.

The hole centering variation is again assumed to be independent from hole to hole, which is reasonable under true position part alignment. Following the development in Section 2.2 we can write

$$\begin{aligned} P(M_K \leq x) &= P(D_1 \leq x, \dots, D_K \leq x) = P(D_1 \leq x) \cdots P(D_K \leq x) \\ &= \left[1 - \exp\left(-\frac{x^2}{2\tau_1^2}\right) \right] \cdots \left[1 - \exp\left(-\frac{x^2}{2\tau_K^2}\right) \right], \end{aligned} \quad (15)$$

where $\tau_i^2 = \sigma_{i1}^2 + \sigma_{i2}^2$ and σ_{ij} is the standard deviation characterizing the hole centering variability for the i^{th} hole on part j . This formula is exact but not easy to comprehend in relation to K and the hole centering accuracies σ_{ij} . How the σ_{ij} vary from hole to hole has not yet been specified and is not important at this point.

To get a better understanding of (15) we develop an approximation that will be applicable only for large x values, i.e., for which $P(M_K \leq x) \approx 1$. Such large x values are of primary concern because they cover the typical range for tolerancing M_K .

We can rewrite (15) as

$$P(M_K \leq x) = \left[\exp\left(\frac{1}{K} \sum_{i=1}^K \log \left[1 - \exp\left\{-\frac{x^2}{2\tau_i^2}\right\}\right]\right) \right]^K.$$

In the approximation we will replace

$$\frac{1}{K} \sum_{i=1}^K \log \left[1 - \exp\left\{-\frac{x^2}{2\tau_i^2}\right\}\right] \quad \text{by} \quad -\exp\left(-\frac{x^2}{2\tau_0^2}\right)$$

for some appropriately chosen value of τ_0^2 . Using the approximation

$$\log \left[1 - \exp\left\{-\frac{x^2}{2\tau_i^2}\right\}\right] \approx -\exp\left(-\frac{x^2}{2\tau_i^2}\right)$$

for large enough x we see that only the terms with large τ_i values will amount to anything when averaging these approximations in

$$\frac{1}{K} \sum_{i=1}^n \log \left[1 - \exp \left\{ -\frac{x^2}{2\tau_i^2} \right\} \right] \approx -\frac{1}{K} \sum_{i=1}^K \exp \left\{ -\frac{x^2}{2\tau_i^2} \right\} . \quad (16)$$

Thus it seems reasonable to find a value τ_0^2 as some kind of weighted average of the τ_i^2 with high weights given to high values of τ_i^2 .

We will work with the following hole pattern and associated hole centering accuracies. Assume that the nominal hole centers are equally spaced in a plane, along a line perpendicular to a given datum line. It is stipulated that

$$3\sigma_x = .0005'' + .00001 \times x$$

where x is the distance (in inches) of the nominal hole center from the datum line. The spacing between adjacent holes is assumed to be $\Delta = 20''$. In particular it is assumed that

$$3\sigma_{i1} = .0005'' + .00001 \times \Delta(i-1) \quad \text{for } i = 1, \dots, K , \quad (17)$$

so that $3\sigma_{i1} = .0005''$ and $3\sigma_{iK} = .0005 + (K-1).0002''$.

For σ_{i2} we could either assume the same model, i.e., $\sigma_{i2} = \sigma_{i1}$, or one can investigate what happens when the datum line is at opposite ends on the two parts, i.e., we would then assume that

$$3\sigma_{i2} = 3\sigma_{(K-i+1)1} = .0005'' + .00001 \times \Delta(K-i) \quad \text{for } i = 1, \dots, K .$$

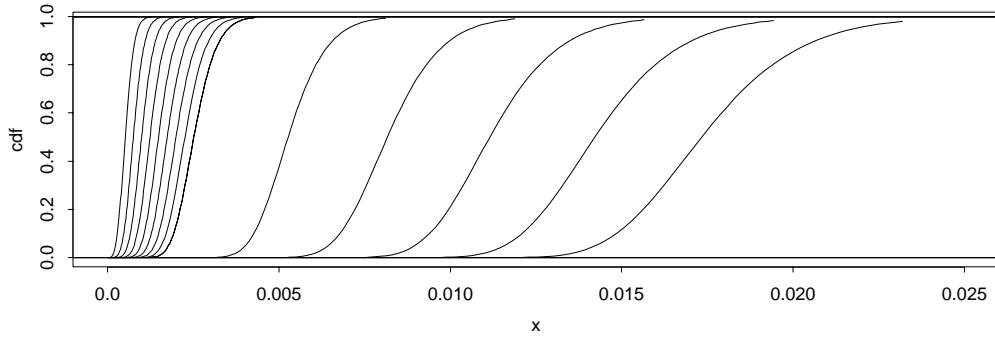
In view of the dominant contributions from terms with large τ_i in (16) it is hoped that with this latter scheme the large centering variation at one hole center is balanced out by the small variation at the corresponding hole on the other part.

Figure 25 shows a comparison of the two datum schemes ($\sigma_{i2} = \sigma_{(K-i+1)1}$ and $\sigma_{i2} = \sigma_{i1}$) in addition to assuming constant maximum σ_0 , namely $\sigma_0 = \sigma_{K1}$ for all holes on both parts, by showing the exact cumulative distribution functions (15) for $K = 2, \dots, 10, 20, \dots, 60$, using the above formula (17) for σ_{i1} .

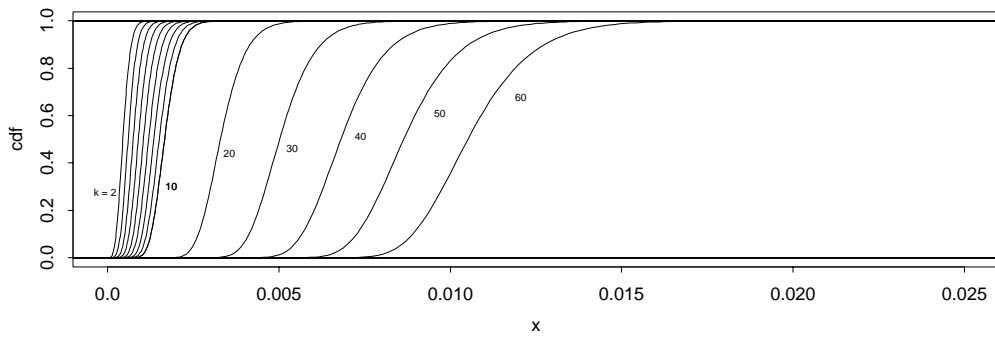
It is clear that the strategy of using opposite end datums paid off by yielding distributions for M_K which are positioned closer to zero than the corresponding distributions under same end part datum and under constant maximum σ_0 . The 99% quantiles of these distribution functions, denoted by $m_{0,K,.99}$ (constant maximum σ_0), $m_{1,K,.99}$ (opposite end datums), and $m_{2,K,.99}$ (same end datums) are compared in ratio form $m_{1,K,.99}/m_{0,K,.99}$ and $m_{2,K,.99}/m_{0,K,.99}$ in Table 4. Clearly the opposite datum indexing scheme is best. However, implementation of that scheme needs to be weighed against the cost of doing so.

Figure 25: Distributions of Maximal Hole Center Distances

assuming constant maximum sigma



part datum references at opposite ends, linearly increasing sigma



part datum references at same end, linearly increasing sigma

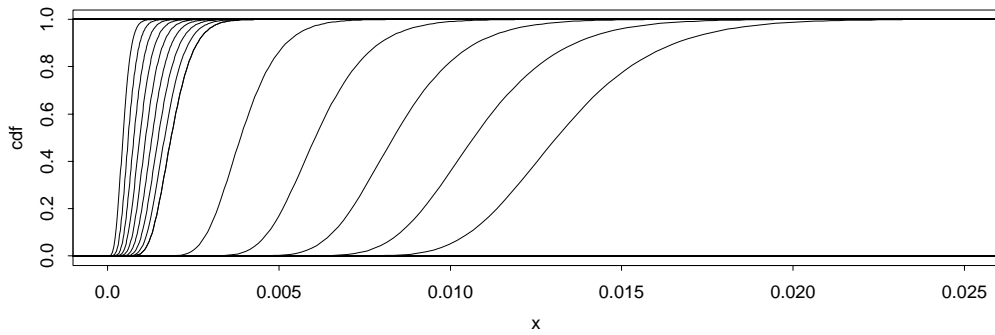


Table 4: Comparison of .99-Quantiles for the Three Schemes

K	2	3	4	5	6	7	8
$m_{1,K,.99}/m_{0,K,.99}$	0.869	0.800	0.758	0.730	0.711	0.696	0.686
$m_{2,K,.99}/m_{0,K,.99}$	0.934	0.903	0.886	0.875	0.867	0.861	0.857
K	9	10	20	30	40	50	60
$m_{1,K,.99}/m_{0,K,.99}$	0.678	0.671	0.643	0.635	0.632	0.630	0.629
$m_{2,K,.99}/m_{0,K,.99}$	0.853	0.851	0.841	0.840	0.840	0.840	0.840

With regard to the approximation

$$\begin{aligned}
 P(M_K \leq x) &= \left[\exp \left(\frac{1}{K} \sum_{i=1}^K \log \left[1 - \exp \left\{ -\frac{x^2}{2\tau_i^2} \right\} \right] \right) \right]^K \approx \exp \left[-K \exp \left(-\frac{x^2}{2\tau_0^2} \right) \right] \\
 &= \exp \left[-\exp \left(-\frac{x^2}{2\tau_0^2} + \log K \right) \right] = \mathcal{G} \left(\frac{x^2}{2\tau_0^2} - \log K \right)
 \end{aligned} \tag{18}$$

for some appropriate weighted average τ_0^2 of the τ_i^2 values, several such averages were tried. The one that gave the best results was

$$\tau_0^2 = \frac{\sum_{i=1}^K \tau_i^{5.5}}{\sum_{i=1}^K \tau_i^{3.5}} = \sum_{i=1}^K w_i \tau_i^2 \quad \text{with} \quad w_i = \tau_i^{3.5} / \sum_{j=1}^K \tau_j^{3.5} .$$

The quality of the approximation is illustrated in Figures 26-29 by showing the relevant upper end of the cumulative distribution functions (cdf), as computed by (15), and their approximations, as computed by (18), for some representative values of K and the σ_{i1} in (17). The approximation is quite good for opposite end datums. For datums at the same end it is still acceptable for $P(M_K \leq x) \geq .99$, although there is some deterioration for large K .

Figure 26: Comparison of Approximation Quality for $K = 3$

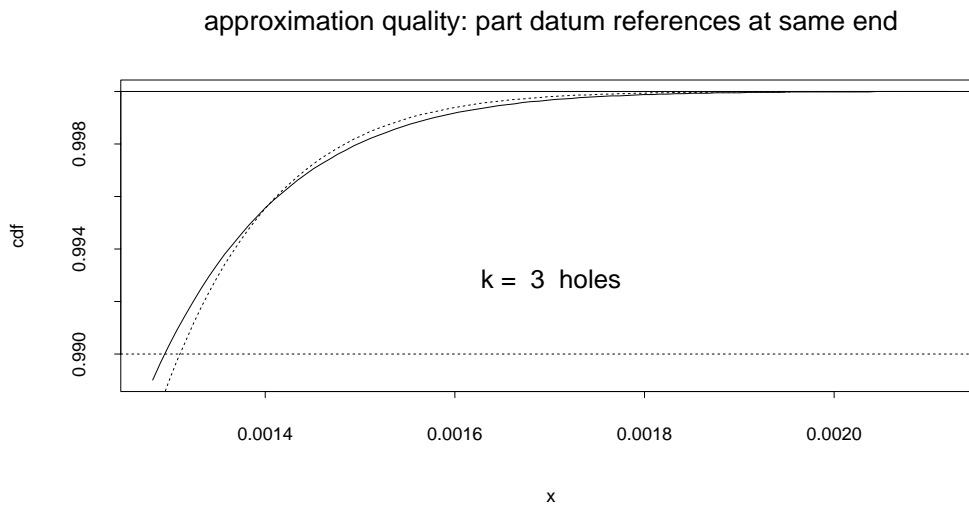
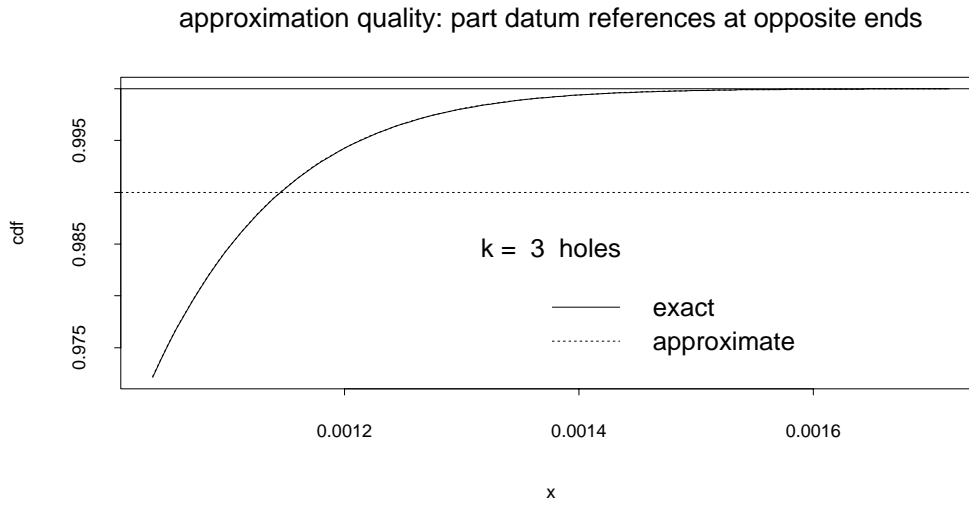


Figure 27: Comparison of Approximation Quality for $K = 7$

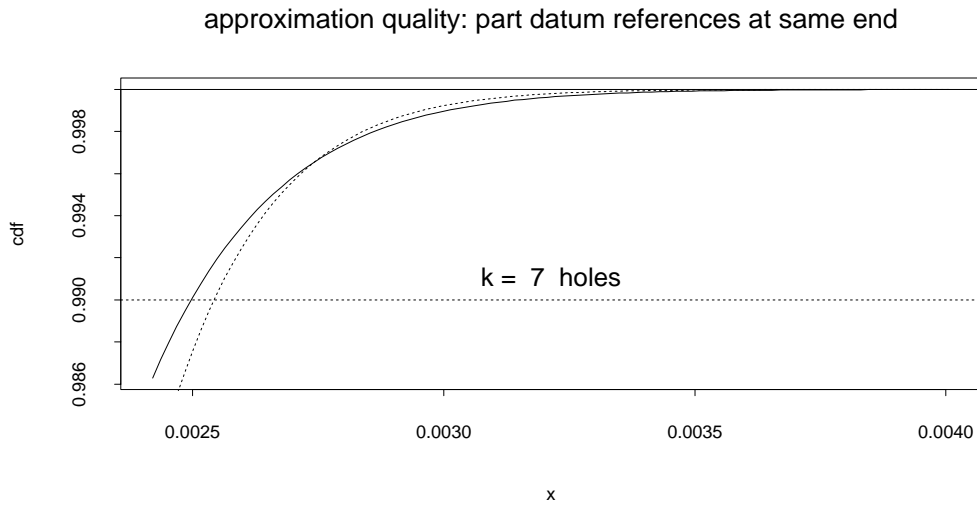
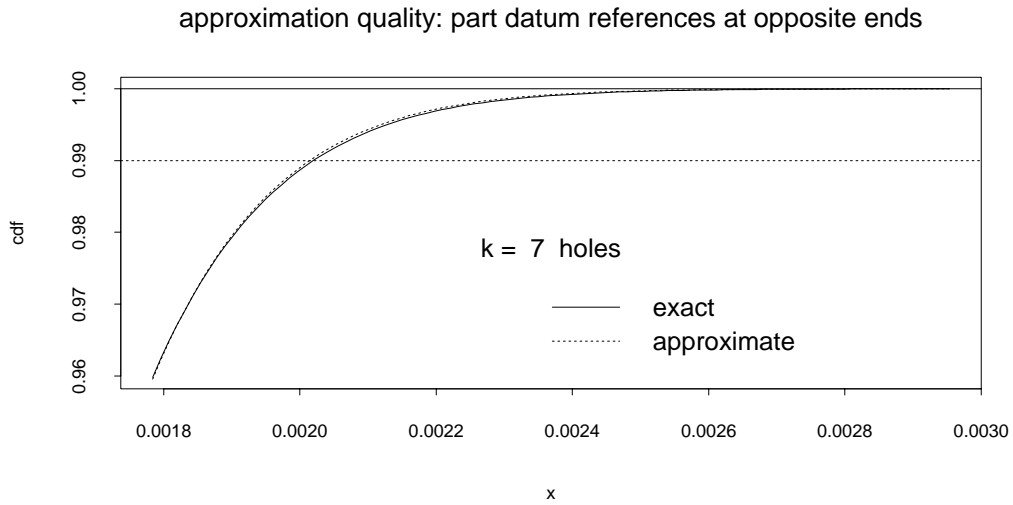


Figure 28: Comparison of Approximation Quality for $K = 20$

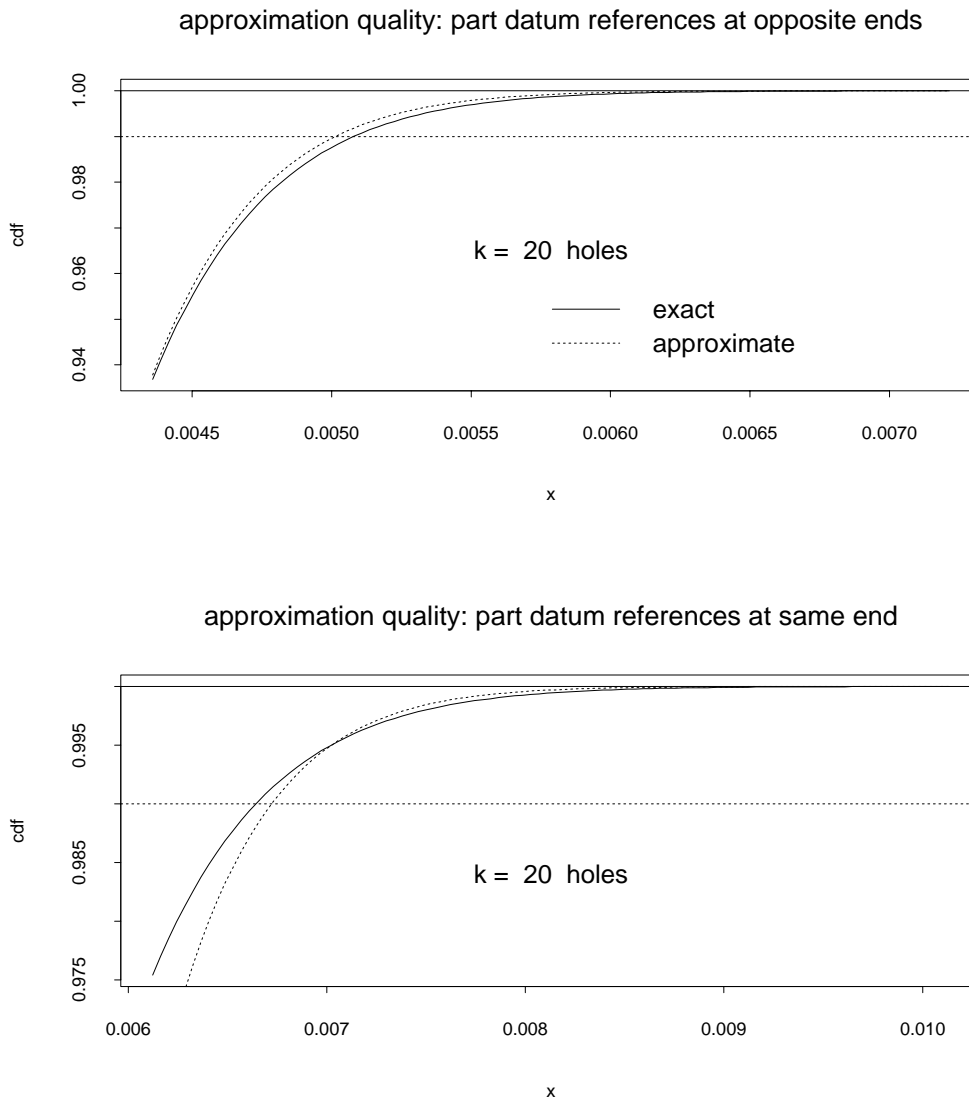
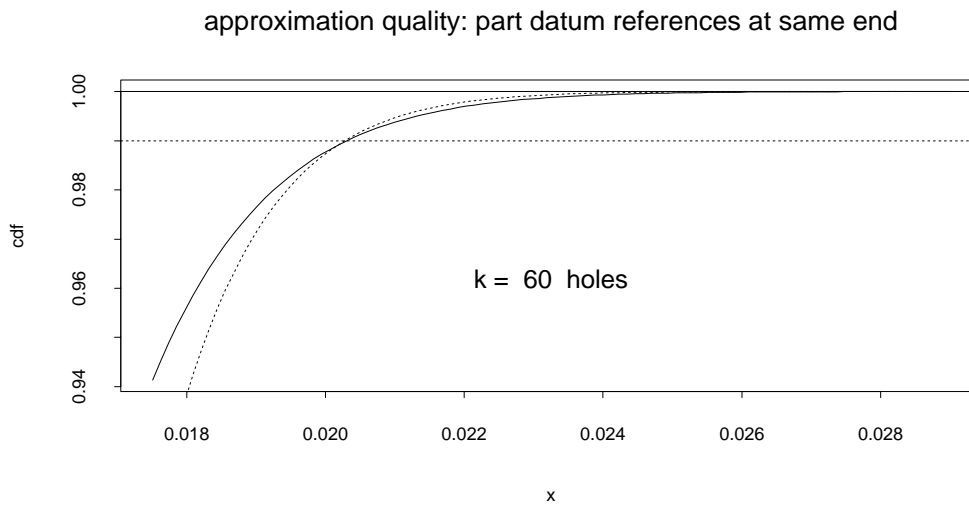
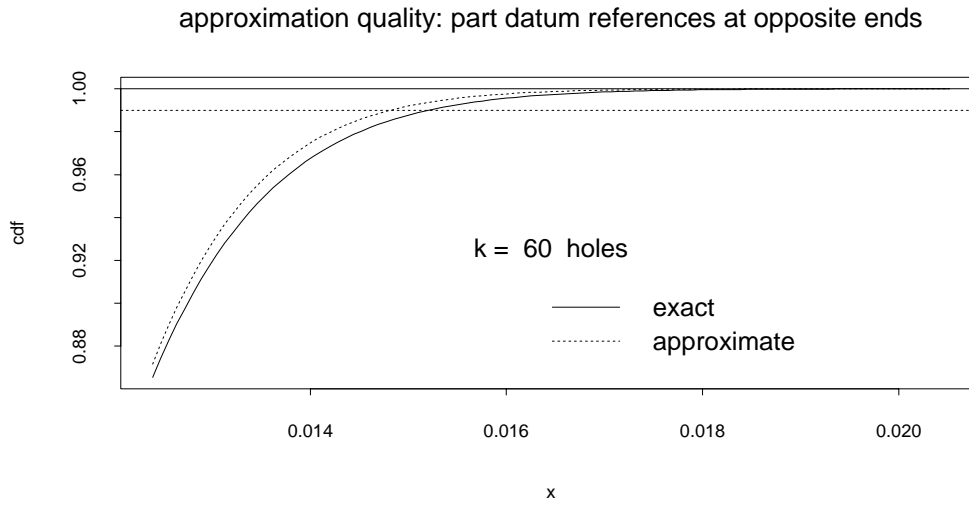


Figure 29: Comparison of Approximation Quality for $K = 60$



The merit in using the approximation (18) is that it gives some insight into the effect of K . Since the approximation has the same form as in our original simple situation based on true position alignment, except for a modified τ_0 value, we see that p -quantiles $m_{K,p}$ of M_K are again of the form

$$m_{K,p} \approx \tau_0 \sqrt{-2 \log[-\log(p)] + 2 \log(K)}$$

for $p \approx 1$. Hence $m_{K,p}$ grows only slowly with K and the accuracy enters again through the scalar multiplier τ_0 , although the latter is obtained in weighted fashion from the τ_i^2 .

Whether one can now take the same step of extrapolating this behavior under true position alignment to the practical primary/secondary hole pair alignment using the same linear relationship with coefficients α_K and β_K from Table 1 is not clear.

It is not even clear yet whether the weighted average of the τ_i 's found above works well for all choices of linear growth in σ_x .

7 Mating Coordination Holes on Assembled Parts

So far it has been assumed that the “matching” hole patterns were on two monolithic parts and at issue was how well the K hole centers on one part matched the K hole centers on the other part. The quality of matching was judged while the nominal hole centers on each part were held in matching nominal positions.

Here we introduce the complication that the two mating parts are not monolithic but are assembled in some fashion from smaller parts. During the assembly these smaller parts are experiencing small shifts and rotations which leave these subparts in not exactly the desired nominal position relative to each other. Of interest is how well the hole center patterns on all these subparts combine in matching the hole center patterns of another mating assembly also made up of subparts.

Ideally all the hole centers on these two assemblies should match, but because of all the variation sources (drilling holes on subparts and aligning subparts relative to each other in one of the two halves of the mating assembly) there will be mismatches. Whereas we have viewed the hole centering variation on a subpart as independent from hole to hole, we now get the complication that any positioning error of such a subpart will affect all hole centers on that subpart in some common way. This introduces dependencies which make an analytical solution infeasible. As alternate recourse we explore this problem via simulations and study how these results relate to our simple, true positioning approach for the monolithic case. If the relationship is simple enough, then useful extensions to our results may be possible.

In order to build a simulation model we need to conceptualize the various sources of

variation in some acceptable way. Again we assume that the assembled part halves will be aligned on their nominal hole centers and that the actual hole centers may deviate from the nominal hole centers subject to the various sources of variation. This may be simplistic since in practice there is no way of knowing where exactly the nominal hole centers are located after the subparts have been joined into an assembly half. However, determining the worst case hole center mismatch under such an alignment should be conservative since through some motion of the assembly halves relative to each other one should be able to get smaller mismatches than under the true position alignment.

To simplify matters we assume that each assembly half is made up of k subparts, each with n holes drilled in it. The nominal hole centers for both assembly halves are

$$\begin{pmatrix} \mu_{ij} \\ \nu_{ij} \end{pmatrix} \quad i = 1, \dots, k, \quad j = 1, \dots, n .$$

For further simplicity we assume that the nominal hole centers are along some common axis or seam, here taken to be the x -axis. Hence we assume that $\nu_{ij} = 0$, $i = 1, \dots, k$, $j = 1, \dots, n$. This simplicity is mainly for purposes of exposition. The obtained results or insights should be valid for general hole center patterns.

We entertain the following model for the j^{th} actual hole center on the i^{th} subpart of the first assembly half:

$$\begin{pmatrix} X_{ij} \\ Y_{ij} \end{pmatrix} = \begin{pmatrix} \mu_{ij} \\ 0 \end{pmatrix} + \sigma \begin{pmatrix} U_{ij} \\ V_{ij} \end{pmatrix} + \tau_1 \begin{pmatrix} U_i \\ V_i \end{pmatrix} + \tau_2 \begin{pmatrix} 0 \\ Z_i \end{pmatrix} \rho_{ij} \quad (19)$$

where

$$\rho_{ij} = \frac{\mu_{ij} - (\mu_{i1} + \mu_{in})/2}{\mu_{in} - (\mu_{i1} + \mu_{in})/2} = \frac{\mu_{ij} - (\mu_{i1} + \mu_{in})/2}{(\mu_{in} - \mu_{i1})/2} .$$

Here all terms $U_{ij}, V_{ij}, U_i, V_i, Z_i$, $i = 1, \dots, k$, $j = 1, \dots, n$ are independent standard normal random variables. The first term on the right side of equation (19) is the nominal hole center and the second term varies independently from hole to hole within the same subpart and between subparts and represents the circular symmetric bivariate normal hole centering variation. The amount of this variation is regulated by the scalar parameter σ . The third term on the right side of (19) is the same for all holes within the same i^{th} subpart. This variation term represents a random translation of the part as it occurs during assembly. Its scale is regulated by the parameter τ_1 . The fourth and last term on the right of (19) is driven by the same random component Z_i for all holes within the same i^{th} subpart. However that term varies from hole to hole due to the deterministic multiplier ρ_{ij} . This fourth term represents a small random tilt or rotation variation from the x -axis. Its effect is nil at the

midpoint $(\mu_{i1} + \mu_{in})/2$ between the two extreme nominal hole centers on the i^{th} subpart and is maximal at those extreme locations. It is easy to see that $\rho_{ij} \in [-1, 1]$ for $j = 1, \dots, n$ for each $i = 1, \dots, k$.

Figure 30: Hole Center Variation on a Single Subpart (5 Replications)

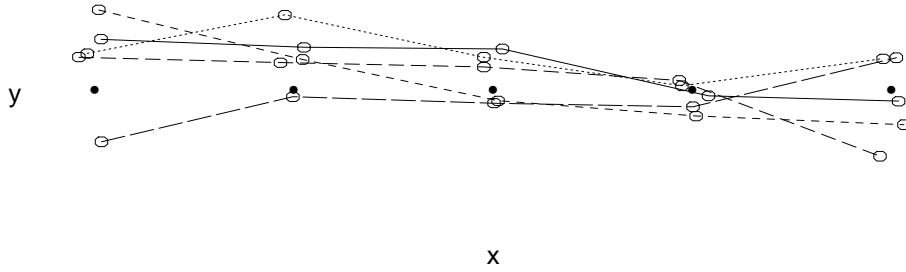


Figure 7 shows five example hole center patterns on the same subpart using the above variation scheme. The unconnected solid dots represent the nominal hole centers for that subpart and the open ellipses connected by five different line types represent the hole centers for five different drilled patterns. Note that some polygons show a definite shift or tilt from the horizontal nominal x -axis.

Similar to (19) we also have a variation model for the hole centers on the other assembly half, built up again from k subparts with n hole centers each, namely

$$\begin{pmatrix} X'_{ij} \\ Y'_{ij} \end{pmatrix} = \begin{pmatrix} \mu_{ij} \\ 0 \end{pmatrix} + \sigma \begin{pmatrix} U'_{ij} \\ V'_{ij} \end{pmatrix} + \tau_1 \begin{pmatrix} U'_i \\ V'_i \end{pmatrix} + \tau_2 \begin{pmatrix} 0 \\ Z'_i \end{pmatrix} \rho_{ij} \quad (20)$$

Here all terms $U'_{ij}, V'_{ij}, U'_i, V'_i, Z'_i$, $i = 1, \dots, k$, $j = 1, \dots, n$ are again independent standard normal random variables, which are also independent of the corresponding terms relating to the other assembly half. Note, that we used the same nominal hole centers for both assembly halves. This expresses our assumption that both assembly halves are held in nominal position while examining the hole center mismatch. Also assumed as the same for both halves are the variation controlling parameters σ , τ_1 and τ_2 . We will choose τ_1 and τ_2 such that the shift variation, controlled by τ_1 is about the same as the rotation variation at the extreme subpart

nominal hole centers, where $|\rho_{ij}| = 1$, i.e., we assume

$$P(\tau_1 \sqrt{U_i^2 + V_i^2} \leq c) = P(\tau_2 \sqrt{Z_i^2 + 0^2} \leq c) = .9973 .$$

From this one gets $c = 3\tau_2$ and

$$.9973 = P\left(\sqrt{U_i^2 + V_i^2} \leq \frac{3\tau_2}{\tau_1}\right) = P\left(U_i^2 + V_i^2 \leq \left[\frac{3\tau_2}{\tau_1}\right]^2\right) = 1 - \exp\left(-\frac{3^2\tau_2^2}{2\tau_1^2}\right)$$

i.e.,

$$\sqrt{-\frac{2}{9} \log(1 - .9973)} = \frac{\tau_2}{\tau_1} \quad \text{or} \quad \tau_2 = 1.14644 \tau_1 .$$

With this we have modeled the tilt of the extreme subpart ends on the same level as subpart translation. The ratio of τ_1 to σ we denote by $r = \tau_1/\sigma$. When $r = 0$ we actually have no subpart translation or tilt, i.e., we are back to the case of monolithic assembly halves.

In the simulation we use the above models (19) and (20) to generate (X_{ij}, Y_{ij}) and (X'_{ij}, Y'_{ij}) and compute

$$D = \max\left(\sqrt{(X_{ij} - X'_{ij})^2 + (Y_{ij} - Y'_{ij})^2} : i = 1, \dots, k; j = 1, \dots, n\right)$$

which is the maximal hole center discrepancy among all $n \times k$ hole center pairs while the assembly halves are held in nominal position. It is certainly possible that smaller values for this maximal hole center discrepancy can be realized by moving the assembly halves relative to each other into a more advantageous mating configuration. However, any such attempt would add complications into which we don't wish to enter. This is in keeping with the approach taken previously in the monolithic part case. By giving up the optimal configuration we gain significantly in simplicity of the results.

The above discrepancy measure D can be simulated many times over and its distribution can be studied. Since $r = 0$ represents a known case for which we can express the distribution of D by a simple formula we will study the distribution of these simulated D values for other r values in relation to this known distribution. Recall that for $r = 0$ we have

$$F_0(d) = P(D \leq d) = \left[1 - \exp\left(-\frac{d^2}{4\sigma^2}\right)\right]^{nk}$$

and the p -quantile $d_{0,p}$, defined by $F_0(d_{0,p}) = p$, is obtained as

$$d_{0,p} = 2\sigma \sqrt{-\log\left(1 - p^{\frac{1}{nk}}\right)} .$$

Suppose the simulated values of D for $r = 0$ are D_1, \dots, D_N and denote their ordered values by $D_{(1)} \leq \dots \leq D_{(N)}$. Plotting these sorted values $D_{(s)}$ versus $d_{0,p(s)}$ with $p(s) = s/(N + 1)$ one would expect to see a point pattern that follows the main diagonal reasonably closely. Of course, for the low and high extremes of this simulated sample of D values (i.e., for s values near 1 and N) the deviations from the straight line pattern will be more substantial. Since such a straight line pattern is simple, it is suggestive to plot the ordered $D_{(s)}$ values, as simulated for other values of r , also against $d_{0,p(s)}$. This program was carried out with values of $r = 0, .5, .75, 1, 1.5, 2, 2.5, 3$ with $N = 10,000$ simulated D values in each case. This was done for each (k, n) configuration with $k = 2, 3, 4, 5, 7, 10$ and $n = 2, 3, 4, 5, 7, 10$. Of the resulting 36 plots for each (k, n) configuration only a few representative ones are shown in Figures 31-36, since the basic character of all 36 plots is the same. Each point pattern of 10,000 simulated points is shown by a connecting polygonal line. The bottom one, representing the case $r = 0$, is expected to be linear except for the fringes at either end, since the observed sample quantiles are plotted against the actual quantiles $d_{0,p}$ of the D distribution. It is remarkable that the point patterns for all the other r values and for all (k, n) configurations also exhibit a mostly linear pattern, at least up to the cumulative probability level of .99. Beyond that level it is difficult to separate real deviation from linearity from the natural and typically strong tail variation.

Also indicated on each plot is the radial hole centering accuracy as $\rho = .01$ which means that $\sigma = .29075 \times .01 = .0029075$. This does not mean that the obtained results will be valid only for this accuracy. The results will be valid for any accuracy, since σ modifies $d_{0,p}$ as a simple scalar multiplier and since σ drives all variation terms in (19) and (20) as a scalar multiplier.

The strongly linear patterns in the plots mean that for other r values in the range $(0, 3]$ and possibly for some $r > 3$ the character of the D distribution does not change and that only the location and scale of the distribution is affected. This observation permits us to summarize the quantiles $d_{r,p}$ of the D distribution function $F_r(d)$ by

$$d_{r,p} = \alpha + \beta d_{0,p} = \alpha + 2\beta\sigma\sqrt{-\log\left(1 - p^{\frac{1}{nk}}\right)},$$

where the coefficients $\alpha = \alpha(r)$ and $\beta = \beta(r)$ are estimated from the middle 80% of the plotted linear point pattern in each case. From the defining relationship $F_r(d_{r,p}) = p$ it then follows that we may represent the distribution function of D under r as

$$F_r(d) = P(D \leq d) = \left[1 - \exp\left(-\left\{\frac{d - \alpha(r)}{2\beta(r)\sigma}\right\}^2\right)\right]^{nk}.$$

The values of $\alpha = \alpha(r)$ and $\beta = \beta(r)$ are given in Tables 5 and 6.

It should be noted that the negative values for α do not suggest that the low end threshold of the distributions is negative. This would not make sense for the inherently nonnegative quantity D . Such negative α values are just a result of fitting a line to the middle 80% of the observations. At the very low end the linear pattern may not hold, but that end of the distribution is of little concern to us.

The results of the present investigation are limited in that we assumed equal bounds on shift and tilt effects at the subpart ends. This may or may not be reasonable.

This investigation should be viewed as preliminary and one can only speculate how these results may extend to the practical alignment based on primary/secondary hole pairs. Given that above we found a linear modification which accounted for the subpart alignment variation and given that primary/secondary hole pair alignment was accounted for by another linear modification when dealing with the pinning of two monolithic parts, one may suspect that a compounding of such linear effects would be a reasonable procedure.

Table 5: Adjustment Coefficients for $k = 2, 3, 4$ Parts

	r	$k = 2$		$k = 3$		$k = 4$	
		α	β	α	β	α	β
all n	0.00	0.0000	1.0000	0.0000	1.0000	0.0000	1.0000
$n = 2$	0.50	0.0000	1.1769	-0.0001	1.2008	-0.0001	1.2000
	0.75	-0.0002	1.4143	-0.0003	1.4308	-0.0004	1.4434
	1.00	-0.0006	1.6841	-0.0007	1.7174	-0.0005	1.6878
	1.50	-0.0011	2.3035	-0.0016	2.3633	-0.0018	2.3712
	2.00	-0.0023	3.0049	-0.0031	3.1031	-0.0027	3.0641
	2.50	-0.0032	3.7379	-0.0032	3.7369	-0.0044	3.8547
	3.00	-0.0041	4.4533	-0.0045	4.4890	-0.0052	4.5597
$n = 3$	0.50	0.0000	1.1663	-0.0001	1.1783	-0.0003	1.1901
	0.75	-0.0007	1.4182	-0.0009	1.4338	-0.0005	1.4008
	1.00	-0.0014	1.7055	-0.0015	1.7065	-0.0015	1.7055
	1.50	-0.0032	2.3820	-0.0037	2.4304	-0.0035	2.4202
	2.00	-0.0051	3.1064	-0.0056	3.1577	-0.0058	3.1706
	2.50	-0.0080	3.9758	-0.0077	3.9352	-0.0084	4.0065
	3.00	-0.0092	4.6745	-0.0103	4.8012	-0.0098	4.7328
$n = 4$	0.50	-0.0005	1.2041	-0.0002	1.1780	-0.0003	1.1877
	0.75	-0.0010	1.4137	-0.0009	1.4171	-0.0011	1.4305
	1.00	-0.0019	1.7160	-0.0020	1.7181	-0.0021	1.7313
	1.50	-0.0042	2.4018	-0.0047	2.4443	-0.0049	2.4729
	2.00	-0.0068	3.1594	-0.0070	3.1859	-0.0076	3.2449
	2.50	-0.0101	4.0005	-0.0104	4.0394	-0.0112	4.1312
	3.00	-0.0128	4.8436	-0.0133	4.8514	-0.0134	4.8754
$n = 5$	0.50	-0.0003	1.1866	-0.0005	1.1944	-0.0003	1.1801
	0.75	-0.0012	1.4280	-0.0009	1.3935	-0.0010	1.4087
	1.00	-0.0024	1.7328	-0.0021	1.7048	-0.0026	1.7538
	1.50	-0.0052	2.4277	-0.0057	2.4859	-0.0056	2.4801
	2.00	-0.0080	3.1836	-0.0088	3.2675	-0.0091	3.2911
	2.50	-0.0111	3.9917	-0.0125	4.1342	-0.0116	4.0319
	3.00	-0.0154	4.9233	-0.0156	4.9386	-0.0158	4.9568
$n = 7$	0.50	-0.0004	1.1873	-0.0004	1.1796	-0.0003	1.1704
	0.75	-0.0013	1.4144	-0.0016	1.4465	-0.0014	1.4212
	1.00	-0.0027	1.7295	-0.0028	1.7354	-0.0028	1.7369
	1.50	-0.0068	2.5195	-0.0069	2.5267	-0.0063	2.4725
	2.00	-0.0105	3.3063	-0.0107	3.3304	-0.0104	3.3120
	2.50	-0.0148	4.1827	-0.0152	4.2161	-0.0148	4.1881
	3.00	-0.0187	5.0159	-0.0200	5.1418	-0.0190	5.0426
$n = 10$	0.50	-0.0007	1.2084	-0.0009	1.2166	-0.0005	1.1901
	0.75	-0.0019	1.4500	-0.0020	1.4689	-0.0017	1.4404
	1.00	-0.0036	1.7839	-0.0035	1.7764	-0.0035	1.7728
	1.50	-0.0082	2.5721	-0.0083	2.5855	-0.0080	2.5593
	2.00	-0.0127	3.3941	-0.0137	3.4883	-0.0128	3.4047
	2.50	-0.0180	4.3148	-0.0177	4.2773	-0.0191	4.3958
	3.00	-0.0227	5.1746	-0.0235	5.2512	-0.0236	5.2568

Table 6: Adjustment Coefficients for $k = 5, 7, 10$ Parts

	r	$k = 5$		$k = 7$		$k = 10$	
		α	β	α	β	α	β
all n	0.00	0.0000	1.0000	0.0000	1.0000	0.0000	1.0000
$n = 2$	0.50	-0.0003	1.2202	-0.0001	1.2012	-0.0002	1.2046
	0.75	-0.0004	1.4399	-0.0005	1.4478	-0.0006	1.4538
	1.00	-0.0009	1.7380	-0.0009	1.7271	-0.0012	1.7584
	1.50	-0.0019	2.3832	-0.0021	2.4087	-0.0020	2.3900
	2.00	-0.0032	3.1154	-0.0031	3.1070	-0.0032	3.1165
	2.50	-0.0040	3.8203	-0.0050	3.9119	-0.0038	3.8024
	3.00	-0.0054	4.5813	-0.0052	4.5646	-0.0060	4.6467
$n = 3$	0.50	-0.0003	1.1897	-0.0005	1.2122	-0.0001	1.1810
	0.75	-0.0010	1.4483	-0.0007	1.4171	-0.0009	1.4297
	1.00	-0.0017	1.7320	-0.0017	1.7372	-0.0022	1.7724
	1.50	-0.0037	2.4376	-0.0041	2.4629	-0.0042	2.4786
	2.00	-0.0063	3.2324	-0.0064	3.2505	-0.0063	3.2272
	2.50	-0.0080	3.9654	-0.0083	3.9999	-0.0083	4.0108
	3.00	-0.0100	4.7578	-0.0097	4.7205	-0.0111	4.8455
$n = 4$	0.50	-0.0004	1.1905	-0.0003	1.1854	-0.0004	1.1955
	0.75	-0.0010	1.4158	-0.0010	1.4166	-0.0010	1.4273
	1.00	-0.0023	1.7469	-0.0023	1.7564	-0.0024	1.7588
	1.50	-0.0050	2.4890	-0.0049	2.4662	-0.0052	2.4939
	2.00	-0.0078	3.2564	-0.0076	3.2421	-0.0085	3.3075
	2.50	-0.0116	4.1693	-0.0111	4.0945	-0.0112	4.1180
	3.00	-0.0138	4.9110	-0.0134	4.8750	-0.0142	4.9547
$n = 5$	0.50	-0.0004	1.1905	-0.0005	1.1958	-0.0005	1.1952
	0.75	-0.0012	1.4229	-0.0012	1.4316	-0.0010	1.4071
	1.00	-0.0027	1.7603	-0.0026	1.7522	-0.0023	1.7198
	1.50	-0.0053	2.4616	-0.0058	2.4919	-0.0057	2.4829
	2.00	-0.0089	3.2731	-0.0094	3.3119	-0.0092	3.3012
	2.50	-0.0125	4.1282	-0.0131	4.1984	-0.0118	4.0711
	3.00	-0.0151	4.9012	-0.0151	4.8963	-0.0164	4.9959
$n = 7$	0.50	-0.0004	1.1852	-0.0006	1.2036	-0.0003	1.1776
	0.75	-0.0016	1.4439	-0.0012	1.4162	-0.0015	1.4363
	1.00	-0.0027	1.7300	-0.0031	1.7670	-0.0024	1.7048
	1.50	-0.0067	2.5135	-0.0068	2.5151	-0.0068	2.5199
	2.00	-0.0106	3.3186	-0.0113	3.3797	-0.0111	3.3581
	2.50	-0.0157	4.2704	-0.0153	4.2302	-0.0154	4.2303
	3.00	-0.0208	5.2030	-0.0197	5.1065	-0.0201	5.1430
$n = 10$	0.50	-0.0005	1.1887	-0.0006	1.1926	-0.0006	1.1920
	0.75	-0.0016	1.4265	-0.0016	1.4335	-0.0018	1.4434
	1.00	-0.0033	1.7537	-0.0035	1.7701	-0.0035	1.7706
	1.50	-0.0079	2.5569	-0.0080	2.5586	-0.0083	2.5861
	2.00	-0.0129	3.4150	-0.0131	3.4296	-0.0134	3.4399
	2.50	-0.0186	4.3631	-0.0179	4.2932	-0.0178	4.2965
	3.00	-0.0223	5.1510	-0.0228	5.1872	-0.0231	5.2219

Figure 31: Approximation quality for $k = 2$ parts and $n = 2$ holes per part

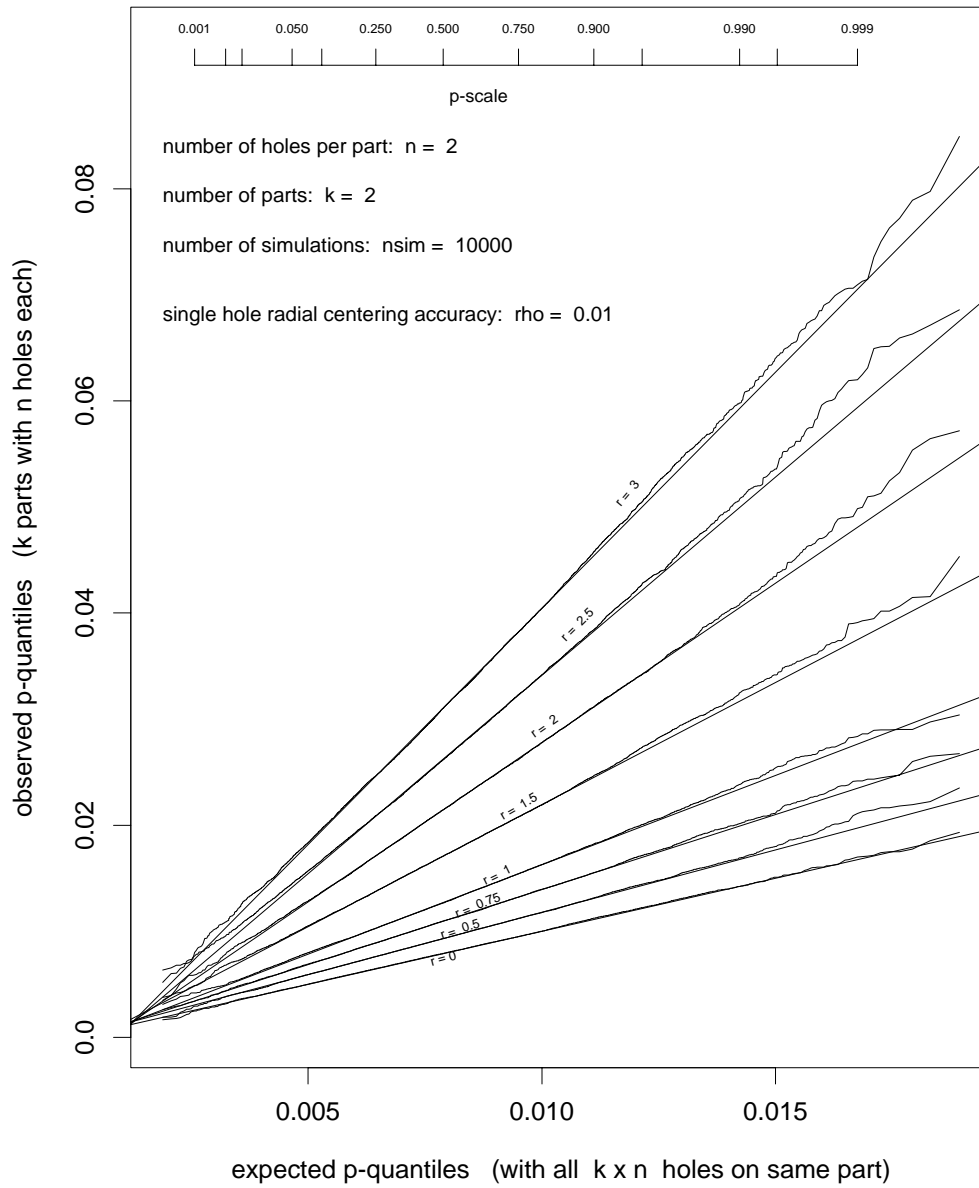


Figure 32: Approximation quality for $k = 2$ parts and $n = 10$ holes per part

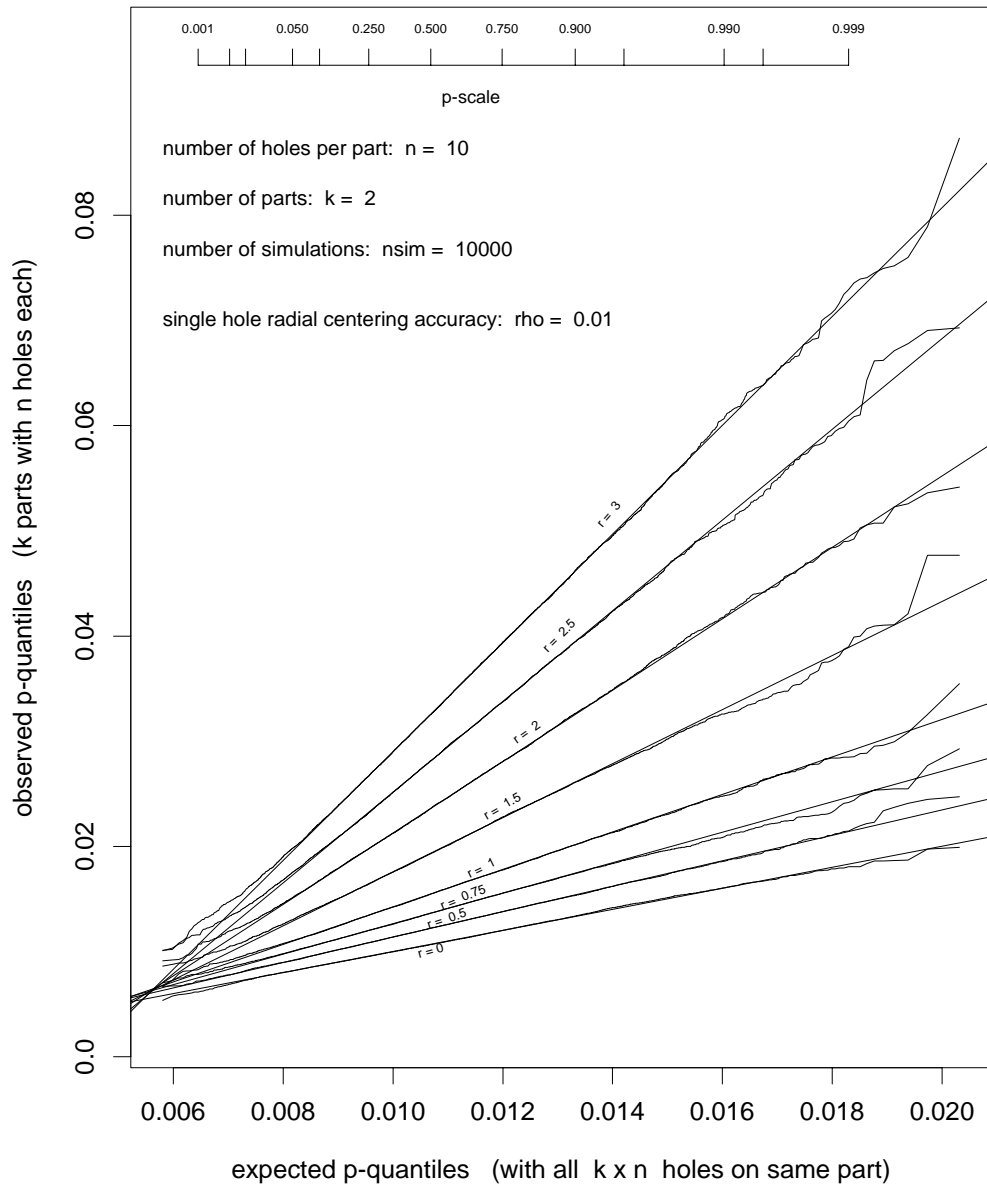


Figure 33: Approximation quality for $k = 3$ parts and $n = 7$ holes per part

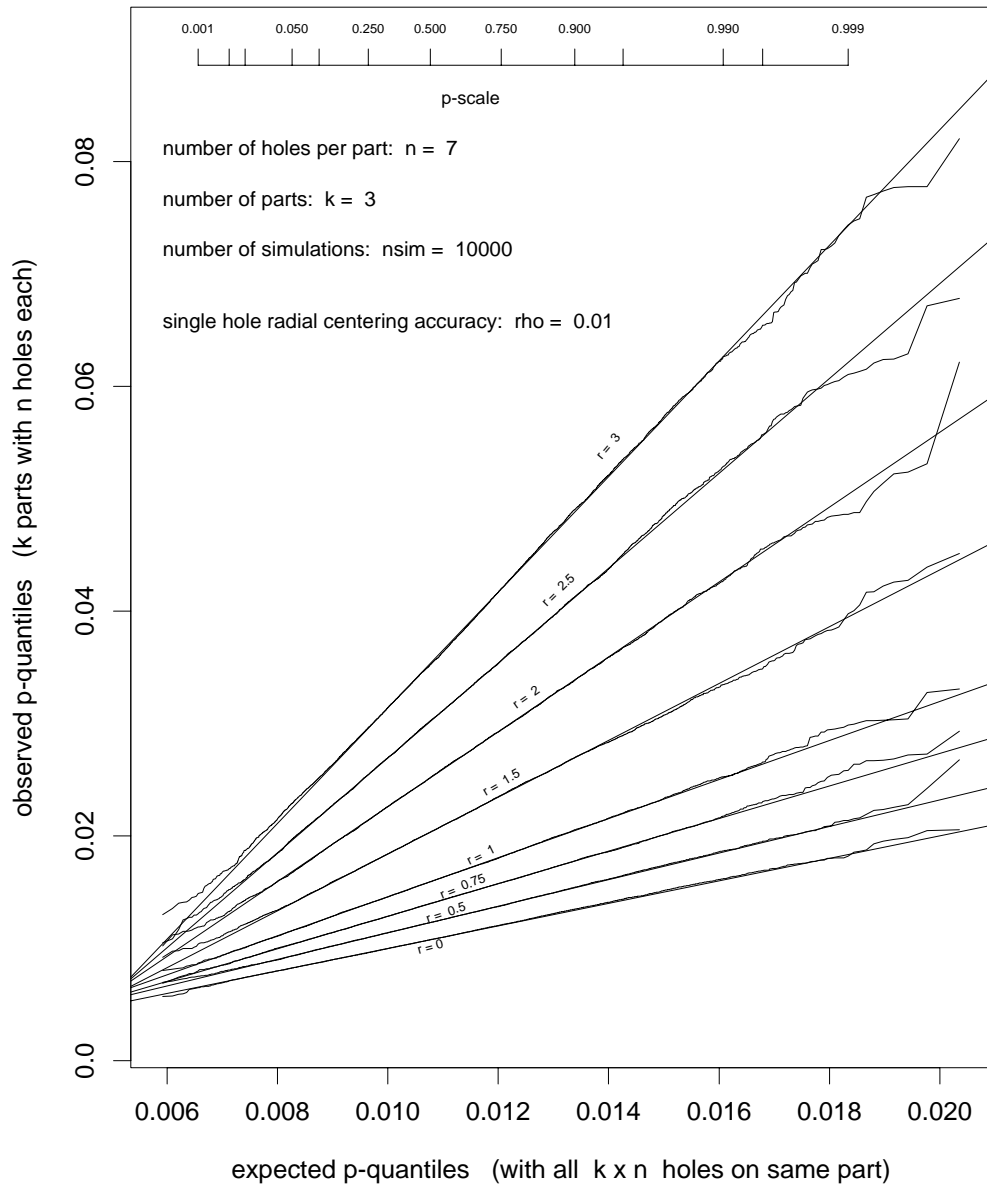


Figure 34: Approximation quality for $k = 7$ parts and $n = 4$ holes per part

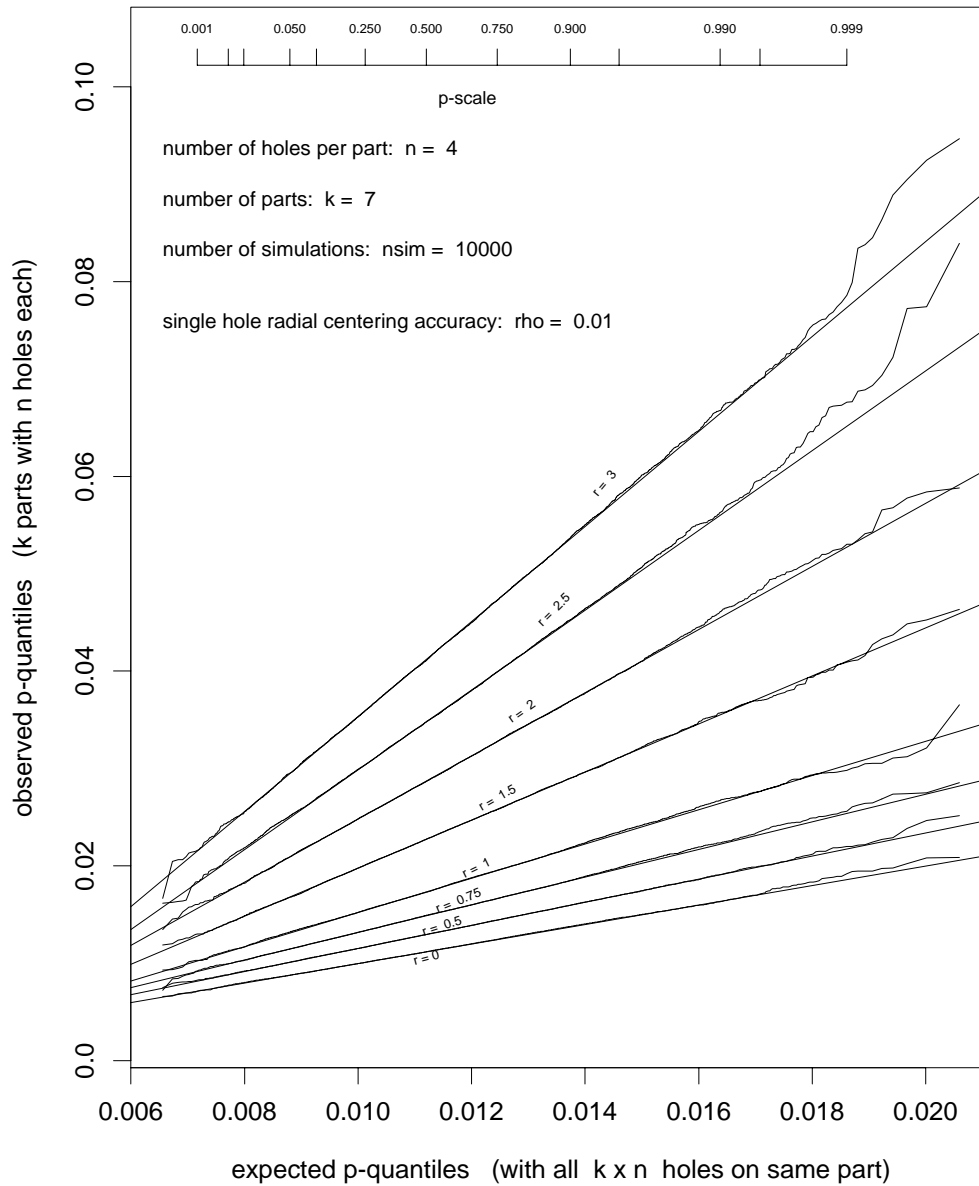


Figure 35: Approximation quality for $k = 10$ parts and $n = 2$ holes per part

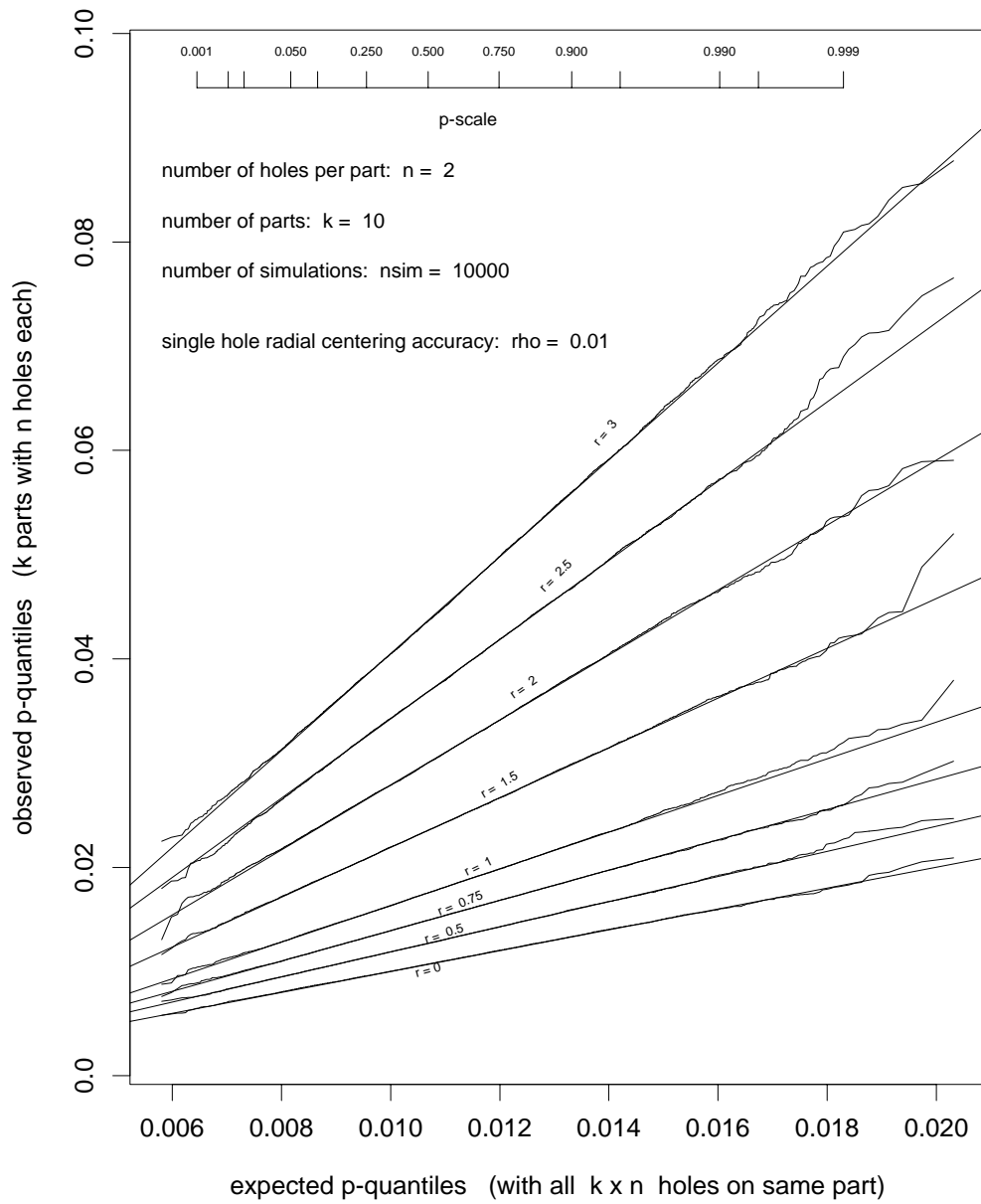
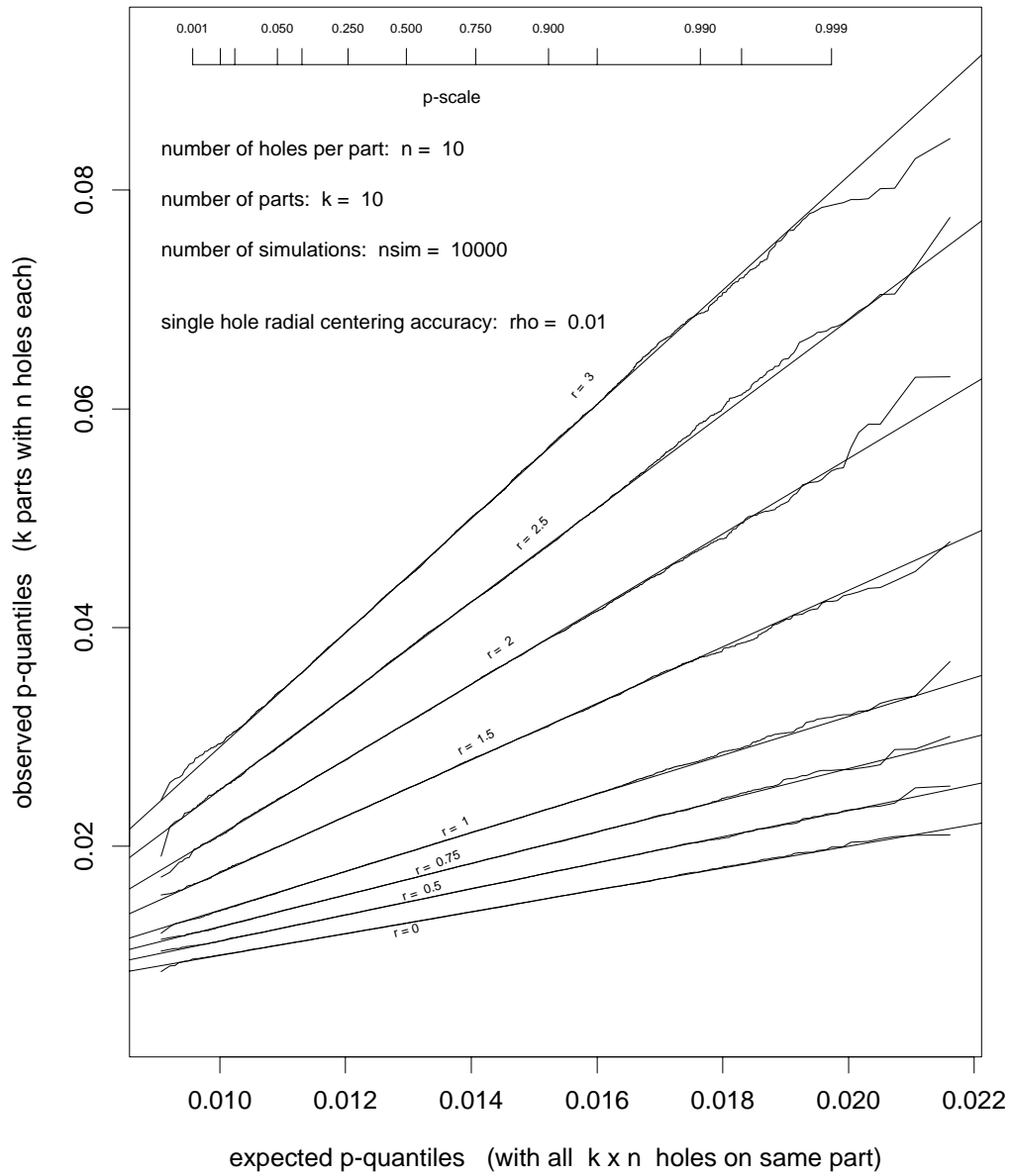


Figure 36: Approximation quality for $k = 10$ parts and $n = 10$ holes per part



8 References

- [1] F.W. Scholz, (1993). "Coordination Hole Tolerance Stacking." *BCSTECH-93-048*, Boeing Information & Support Services, P.O. Box 3707, MS 7L-22, Seattle WA 98124-2207.

- [2] F.W. Scholz, (1994). "Coordination Hole Tolerance Stacking, Panel/Panel/Stringer Join." *BCSTECH-94-017*, Boeing Information & Support Services, P.O. Box 3707, MS 7L-22, Seattle WA 98124-2207.

- [3] F.W. Scholz, (1994). "Cylinder Section Tolerance Stacking Issues." *BCSTECH-94-018*, Boeing Information & Support Services, P.O. Box 3707, MS 7L-22, Seattle WA 98124-2207.

- [4] F.W. Scholz, (1996). "Hole Pinning Clearance." *ISSTECH-96-028*, Boeing Information & Support Services, P.O. Box 3707, MS 7L-22, Seattle WA 98124-2207.

9 Appendix A Extreme Value Approximation

Using the notation introduced in Sections 2.2 and 2.3 we have for $b_K > 0$

$$\begin{aligned}
 P(b_K[M_K - a_K] \leq x) &= P(M_K \leq x/b_K + a_K) \\
 &= \left[1 - \exp\left(-\frac{\{x/b_K + a_K\}^2}{2\tau^2}\right) \right]^K \\
 &= \left[1 - \exp\left(-\frac{x^2}{2\tau^2 b_K^2} - \frac{x a_K}{b_K \tau^2} - \frac{a_K^2}{2\tau^2}\right) \right]^K
 \end{aligned}$$

and with $a_K = \tau\sqrt{2\log(K)}$ and $b_K = \sqrt{2\log(K)}/\tau$

$$\begin{aligned}
 &= \left[1 - \frac{1}{K} \exp\left(-x - \frac{x^2}{4\log(K)}\right) \right]^K \\
 &\longrightarrow \exp[-\exp(-x)] = \mathcal{G}(x) \quad \text{as } K \rightarrow \infty.
 \end{aligned}$$

This follows since

$$K \left[\frac{1}{K} \exp\left(-x - \frac{x^2}{4\log(K)}\right) \right] \longrightarrow \exp(-x) \quad \text{as } K \rightarrow \infty.$$

We also see that for large $|x|$ the term

$$\exp\left(-\frac{x^2}{4\log(K)}\right)$$

converges to 1 only very slowly due to the slow growth of $\log(K)$.

10 Appendix B Geometry of Primary/Secondary Hole Pair Alignment

Setup and Alignment Transformation

As discussed in Section 3, the alignment of the two parts will be accomplished by using two sets of paired coordination holes, two holes on one part are paired with corresponding holes on the other. In this alignment the first hole pair is matched exactly and the second hole pair is aligned by rotation in the best possible way. It is assumed that the relevant aspects of the two hole pairs can be viewed as two sets of circles in the same plane³. It is assumed that nothing impedes the motions of the above alignment process.

Because of the above planar view we may denote the coordinates of the primary hole pair by (X_1, Y_1) and (X'_1, Y'_1) for the first and second part, respectively. Similarly, we denote the coordinates of the secondary hole pair by (X_2, Y_2) and (X'_2, Y'_2) . These coordinates are with respect to a fixed coordinate system. The first part will stay firmly fixed within that system whereas the second part will undergo motions with respect to that system. Throughout we will observe the convention that coordinates with a ' refer to points on the second part. Coordinates with a '' refer to the same points after the alignment transformation. We view (X_i, Y_i) and (X'_i, Y'_i) as bivariate normal random vectors, i.e.,

$$\begin{pmatrix} X_i \\ Y_i \end{pmatrix} \quad \text{and} \quad \begin{pmatrix} X'_i \\ Y'_i \end{pmatrix} \sim N_2 \left(\begin{pmatrix} \mu_i \\ \nu_i \end{pmatrix}, \sigma^2 \begin{pmatrix} 1 & 0 \\ 0 & 1 \end{pmatrix} \right) \quad \text{for } i = 1, 2$$

where the (μ_i, ν_i) represent the nominal hole center locations, which are supposed to be the same for a matched set of holes. Another way of expressing this is as follows

$$X_i = \mu_i + \sigma U_i, \quad Y_i = \nu_i + \sigma V_i, \quad X'_i = \mu_i + \sigma U'_i, \quad Y'_i = \nu_i + \sigma V'_i,$$

where U_i, V_i, U'_i, V'_i are independent standard normal random variables. This representation turns out to be very useful when tracking the influence of the parameters μ_i, ν_i, σ on various key characteristics.

The translation to match the primary hole centers on both parts is clearly given by (Δ_x, Δ_y) , where

$$\Delta_x = X_1 - X'_1 = \sigma(U_1 - U'_1) \quad \text{and} \quad \Delta_y = Y_1 - Y'_1 = \sigma(V_1 - V'_1).$$

These lateral and longitudinal offsets are normally distributed with means zero and standard deviation $\sqrt{2}\sigma$.

³This may involve a projection if the two hole pairs are on two parallel planes.

We now rotate the translated second part around (X_1, Y_1) until the segment connecting (X_1, Y_1) with (X_2, Y_2) coincides with the direction of the translated segment connecting (X'_1, Y'_1) with (X'_2, Y'_2) . We have the following expressions for the cosine and sine of that rotation angle ϕ :

$$\cos \phi = \frac{(X_2 - X_1)(X'_2 - X'_1) + (Y_2 - Y_1)(Y'_2 - Y'_1)}{\sqrt{(X_2 - X_1)^2 + (Y_2 - Y_1)^2} \sqrt{(X'_2 - X'_1)^2 + (Y'_2 - Y'_1)^2}}$$

and

$$\sin \phi = \frac{(X_2 - X_1)(Y'_2 - Y'_1) - (Y_2 - Y_1)(X'_2 - X'_1)}{\sqrt{(X_2 - X_1)^2 + (Y_2 - Y_1)^2} \sqrt{(X'_2 - X'_1)^2 + (Y'_2 - Y'_1)^2}}.$$

By this translation and rotation we move any point (X', Y') to a new position, namely

$$\begin{pmatrix} X' \\ Y' \end{pmatrix} \longrightarrow \begin{pmatrix} X_1 \\ Y_1 \end{pmatrix} + R_\phi \left(\begin{pmatrix} X' + \Delta_x \\ Y' + \Delta_y \end{pmatrix} - \begin{pmatrix} X_1 \\ Y_1 \end{pmatrix} \right) = \begin{pmatrix} X'' \\ Y'' \end{pmatrix},$$

where

$$R_\phi = \begin{pmatrix} \cos \phi & \sin \phi \\ -\sin \phi & \cos \phi \end{pmatrix}.$$

Note that only part 2 is moved and part 1 remains fixed in the chosen coordinate system.

Approximations

It turns out that the above complicated expressions for $\sin \phi$ and $\cos \phi$ can be approximated very well, leading to useful approximations in the transformation formulas. The benefit of such approximations is that it becomes easier to get a sense of what drives the variability of certain key characteristics.

There is no loss in generality in assuming $\nu_1 = \nu_2$, since we can always set up the reference coordinate system that way. Typically σ is relatively small compared to $|\mu_2 - \mu_1|$, i.e., terms like $(U_2 - U_1)\sigma/(\mu_2 - \mu_1)$ can be neglected when compared to 1. The reason is that standard normal random variables tend to be mostly restricted to the interval $[-3, 3]$ and convolutions such as $U_2 - U_1$ will be mostly within the same interval scaled up by a factor $\sqrt{2}$. Thus such random quantities are reasonably limited or bounded and multiplication by $\sigma/(\mu_2 - \mu_1)$ will render such contributions negligible.

This can be used to simplify the above expressions for $\cos \phi$ and $\sin \phi$. For example,

$$\cos \phi \approx 1$$

since

$$\begin{aligned}
(X_2 - X_1)(X'_2 - X'_1) &= (\mu_2 - \mu_1 + \sigma(U_2 - U_1))(\mu_2 - \mu_1 + \sigma(U'_2 - U'_1)) \\
&= (\mu_2 - \mu_1)^2 \left(1 + \frac{\sigma(U_2 - U_1)}{\mu_2 - \mu_1}\right) \left(1 + \frac{\sigma(U'_2 - U'_1)}{\mu_2 - \mu_1}\right) \\
&\approx (\mu_2 - \mu_1)^2
\end{aligned}$$

and (using $\nu_1 = \nu_2$)

$$\begin{aligned}
(Y_2 - Y_1)(Y'_2 - Y'_1) &= (\nu_2 - \nu_1 + \sigma(V_2 - V_1))(\nu_2 - \nu_1 + \sigma(V'_2 - V'_1)) \\
&= \sigma^2(V_2 - V_1)(V'_2 - V'_1)
\end{aligned}$$

so that the numerator in $\cos \phi$ becomes approximately

$$\begin{aligned}
(\mu_2 - \mu_1)^2 + \sigma^2(V_2 - V_1)(V'_2 - V'_1) &= (\mu_2 - \mu_1)^2 \left(1 + \frac{\sigma^2(V_2 - V_1)(V'_2 - V'_1)}{(\mu_2 - \mu_1)^2}\right) \\
&\approx (\mu_2 - \mu_1)^2.
\end{aligned}$$

The same process leads to $(\mu_2 - \mu_1)^2$ as an approximation for the denominator of $\cos \phi$ and thus $\cos \phi \approx 1$ to a good approximation. Similarly one finds

$$\phi \approx \sin \phi \approx \frac{\sigma(V'_2 - V'_1 - V_2 + V_1)}{\mu_2 - \mu_1} = \frac{Y'_2 - Y'_1 - Y_2 + Y_1}{\mu_2 - \mu_1}.$$

This clearly shows the influence of σ , μ_1 , and μ_2 on ϕ . What also stands out is that the variation of ϕ is dominated mainly by the variation of the Y coordinates, which should come as no surprise. Using this approximation we can approximate the standard deviation of ϕ by

$$\sigma_\phi \approx \frac{2\sigma}{|\mu_2 - \mu_1|},$$

which is proportional to σ and inversely proportional to the nominal distance between the two holes used for alignment. As far as the misalignment angle is concerned it is most advantageous to space the primary and secondary alignment holes as far apart as possible.

The above approximations for $\cos \phi$ and $\sin \phi$ yield the following approximations for the points (X'', Y'') obtained by transformation from $(X', Y') = (\mu, \nu) + \sigma(U', V')$ which

may represent the center of some coordination hole anywhere on the second part, i.e., not necessarily collinear with the two used for alignment:

$$\begin{aligned}
X'' &= X_1 + (X' - X'_1) \cos \phi + (Y' - Y'_1) \sin \phi \\
&\approx X' + X_1 - X'_1 + \frac{\sigma}{\mu_2 - \mu_1} (Y' - Y'_1) (Y'_2 - Y'_1 - Y_2 + Y_1) \\
&= \mu + \sigma U' + \sigma (U_1 - U'_1) + \frac{\sigma}{\mu_2 - \mu_1} (\nu + \sigma V' - \nu_1 - \sigma V'_1) (V'_2 - V'_1 - V_2 + V_1) \\
&\approx \mu + \sigma \left[U' + U_1 - U'_1 + \frac{\nu - \nu_1}{\mu_2 - \mu_1} (V'_2 - V'_1 - V_2 + V_1) \right]
\end{aligned}$$

neglecting the term $\sigma^2 (V' - V'_1) (V'_2 - V'_1 - V_2 + V_1) / (\mu_2 - \mu_1)$ against the other terms involving only σ . Further

$$\begin{aligned}
Y'' &= Y_1 - (X' - X'_1) \sin \phi + (Y' - Y'_1) \cos \phi \\
&\approx Y' + Y_1 - Y'_1 - \frac{\sigma}{\mu_2 - \mu_1} (X' - X'_1) (Y'_2 - Y'_1 - Y_2 + Y_1) \\
&= \nu + \sigma V' + \sigma (V_1 - V'_1) - \frac{\sigma}{\mu_2 - \mu_1} (\mu - \mu_1 + \sigma (U' - U'_1)) (V'_2 - V'_1 - V_2 + V_1) \\
&\approx \nu + \sigma \left[V' + V_1 - V'_1 - \frac{\mu - \mu_1}{\mu_2 - \mu_1} (V'_2 - V'_1 - V_2 + V_1) \right]
\end{aligned}$$

neglecting the term $\sigma^2 (U' - U'_1) (V'_2 - V'_1 - V_2 + V_1) / (\mu_2 - \mu_1)$ against the other terms involving only σ .

If $(X, Y) = (\mu, \nu) + \sigma(U, V)$ (again with U, V independent standard normal random variables) is the point on the first panel paired with (X', Y') on the second panel, then we can express the approximate distance between the two points after alignment as

$$\begin{aligned}
D &= D(X, Y, X', Y') = \sqrt{(X - X'')^2 + (Y - Y'')^2} \\
&\approx \sigma \left\{ \left[U - U' - U_1 + U'_1 - \frac{\nu - \nu_1}{\mu_2 - \mu_1} (V'_2 - V'_1 - V_2 + V_1) \right]^2 \right. \\
&\quad \left. + \left[V - V' - V_1 + V'_1 + \frac{\mu - \mu_1}{\mu_2 - \mu_1} (V'_2 - V'_1 - V_2 + V_1) \right]^2 \right\}^{1/2}.
\end{aligned} \tag{21}$$

Note the direct proportionality between D and σ and the fact that a common rescaling of the μ 's and ν 's has no effect on D , since such scale factors would simply drop out in $(\nu - \nu_1)/(\mu_2 - \mu_1)$ and $(\mu - \mu_1)/(\mu_2 - \mu_1)$. Such rescaling is of course limited by our earlier assumption that $\sigma/(\mu_2 - \mu_1)$ be negligible against one, i.e., we can't scale these means too small in order for this observation to hold.

In the special case when $(X, Y) = (X_2, Y_2)$ and $(X', Y') = (X'_2, Y'_2)$ the above expression for D simplifies to

$$D = D(X_2, Y_2, X'_2, Y'_2) \approx \sigma |U_2 - U'_2 - U_1 + U'_1| .$$

Figure 37 illustrates the quality of the above approximations by plotting the approximate value of D against its actual value. For the two alignment hole locations we took $\mu_1 = 0$ and $\mu_2 = 20$ ($\nu_1 = \nu_2 = 0$) and for the location error standard deviation we took a relatively large value of $\sigma = .1$. The top half of Figure 37 shows the approximate D plotted against the actual D of the second matched hole pair for 100 randomly generated alignment situations. The points lie close to the main diagonal indicating that the approximation is excellent. The bottom half of Figure 37 shows the corresponding comparison of a third coordination hole at $(\mu, \nu) = (10, 0)$ (not used for alignment) for 100 randomly generated alignment situations and third coordination hole choices. Again the approximation is excellent and it appears that we can use it with confidence.

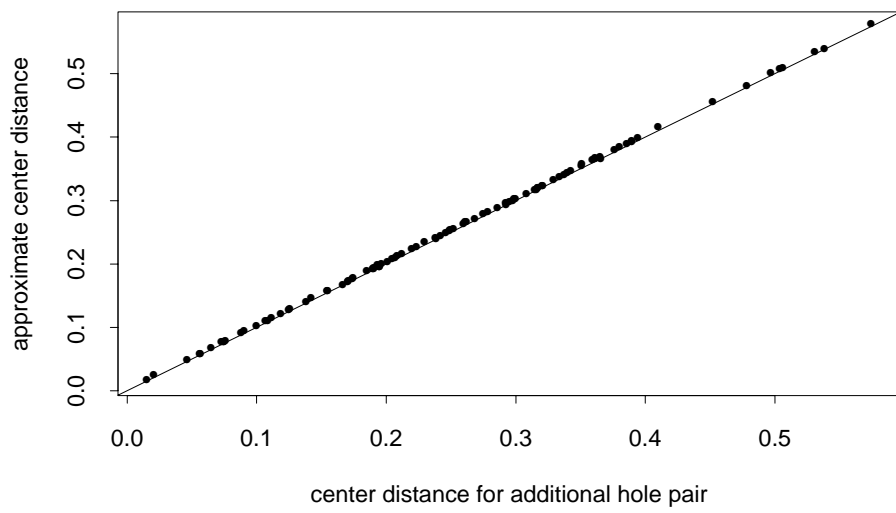
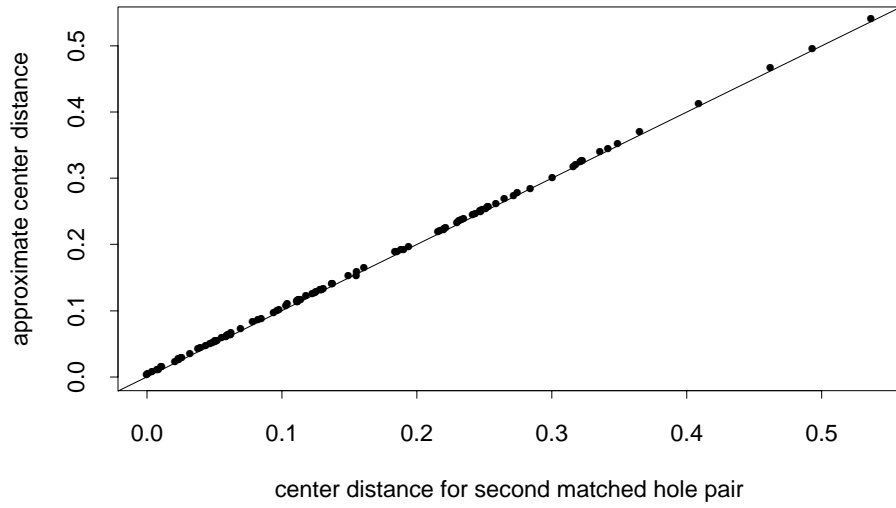
Simulation of Maximal Hole Center Distances

When we have a set of K coordination hole pairs in some matching patterns on two parts it becomes notationally more convenient to treat the K^{th} pair as the secondary hole pair used in the alignment, whereas the holes corresponding to indices $i = 2, \dots, K - 1$ are viewed as intermediate holes. Thus we should modify the above expression (21) for the hole center distance by replacing the index 2 by K throughout. Taking the thus modified expression (21) for the hole center distance at any hole pair $(X, Y) = (X_i, Y_i)$ and $(X', Y') = (X'_i, Y'_i)$ and finding the largest of these distances, namely

$$\tilde{M}_K = \max [D(X_i, Y_i, X'_i, Y'_i) ; i = 1, \dots, K]$$

leads to

Figure 37: Approximation Quality



$$\tilde{M}_K = \sigma \max \left(\left\{ \left[U_i - U'_i - U_1 + U'_1 - \frac{\nu_i - \nu_1}{\mu_K - \mu_1} (V'_K - V'_1 - V_K + V_1) \right]^2 + \left[V_i - V'_i - V_1 + V'_1 + \frac{\mu_i - \mu_1}{\mu_K - \mu_1} (V'_K - V'_1 - V_K + V_1) \right]^2 \right\}^{1/2} ; i = 1, \dots, K \right) .$$

The distribution of \tilde{M}_K/σ is easily simulated for various nominal hole center patterns. One pattern of interest is when all K holes are equally spaced along a line and another is when they are symmetrically arranged around the perimeter of a square including the corners of the square. In the latter case K should be divisible by 4. The relative spacing between nominal hole centers does not affect the distribution of \tilde{M}_K/σ , since any common scaling factor of the (μ_i, ν_i) drops out in the ratios $(\nu_i - \nu_1)/(\mu_K - \mu_1)$ and $(\mu_i - \mu_1)/(\mu_K - \mu_1)$. This of course assumes that any such scaling does not violate our earlier assumption that $\sigma/(\mu_K - \mu_1)$ (before it was $\sigma/(\mu_2 - \mu_1)$) be negligible against one. In practical situations such violating scalings should not arise.

In the above derivation and simulation description it was assumed that the hole centering variation, characterized by σ , is the same on both parts. Observe that in \tilde{M}_K the contributions from the two parts always appear paired, such as in

$$\sigma(V_i - V'_i) = Y_i - Y'_i .$$

If we assume that the Y_i and Y'_i have different standard deviations, say σ_1 and σ_2 , we can view $Y_i - Y'_i$ as having the same distribution as

$$\sigma(V_i - V'_i) \quad \text{with} \quad \sigma^2 = (\sigma_1^2 + \sigma_2^2)/2 .$$

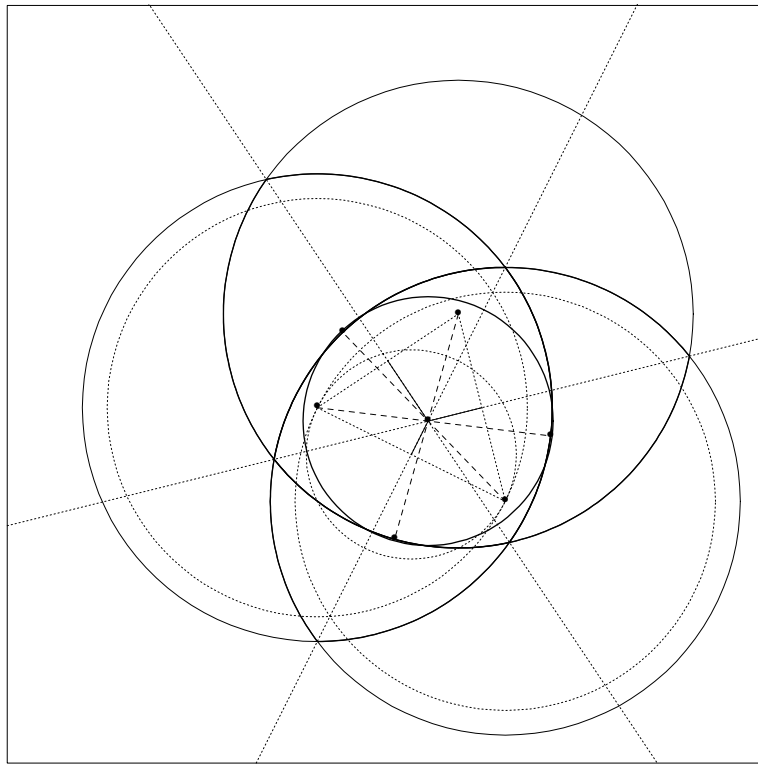
This leaves the situation in the same state as originally assumed.

11 Appendix C

Clearance and Cleanout for Three Overlapping Holes

The problem discussed here is that of finding the largest circle that can be inscribed into the intersection of three circles with same radius r and centers that deviate to some extent from a nominal, common center position. What is desired is a criterion that tells us whether the intersection will accommodate a clearance circle at all and if so, we would like to characterize the diameter of the maximum clearance circle that can be inscribed.

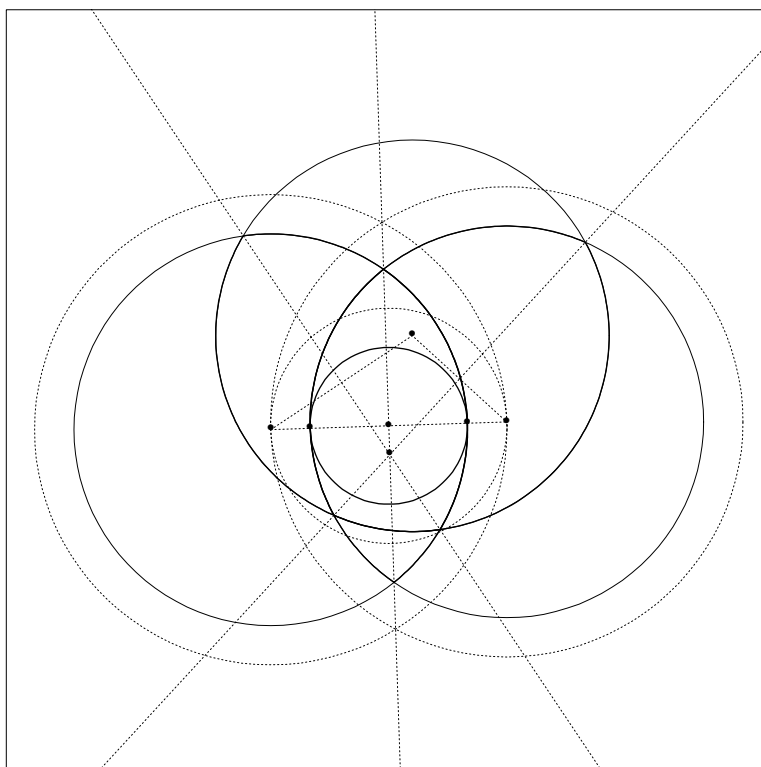
Figure 38: Three Holes (Case A): Clearance Circle Tangent to All Three Circles



It turns out that there are two intrinsically different cases (A and B) aside from the

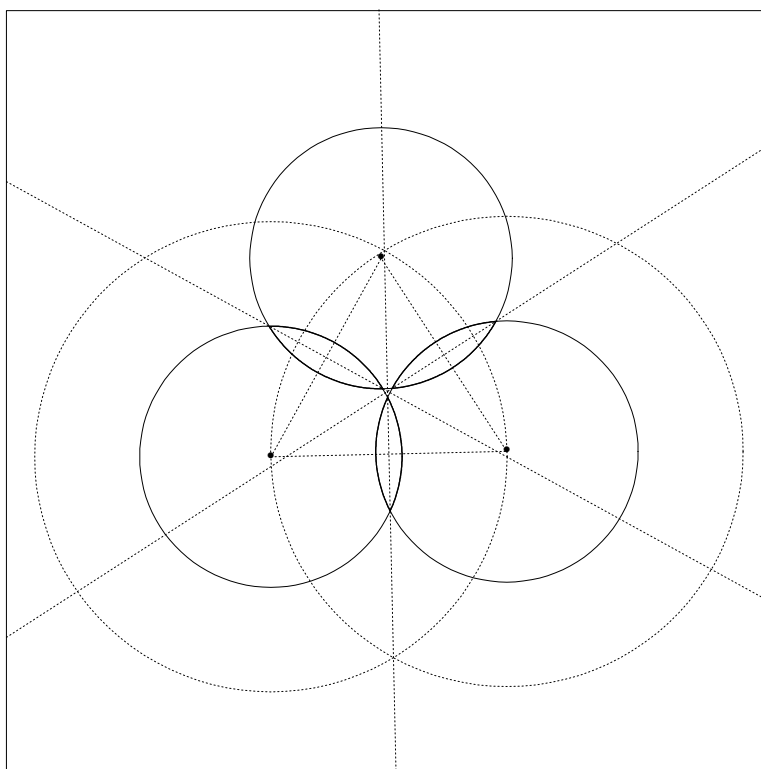
situation when there is no clearance circle (case C). In the first case the clearance circle touches all three given circles and in the second case only two of the circles are touched, i.e., it is as though the third circle is not present. Figures 38 and 39 depict cases A and B , respectively. Figure 40 shows an example with nonempty intersection for each pair of circles but with empty overall intersection, i.e., no clearance. The various geometric entities in those Figures will be explained in the next section. Much of the geometric insight and solution to this problem is due to Tom Grandine.

Figure 39: Three Holes (Case B): Clearance Circle Tangent to Only Two Circles



A second problem in this context is that of finding the smallest circle that is centered on one of the three circle centers and which contains all three circles. This circle is the clean-out circle.

Figure 40: Three Holes (Case *C*): No Clearance Circle



The Clearance Diameter

Let $P_i = (x_i, y_i)$ denote the center of circle C_i , $i = 1, 2, 3$. The common diameter of the three circles is denoted by $2r$. In order to see whether there is a positive clearance at all, we consider those two circle centers that are farthest apart, say P_1 and P_2 , i.e., $|\overline{P_1P_2}| \geq |\overline{P_1P_3}|$ and $|\overline{P_1P_2}| \geq |\overline{P_2P_3}|$, where $|\overline{P_iP_j}|$ denotes the distance between P_i and P_j . It is evident that there will be a positive clearance for circle C_1 and circle C_2 provided $2r > |\overline{P_1P_2}|$. This situation is illustrated in Figure 38. There the two circles, lower left and lower right, are farthest apart. Concentric to these two circles are drawn two dotted line circles with common radius $|\overline{P_1P_2}|$. By the maximality assumption of the distance $|\overline{P_1P_2}|$ it follows that the center P_3 of the upper circle must be within the intersection of the dotted line circles. However, even if P_3 is in that intersection it does not guarantee that the three circles, C_1, C_2, C_3 , will have a positive clearance diameter, as Figure 40 illustrates.

In order to understand the clearance diameter we connect P_1, P_2 , and P_3 to form the sides of a triangle. Next we erect the midperpendiculars on each triangle side, indicated by the straight dotted lines. These intersect at exactly one point, say Q . Using $\overline{P_1P_2}$ as diameter a smaller dotted line circle is drawn in Figure 38. If the third center point P_3 lies outside this dotted line circle (as in Figure 38), then the point Q will lie within the triangle. Otherwise (as shown in Figure 39) it will lie outside the triangle.

This can be seen from Thales' theorem which states that the triangle is a right triangle whenever P_3 lies on this dotted line circle. In that case Q is easily seen to lie on the side opposite to P_3 , i.e., the dividing line between inside and outside of that triangle.

The significance of the midperpendiculars is as follows. If the clearance circle touches two of the given circles, then the perpendiculars to these two tangency points have to meet on the midperpendicular defined by these two circles. If the clearance circle touches all three given circles, then the perpendiculars at the three tangency points (given by the dashed line segments in Figure 38) simultaneously meet on all three midperpendiculars of the triangle P_1, P_2, P_3 , i.e., in Q .

This point Q is equidistant from all the P_i . Denote this distance by r' , which is the radius of the circle through the P_i 's with center at Q . The dashed lines going from P_i through Q to the edge of circle C_i have length r . Hence the segment from Q to the clearance circle edge has length $\rho = r - r'$. Based on the above discussion 2ρ is the clearance diameter of the largest circle fitting into the intersection of the three given circles. As mentioned above, the intersection may be empty, which is indicated by ρ being negative. However, this latter contingency only occurs when the P_i are all far apart.

In Figure 39 the third center point is within the circle spanning the diameter $\overline{P_1P_2}$.

Because of that the midperpendiculars meet below the triangle. The corresponding inscribed clearance circle that would touch all three original circles is not the largest possible. The circle with midpoint halfway between P_1 and P_2 and touching circles C_1 and C_2 is clearly bigger. It does not touch circle C_3 and it is the maximal circle within the intersection of C_1 and C_2 .

It remains to calculate the clearance diameter from the coordinates of P_1, P_2, P_3 . Case *B* is the easiest. It is characterized (assuming P_1 and P_2 being furthest apart) by the condition

$$|\overline{P_1P_2}|^2 > |\overline{P_1P_3}|^2 + |\overline{P_2P_3}|^2 .$$

In that case the maximal clearance diameter is

$$D = 2r - |\overline{P_1P_2}| = 2r - \sqrt{(x_1 - x_2)^2 + (y_1 - y_2)^2} .$$

In case *A* we need to establish the radius r' of the circle passing through P_1, P_2, P_3 . This is given by the sine theorem which states

$$\frac{|\overline{P_1P_2}|}{\sin \alpha_3} = \frac{|\overline{P_1P_3}|}{\sin \alpha_2} = \frac{|\overline{P_2P_3}|}{\sin \alpha_1} = 2r' ,$$

where α_i is the angle of the triangle P_1, P_2, P_3 at P_i . We can express $\sin \alpha_1$ as

$$\sin \alpha_1 = \frac{|(x_2 - x_1)(y_3 - y_1) - (y_2 - y_1)(x_3 - x_1)|}{\sqrt{(x_2 - x_1)^2 + (y_2 - y_1)^2} \sqrt{(x_3 - x_1)^2 + (y_3 - y_1)^2}}$$

and

$$|\overline{P_2P_3}| = \sqrt{(x_3 - x_2)^2 + (y_3 - y_2)^2} .$$

After obtaining $2r'$ as the above ratio we obtain $2\rho = 2r - 2r'$ as the clearance diameter, provided it is positive. If not, then there is no clearance.

The Clean-Out Diameter

Here we find the smallest circle that contains the three given circles C_1, C_2 , and C_3 and which is centered on one of these three circles. Although one could optimize over the centering of the clean-out circle by trying out all three circles as possible centers we will not pursue this here. The reason is that the circle center found to be optimal may not be accessible, being either at the bottom or in the middle of the three hole stack and assuming that we can drill the clean-out hole only from the top of the stack. An optimal center location sandwiched as the middle hole would always be inaccessible, no matter from which side we

can drill. Thus we will assume that the centering hole is given as circle C_1 and the only question is how large must the clean-out diameter be in order to clean out all three given circles.

In order to clean out C_1 and C_2 we need a hole diameter of

$$D_1 = 2 \left(r + \sqrt{(x_1 - x_2)^2 + (y_1 - y_2)^2} \right)$$

and in order to clean out C_1 and C_3 we need a hole diameter of

$$D_2 = 2 \left(r + \sqrt{(x_1 - x_3)^2 + (y_1 - y_3)^2} \right) .$$

In order to clean out all three holes at the same time while centering on C_1 we need a clean-out diameter of

$$\begin{aligned} D_U &= \max(D_1, D_2) \\ &= 2r + 2 \max \left(\sqrt{(x_1 - x_2)^2 + (y_1 - y_2)^2}, \sqrt{(x_1 - x_3)^2 + (y_1 - y_3)^2} \right) . \end{aligned}$$

Previously, when cleaning out two hole pairs, we also considered centering the clean-out hole halfway between the two hole centers. When three holes are involved this type of centering is probably even more difficult to accomplish because of three levels of stacking holes. We will not analyze this further. In any case, the above formulation of D_U (based on centering on C_1) is likely to be conservative, by providing the largest clean-out diameter. If that leads to satisfactory full-sized hole diameters, we will have the same or higher degree of satisfaction with whatever clean-out centering is accomplished in practice.

12 Appendix D

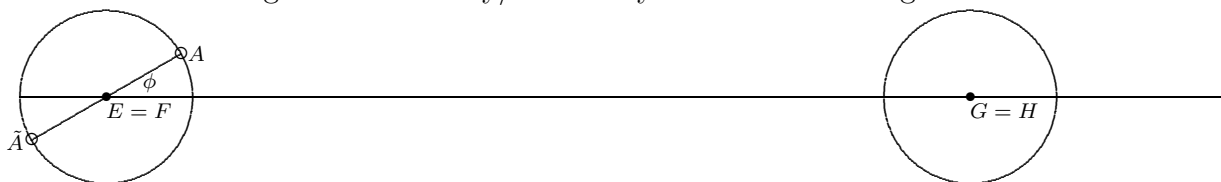
Worst Case for Primary/Secondary Hole Pair Alignment

The following is a worst case analysis when parts are aligned by primary and secondary coordination holes. The arguments put forth are not a mathematical proof that this analysis actually represents the worst case but we believe that they are very persuasive nevertheless. Furthermore, simulations appear to confirm the conclusions. This type of analysis seems new and the results are somewhat surprising at first glance.

Figure 41 shows a pair of circles which represent the hole centering tolerance zones for two holes each on two parts \mathcal{X} and \mathcal{Y} . The left circle represents the matching tolerance zones for the primary hole centers (with matched nominal centers $E = F$) for parts \mathcal{X} and \mathcal{Y} whereas the right circle (with matched nominal centers $G = H$) represents the matching tolerance zones for the secondary hole centers on the same parts. We emphasize that these circles *do not* represent the actual holes themselves.

On the perimeter of the primary centering zones two extreme realizations of actual hole centers are shown as \circ , one for part \mathcal{X} and one for part \mathcal{Y} and denoted by \tilde{A} and A , respectively. These realizations of actual hole centers are extreme in the sense that they are as far apart as possible and still within the same matched tolerance zones. There are many other such extreme realizations which can be distinguished by the angle ϕ which the segment $A\tilde{A}$ forms with the baseline which connects the centers F and H .

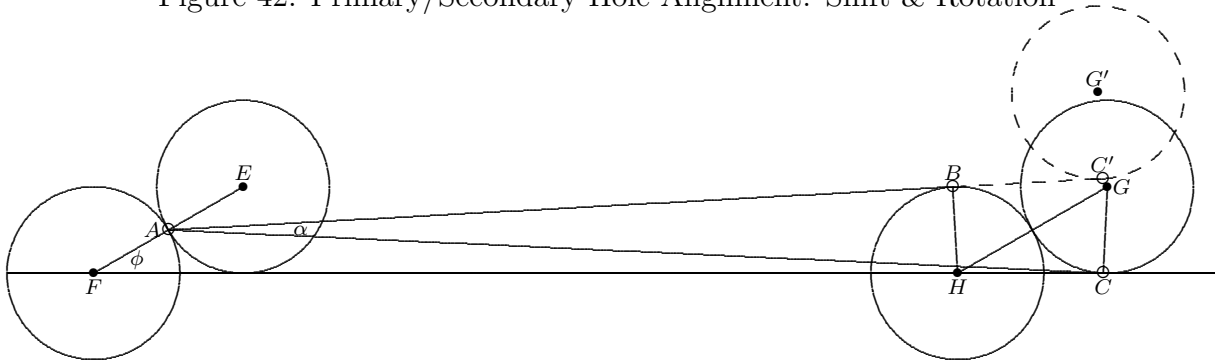
Figure 41: Primary/Secondary True Position Alignment



These extreme primary hole centers can be aligned perfectly by moving part \mathcal{X} along the segment $\tilde{A}A$. The result after this shift is illustrated in Figure 42, showing the offset primary and secondary tolerance zones as solid line circles centered at E , F , G , and H . We will use the convention of referring to the tolerance zones by the same letters.

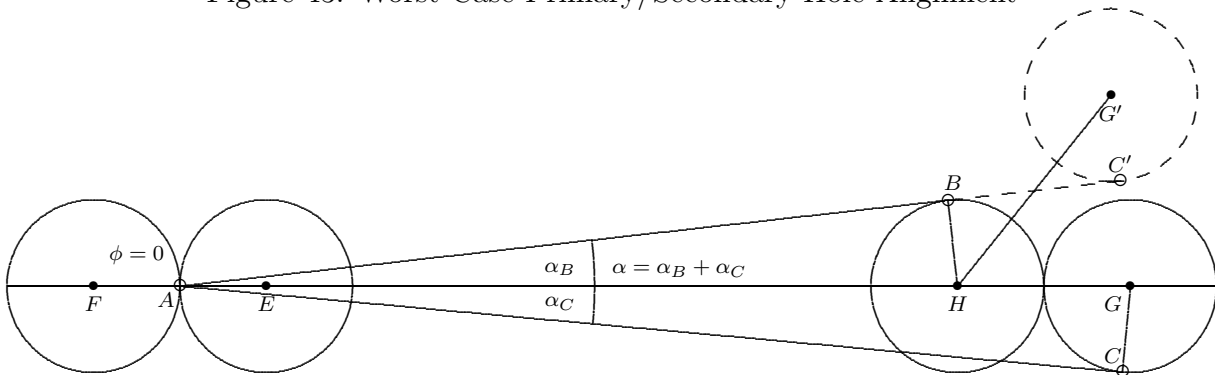
Also shown on the perimeter of the secondary tolerance zones are two extreme actual hole centers, again indicated by \circ and labeled by B and C respectively. This choice of hole centers is special in that the segments AB and AC are tangent to the respective zones H and G . These tangents have angle α between them, which itself is a function of ϕ .

Figure 42: Primary/Secondary Hole Alignment: Shift & Rotation



In order to align these secondary hole centers as best as possible (while keeping the perfect alignment at A) we should rotate part \mathcal{X} with E and G on it around A so that $A, B,$ and C become collinear. The result of this rotation is shown in Figure 42 as the dashed circle with center at G' , with $A, B,$ and C' collinear. A little reflection should convince that for fixed ϕ this rotation by the angle α will separate G' and H as much as possible for any choice of actual hole centers within the zones G and H .

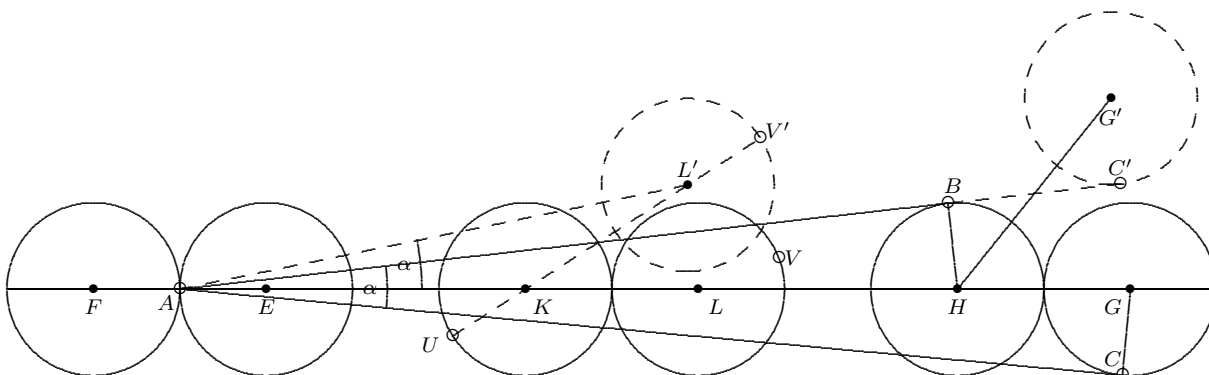
Figure 43: Worst Case Primary/Secondary Hole Alignment



Typically the primary and secondary hole pairs are chosen to be those that are nominally farthest apart from each other. Once the primary and secondary holes are aligned as best as possible, the remaining hole centers located in-between (and not shown in Figure 42) will have misaligned hole centers. The question is: What is the maximal separation that the hole centers of any in-between hole pair can experience? It seems plausible⁴ that this maximal separation comes about when $\phi = 0$, which will result in a maximal rotation angle $\alpha = \alpha_B + \alpha_C$. This latter situation is illustrated in Figure 43.

Figure 44 shows an elaboration of Figure 43 in that an intermediate pair of hole center tolerance zones (between primary and secondary) has been added to each part, both shown in their shifted and rotated position according to the previously discussed alignment.

Figure 44: Worst Case Intermediate Hole Center Separation



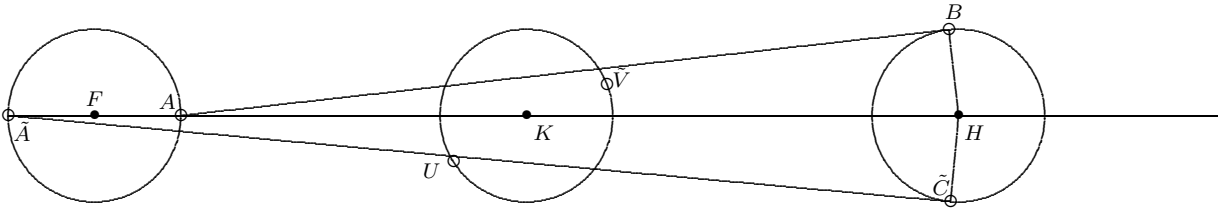
Since the actual hole centers of these intermediate holes are not used during the alignment we can, in worst case fashion, choose the actual hole centers within these aligned tolerance zones (centered at K and L') as far apart as possible, namely at U and V' . Because of the separation of the zones K and L' the distance between U and V' exceeds 4ρ , where ρ is the common radius of all the hole centering tolerance zones. The point V on the perimeter of zone L corresponds to the point V' before rotation by the angle α .

When there are several intermediate holes between the primary and secondary alignment holes then the maximal discrepancy between actual hole centers, i.e., the worst case, can be realized for that intermediate hole pair which is farthest away from the primary hole pair, i.e., just shy of the secondary hole pair.

⁴Although simulations support this conjecture we found it very tedious to prove this rigorously and so far have left this issue unresolved

Figure 45 shows the zones and the worst case choices of actual hole centers in true position alignment. Note that the points \tilde{A} , \tilde{V} , and \tilde{C} in Figure 45 correspond to the shifted points A , V , and C in Figure 44, respectively. The fact that these points A , \tilde{A} , U , \tilde{V} , B , and \tilde{C} represent worst case choices for actual hole centers within their respective tolerance zones is far from obvious when looking just at Figure 45. It only becomes plausible (without the benefit of a tight mathematical proof at this point) through the previous sequence of Figures and explanations.

Figure 45: Worst Case Intermediate Hole Center Separation



It remains to derive a formula for the worst case distance between the hole centers U and V' in Figure 44. This distance is $d = x + 2\rho$, where x is the distance between K and L' . To derive this let ℓ denote the distance between the nominal primary and secondary hole centers, i.e., between F and H . Let λ be the distance between F and the most distant, intermediate, nominal hole center, say between F and K (in Figure 44). Then the distance between A and L' (in Figure 44) is $\lambda + \rho$, the same as the distance between A and L , whereas the distance between A and K is $\lambda - \rho$. By the Cosine Theorem we have

$$\begin{aligned} x &= \sqrt{(\lambda - \rho)^2 + (\lambda + \rho)^2 - 2(\lambda - \rho)(\lambda + \rho) \cos(\alpha)} \\ &= \sqrt{2\lambda^2 + 2\rho^2 - 2(\lambda^2 - \rho^2) \cos(\alpha)} \end{aligned}$$

which is an increasing function of $\lambda > 0$, confirming our earlier assertion that the worst case intermediate hole center pair should be chosen as distant from F as possible.

To obtain $\cos(\alpha)$ we note from Figure 43 that

$$\sin(\alpha_B) = \frac{\rho}{\ell - \rho} \quad \text{and} \quad \sin(\alpha_C) = \frac{\rho}{\ell + \rho}$$

and thus

$$\begin{aligned}
\cos(\alpha) = \cos(\alpha_B + \alpha_C) &= \cos(\alpha_B)\cos(\alpha_C) - \sin(\alpha_B)\sin(\alpha_C) \\
&= \sqrt{1 - \frac{\rho^2}{(\ell - \rho)^2}} \sqrt{1 - \frac{\rho^2}{(\ell + \rho)^2}} - \frac{\rho}{\ell - \rho} \frac{\rho}{\ell + \rho} \\
&= \frac{\ell\sqrt{\ell^2 - (2\rho)^2} - \rho^2}{\ell^2 - \rho^2} = \frac{\sqrt{1 - 4R^2} - R^2}{1 - R^2} \approx 1 - 2R^2,
\end{aligned}$$

abbreviating $R = \rho/\ell$, which typically is very small, say $R < .01$ when the radial tolerance is $.01''$ and $\ell = 1''$ conservatively small. The maximum relative error incurred in the last approximation is 4×10^{-8} for $R < .01$.

Hence we have

$$\begin{aligned}
d &\approx 2\rho + \sqrt{2\rho^2 + 2\lambda^2 - 2(\lambda^2 - \rho^2)(1 - 2R^2)} = 2\rho + \sqrt{4\rho^2 + 4R^2(\lambda^2 - \rho^2)} \\
&= 2\rho + 2\rho\sqrt{1 + (\lambda/\ell)^2 - R^2} \approx 2\rho \left(1 + \sqrt{1 + (\lambda/\ell)^2}\right).
\end{aligned}$$

The maximum relative error in the last approximation is 2.11×10^{-5} for $\lambda/\ell \geq .5$ and $R < .01$.

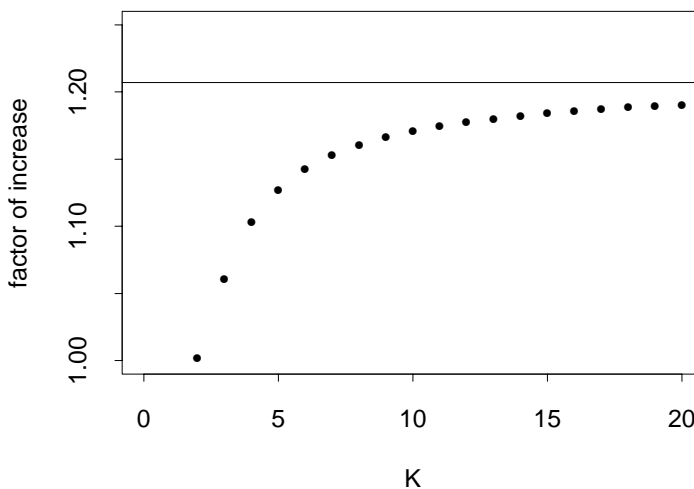
For the special case with K equally spaced and linearly arranged nominal hole centers on both parts one has $\lambda = (K - 2)\ell/(K - 1)$ and thus for $K \geq 3$

$$d_K = d = 4\rho \times \frac{1}{2} \left(1 + \sqrt{1 + \left(\frac{K - 2}{K - 1}\right)^2}\right).$$

For $K = 3$ one has $d_3 \approx 4\rho \times 1.059$, i.e., 5.9% larger than 4ρ , which represents the worst case for $K = 2$. That 4ρ is a worst case separation of actual hole centers when $K = 2$ can be seen from Figures 42 and 43. There the secondary hole center tolerance zones touch after the worst case alignment shift of the primary hole centers. In this touching position any two hole centers in the respective secondary centering zones can be at most 4ρ apart and will only be brought closer together by any alignment rotation around A . If the actual secondary hole centers are at opposite ends of the secondary tolerance zones and on the baseline, then no rotation will take place and 4ρ is achieved. The fact that $d_2 = 4\rho$ in the above formula for d_K is merely an accident.

For large K we get $d_\infty \approx 4\rho \times (1 + \sqrt{2})/2 = 4\rho \times 1.207$, which is 20.7% larger than 4ρ . For $K = 2, \dots, 20$ the factor of increase, $d_K/(4\rho)$, is plotted against K in Figure 46 together with the asymptote at 1.207. It is somewhat surprising that for $K > 2$ the worst case hole center separation is larger than 4ρ . Maybe the reason for it not having shown up in practical situations is that it is a worst case situation and thus statistically rare and the factor of increase is bounded by 1.207 for all K .

Figure 46: Worst Case Increase Factor for 4ρ



From the above we also get $\sin(\alpha) \approx \alpha$ for the worst case angular misalignment between the parts \mathcal{X} and \mathcal{Y} as

$$\sin(\alpha) = \sqrt{1 - \cos^2(\alpha)} \approx \sqrt{1 - (1 - 2R^2)^2} = 2R\sqrt{1 - R^2} \approx 2R.$$

The maximum relative error in the last approximation is at most 5×10^{-5} for $R < .01$.

The effect of this angular misalignment between the parts \mathcal{X} and \mathcal{Y} will be felt most at points (on \mathcal{X} and \mathcal{Y}) which have the greatest perpendicular distance, say ζ , from the baselines connecting the primary and secondary hole centers on each part. The lateral swing at these distant points is approximately $2\zeta R = 2\rho\zeta/\ell$. Aside from the hole centering tolerance zone radius, ρ , this swing is strongly dependent on the ratio of ζ and ℓ . Here ℓ represents the width over which coordination holes are used to join the parts and ζ represents the dimensional extent of the parts in the direction perpendicular to the joining seam. Ideally one would like to have $\zeta/\ell < 1$, or at least not much larger than 1.

The other aspect of part misalignment between the parts \mathcal{X} and \mathcal{Y} is the worst case shift caused by aligning the two primary hole centers. Here “worst case” refers to the previously analyzed case of maximal separation of hole centers when using the primary/secondary hole alignment scheme. Although the subsequent rotation for aligning the secondary hole centers will slightly reduce the actual shift this reduction is negligible, namely at most 5×10^{-5} in relative terms for $R < .01$. Under this worst case misalignment we obtain a shift of 2ρ along the axis defined by the primary and secondary hole centers. Of course such shifts could also occur in the direction perpendicular to this, but then we no longer get worst case separation of hole centers.

The above analysis dealt with a linear nominal hole center pattern. It would be of interest to find the worst case when the hole center pattern is equally spaced around the periphery of a circle. Much of the previous considerations probably still apply and after some analysis one may come up with a closed form formula for worst case hole center here as well.